Role of stromal SPARC in PDAC tumorigenesis and drug delivery

Dissertation

for the award of the degree

"Doctor of Philosophy (Ph.D)"

of the Georg-August-Universität Göttingen

within the doctoral program Molecular medicine,

of the Georg-August University School of Science (GAUSS)

Submitted by

Iswarya Ramu

Born in

Velivayal, India

Göttingen, 2018

Thesis Supervisor

PD Dr. Dr. med. Albrecht Neesse

Members of the thesis advisory committee

PD Dr. Dr. med. Albrecht Neesse (Reviewer)

Department of Gastroenterology and Gastrointestinal Oncology

University Medical center Göttingen

Prof. Dr. Steven Johnsen (Reviewer)

Department of General, Visceral and Pediatric Surgery

University Medical center Göttingen

Prof. Dr. Matthias Dobbelstein

Department of Molecular Oncology

University Medical center Göttingen

Further members of the examination board

Prof. Dr. med. Frauke Alves

Department of Hematology and Oncology, University Medical Center Göttingen

Prof. Dr. Heidi Hahn

Department of Human Genetics, University Medical Center Göttingen

PD Dr. rer. nat. Laura Zelarayan-Behrend

Institute of Pharmacology and Toxicology, University Medical Center Göttingen

Date of oral examination: 10.12.2018

Affidavit

I hereby declare that the PhD thesis entitled “Role of stromal SPARC in PDAC tumorigenesis and drug delivery” has been written independently and with no other sources and aids than quoted.

_____

Iswarya Ramu

October, 2018

Göttingen

Table of Contents

Acknowledgements

With immense gratitude, I take this opportunity to convey my heartfelt thanks to my supervisor PD. Dr. Dr. med. Albrecht Neesse for giving me this chance to work in his research group and for his constant support and motivation throughout the course of my Ph.D project.

I sincerely thank my thesis advisory committee members Prof. Dr. Steven A. Johnsen and Prof. Dr. Matthias Dobbelstein for their support and valuable discussions and suggestions for my project during each thesis committee meeting.

On a special note, I would like to thank Prof. Dr. med. Volker Ellenrieder, PD. Dr. med. Elisabeth Hessmann and Dr. Shiv Singh for providing guidance and discussions about my experiments and for helping with any critical situations. I deeply thank our former colleague Dr. Nai-Ming Chen for teaching the techniques during the initial days of my thesis project.

I am grateful to Prof. Dr. med. Bence Sipos and Prof. Dr. Phillipp Ströbel for their contribution in histological analysis and tumor grading. I would like to sincerely thank Prof. Duncan Jodrell and Dr. Frances Richards for helping us with the pharmacokinetic analysis.

I thank my fellow Ph.D student Melanie Patzak for helping me with some of the mouse experiments and for being available if I needed any help. I also would like to thank the fellow medical dissertation students Lukas Klein and Sören Buchholz for their moral support during the course of my thesis project. I would like to convey my deep thanks to Dr. Robert Goetze and Laurin Wolf for standing at my side in every situation and for their brotherly love and support. I would like to extend my sincere thanks to our talented and hardworking technical assistants Jutta Blumberg and Ulrike Wegner for their constant support and contribution throughout my project.

I thank my fellow Ph.D students Shilpa Patil, Umair Latif, Zhe Zhang (Alice), Mengyu Tu, Marie Hasselluhn, Geske Schmidt, Lennart Versemann, Kevin Weimer, Lina Frank and other technical assistants of our department for creating such a wonderful work atmosphere and for the fruitful scientific discussions regarding my thesis and in general.

I would like to convey a special thanks to my best friend Veera for giving me the moral support throughout the course of my stay in Germany. I am truly grateful to my best friends Ari, Rajeev, Brindha, Shilpa and Maithy for filling me up with the positive energy whenever I was drained.

I would not have survived this long and challenging journey without the constant support from my family. Therefore, I would like dedicate my Ph.D thesis to my family. I would like to thank my mother Mrs. Pazhaniammal Ramu, my sisters Mrs. Sathya Krishnaraj and Sonu and my brother in law Dr. K. Krishnaraj for being my back bone. I like to thank my sister Dr. Sankari Nagarajan for being the inspiration and for her constant support and guidance throughout my career.

At last but most importantly I wish to thank my husband Vino who inspires me greatly with his enthusiastic nature and whose presence influences me positively. Thank you for being who you are. Your efforts and contribution can't be described in words, I am deeply thankful for all your support.

Abbreviations

α	alpha
β	beta
µ	micro
µl	microliter
µm	micrometre
µM	micromole
°C	degree celsius
2D	two dimensional
aa	aminoacid
ABC	avidin-biotin Complex
ADM	acinar to ductal metaplasia
asn	asparagine
α -SMA	alpha-Smooth Muscle Actin
bp	base pair
BM-40	basement membrane protein-40
BSA	bovine serum albumin
BRCA1	breast cancer 1
CAFs	cancer associated fibroblasts
CC3	cleaved caspase 3
CCL	chemokine (C-C motif) Ligand
CD-31	cluster of differentiation 31
CDA	cytidine deaminase
CO_2	carbon dioxide
CTGF	connective tissue growth factor
Da	Dalton
DAB	3,3'-Diaminobenzidine
DAPI	diamidino-2-phenylindole
dCK	deoxycytidine kinase
DDR2	discoidin domain receptor 2
dFdC	2′,2′-difluorodeoxycytidine
dFdCDP	difluorodeoxycytidine diphosphate
dFdCMP	difluorodeoxycytidine monophosphate
dFdCTP	2′,2′-difluorodeoxycytidine-5′-triphosphate
dFdU	2′,2′-difluorodeoxyuridine
DMEM	dulbecco's Modified Eagle's Medium
DNA	deoxyribonucleic acid
EC domain	extra cellular domain
ECM	extra cellular matrix
ECL	enhanced chemiluminescence
EDTA	ethylenediaminetetraacetic acid
EGF	epidermal growth factor
EMT	epithelial to mesenchymal transition
ER	endoplasmic reticulum
ERK	extracellular signal-regulated kinase
FBS	fetal bovine serum
FGF	fibroblast growth factor

Fig.	figure
5-FU	fluorouracil
FOLFIRINOX	folinic acid, fluorouracil, irinotecan and oxaliplatin
g	gram
Gly	glycine
GM-CSF	granulocyte-macrophage colony-stimulating factor
GEMM	genetically engineered mouse models
h	hour
HA	hyaluronic acid
HBSS	hanks' balanced salt solution
HCl	hydrochloric acid
hENTs	human nucleoside transporters
H&E	hematoxylin and eosin
HEPES	4-(2-hydroxyethyl)-1-piperazineethanesulfonic acid
Hh	hedgehog
His	histidine
HRP	horse radish peroxidase
HSP47	heat shock protein47
HSP90	heat shock protein90
H_2O_2	hydrogen peroxide
IgG	immunoglobulin G
IHC	immunohistochemistry
IL6	interleukin 6
IL8	interleukin 8
ILK	integrin linked protein kinase
KC	LSL-$Kras^{G12D}$; Pdx or P48 Cre
kDa	kilo Dalton
KPC	LSL-$Kras^{G12D}$;$Trp53^{172H}$;PdxCre
Lys	lysine
LC-MS	liquid chromatography-mass spectrometry
LSL	Lox-stop-lox
M	mole
MDSC	myeloid derived suppressor cells
MEK1/2	mitogen-activated protein kinase kinase1/2
MEM	minimum essential medium
min	minute
ml	millilitre
mM	millimole
MMP	matrix metalloproteinase
M.O.M kit	mouse on mouse kit
mRNA	messenger RNA
mTORC1	mammalian target of rapamycin complex 1
MTT	3-(4, 5-dimethylthiazol-2-yl)-2,5-diphenyl tetrazolium bromide
NaOH	sodium hydroxide
NEAA	non-essential amino acid
NF-KB	nuclear factor kappa-light-chain-enhancer of activated B-cells

NFKBIA	NF-KB inhibitor α
NT5c1A	5'-Nucleotidase, Cytosolic IA
NTP	nucleoside triphosphate
PanIN	pancreatic intra epithelial neoplasm
PAFs	PanIN associated fibroblasts
PI3K	phosphoinositide 3 kinase
PBS	phosphate Buffered Saline
PBS-T	phosphate Buffered Saline withTween 20
PCR	polymerase chain reaction
PDAC	pancreatic ductal adenocarcinoma
PDGF	platelet derived growth factor
pH	potential of hydrogen
pM	pico mole
PMSF	phenylmethanesulfonyl fluoride
P/S	penicillin/Streptomycin
PSCs	pancreatic stellate cells
RNA	ribonucleic acid
rpm	revolutions per minute
RT	room temperature
SBTI	soy bean trypsin inhibitor
SDS	sodium dodecyl sulfate
SDS-PAGE	SDS-polyacrylamide gel electrophoresis
sec	second
SMOC	secreted modular calcium binding protein
SPARC	secreted protein acidic and rich in cysteine
TAMs	tumor associated macrophages
Taq	*Thermus aquaticus*
TBE	tris-Borase-EDTA
TBS	tris-buffered saline
TBS-T	tris-buffered saline with Tween 20
TGFß	transforming growth factor beta
TNF- α	tumor necrosis factor α
TVA	tierversuchsantrag (animal experiment application)
V	voltage
VEGF	vascular endothelial growth factor
vs	versus
wt	wildtype
ZTE	zentrale Tierexperimentielle Einrichtung (central animal experimental facility)

Abstract

Pancreatic ductal adenocarcinoma (PDAC) is one of the most aggressive solid tumors in humans. Median survival is around 12 months and is due to late diagnosis, early metastatic spread, and a high resistance towards available chemotherapeutic regimens. The desmoplastic reaction is a key feature of PDAC which contributes to disease progression and has also been reported to confer to chemoresistance and impaired drug delivery. Secreted protein acidic and rich in cysteine (SPARC) is an important matricellular protein that regulates collagen deposition and ECM remodeling. In human PDAC, SPARC is expressed by peritumoral fibroblasts and high expression is associated with a poor prognosis. In several other cancer entities, SPARC has been shown to play either tumor promoting or tumor suppressing roles. However, the functional role of SPARC in PDAC is unclear. In my thesis, I investigated the expression of SPARC and its role during tumor progression from preneoplastic lesions to frank carcinomas in genetically engineered mouse models (GEMMs) of PDAC. In order to achieve this, I generated SPARC^{wt}, SPARC$^{-/-}$, KC-SPARC^{wt} and KC-SPARC$^{-/-}$ mice with a global SPARC knock-out for *in vivo* studies. Furthermore, primary epithelial and fibroblast cell lines were derived from preneoplastic murine tissues and murine pancreas tumors for *in vitro* experiments.

The *in vivo* results showed that the development of the murine pancreas was unaffected by germ- line SPARC knock-out. Immunohistochemical and western blot analysis revealed that SPARC is not expressed in the normal pancreas with a marked increase of SPARC in activated fibroblasts during preneoplastic stages and tumor progression. However, loss of SPARC in KC-SPARC$^{-/-}$ mice resulted in a significant reduction of intratumoral collagen deposition. Notably, SPARC and subsequent collagen depletion did not alter pancreatic intraepithelial neoplasia (PanIN) progression, tumor incidence or metastatic frequency to the liver. Both KC-SPARC^{wt} and KC-SPARC$^{-/-}$ tumors exhibited similar tumor characteristic including proliferation, apoptosis and mean vessel density. Primary epithelial and fibroblast cell lines from both genotypes showed comparable morphology and proliferation rates. However, tumor bearing KC-SPARC$^{-/-}$ mice lived significantly shorter than of KC-SPARC^{wt} mice, a finding that was most likely due to more severe clinical complications such as ascites, diarrhea and bile duct obstruction in KC-SPARC$^{-/-}$ mice.

Interestingly, SPARC mediated collagen deposition did not impede the delivery and metabolism of gemcitabine in pre-neoplastic lesions and tumors as determined by LC-MS/MS. Strikingly, the amount of gemcitabine increased from normal pancreas tissues to pancreatic tumors questioning the drug delivery hypothesis for gemcitabine in PDAC.

1. Introduction

1.1 Pancreatic ductal adenocarcinoma (PDAC)

1.1.1 Epidemiology

Pancreatic ductal adenocarcinoma (PDAC) constitutes one of the most aggressive malignancies in humans (Carpelan-Holmstrom, 2005; Howlader et al., 2012) and accounts for 7% of total cancers in both male and female (Carpelan-Holmstrom, 2005; Rahib et al., 2014; Schneider et al., 2005; Siegel et al., 2017). PDAC possesses one of the worst clinical outcomes of all solid tumors, and only about 6-8% of patients survive beyond 5 years. The median survival of untreated patients with advanced or metastatic disease is about 6-12 months. Around 80% of patients are reported to have either locally advanced disease or distant metastases during initial diagnosis and cannot be operated anymore (Siegel et al., 2017).

In 2001, Parkin and colleagues have performed a study to examine the global cancer burden using multiple data sets from various sources including the World Health Organization (WHO), Disease surveillance points (DSP), GLOBCON 2000, International agency for Research on Cancer (IARC), Surveillance, Epidemiology and End Results (SEER) and EUROCARE-2 (Parkin et al., 2001). This study has shown that there were 216,000 new pancreatic cancer cases with an estimated death of 213,000 cases worldwide, while in Europe there were 60,139 newly reported cases with an estimated death of 64,801 cases (Parkin et al., 2001). In 2002, PDAC incidence in the United Kingdom was reported to be 7152 cases with the estimated death of 7250 cases (Ghaneh et al., 2008). More recently, the American Cancer Society reported 53,670 new cases in the US in 2017 with an estimated death of 43,090 cases (Siegel et al., 2017). Evidently, over the years the incidence is increasing while the mortality rate is unchanged (Lowenfels and Maisonneuve, 2004). Therefore, PDAC is the fourth common reason for cancer-related deaths worldwide, and it is expected to be the second leading cause of cancer-related deaths worldwide by 2030.

There are various factors such as age, sex, ethnicity, smoking and alcoholic abuse, chronic pancreatitis, obesity, diabetes and *Helicobacter pylori* infections which have been associated with a slightly increased risk to develop PDAC (Maisonneuve and Lowenfels, 2010). In particular, tobacco and alcohol have been identified to accelerate

the risk of PDAC development up to 2-fold (Iodice et al., 2008; Tramacere et al., 2010). PDAC occurs predominantly in the elderly population (Howlader et al., 2012) and is slightly more often diagnosed in males than in females (Siegel et al., 2017). One proposed explanation for this difference might be the protective role of female hormones against PDAC, though there is no concrete validation for this hypothesis yet (Wahi et al., 2009). Recent studies have also explored the direct correlation between obesity and PDAC risk (Arslan et al., 2010; Incio et al., 2016). The highest incidence is reported among the populations of industrialized/western countries, while the incidence seems to be relatively lower among Indian and Nigerian populations (Boyle et al., 1989).

PDAC is also associated with hereditary factors, in which germ line mutations in certain genes including BRCA1, BRCA2, APC, CDKN2A and PRSS1 result in PDAC development (Rizzato et al., 2013; Shi et al., 2009; Turati et al., 2013). Among these genes, BRCA2 was found to be the most frequently reported mutation to increase the risk of PDAC about 6-12% (Murphy et al., 2002; Shi et al., 2009; Thompson and Easton, 2002).

1.1.2 Current therapies of PDAC

The treatment options for PDAC are extremely limited due to various reasons such as lack of early symptoms and diagnosis, high recurrence rate after surgery, and high resistance towards the existing chemotherapeutic regimens (Neesse et al., 2015). As mentioned earlier, only a small proportion of patients (~20%) are eligible for surgery at the time of diagnosis (Neoptolemos et al., 2010). The prognosis of surgical patients is still poor due to local recurrence or distant metastases shortly after surgery. Therefore, patients who are eligible for surgery receive adjuvant therapy postoperatively. This has been shown to improve overall and disease free survival (Boeck et al., 2008; Stocken et al., 2005). Numerous clinical trials including CONKO-001, CONKO-005, JSAP-02, RTOG9704, European Study Group for Pancreatic cancer-1, 3, 4 (ESPAC-1, 3 and 4) have been performed over three decades to explore the optimal adjuvant therapy for PDAC (Kanji et al., 2018; Neoptolemos et al., 2010, 2017, Oettle et al., 2013, 2007; Sinn et al., 2017). Most of the above mentioned randomized trials studied the efficacy of gemcitabine alone or in combination with a second chemotherapeutic agent as adjuvant therapy following surgical resection.

In 2010, the ESPAC-3 randomized and controlled trial was aimed to explore the therapeutic value of gemcitabine monotherapy compared to 5-fluorouracil (5-FU) plus folinic acid as an adjuvant therapy on a large number of patients who underwent surgical resection of PDAC. Results of this trial have shown that there was no significant difference in terms of overall survival and disease-free survival between the groups treated with gemcitabine alone (median survival- 23.6 months, progression free survival-13.5 months) and the group treated with 5-FU plus folinic acid (median survival- 23.0 months, progression free survival-12.5 months). However, gemcitabine was tolerated well with less adverse side effects. Due to this advantage, gemcitabine has been considered as the standard adjuvant therapy (Neoptolemos et al., 2010). Recently, ESPAC-4 trial has aimed to study the clinical efficacy of gemcitabine and capecitabine combination compared to gemcitabine alone as an adjuvant therapy in surgically resected PDAC patients. This study has revealed that the combination had a significantly improved survival outcome compared to gemcitabine monotherapy while having a tolerable toxicity profile (overall median survival 28.8 months and 25.5 months respectively). Therefore, the combination of gemcitabine and capecitabine could be considered as the standard adjuvant therapy at present (Neoptolemos et al., 2017).

In case of locally advanced and metastatic PDAC palliative treatment represents the only approved treatment option at present. In the past, 5-FU was used to treat patients with advanced pancreatic cancer based on the study results of Cullinan and colleagues in 1985. In this study, the authors compared therapeutic efficacy of 5-FU versus the combination of 5-FU and doxorubicin versus the combination of 5-FU, doxorubicin and mitomycin and reported no significant difference in terms of survival and quality of life of the patients. Thus, 5-FU was considered the better option based on the most acceptable toxicity profile (Cullinan et al., 1985). In 1994, Casper and colleagues conducted a phase II trial using gemcitabine on patients with advanced PDAC with no prior treatment. This study reported an increased therapeutic efficacy of gemcitabine with a tolerable toxicity profile (Casper et al., 1994). Three years later, another randomized trial was conducted on a large cohort of patients (126 patients) to compare the clinical efficacy of gemcitabine versus standard 5-FU therapy. In this study, gemcitabine was shown to improve clinical benefit response (23.8% and 4.8% respectively), and overall survival (5.65 and 4.41 months) compared to standard 5-FU treatment (Burris et al., 1997). Since then gemcitabine was used as a first line therapy for the locally advanced and metastatic

PDAC for several decades. In 2011, Conroy and colleagues showed that FOLFIRINOX (folinic acid, fluorouracil, irinotecan and oxaliplatin) prolonged overall median survival of patients about 4.3 months compared to the gemcitabine monotherapy in a large phase III trial conducted in France (Conroy et al., 2011). Two years later, an international phase III trial reported a significantly prolonged overall survival of metastatic PDAC patients with gemcitabine and nab-paclitaxel combination treatment compared to gemcitabine monotherapy (Von Hoff et al., 2013). However, the above mentioned treatment regimens have more side effects than gemcitabine monotherapy, and not all patients are eligible based on age, performance and nutritional status.

1.1.3 Initiation and progression

Oncogenic Kras mutation occurs in almost 95% of all human PDAC patients (Biankin et al., 2012; Jones et al., 2008; Kanda et al., 2012; Waddell et al., 2015; Witkiewicz et al., 2015). Kras mutations are also found in several other tumor entities including breast, endometrial, cervical, bladder, liver cancers and myeloid leukemia (Anderson et al., 1992; Bos et al., 1987; Downward, 2003; Schubbert et al., 2007). $Kras^{G12D}$ is the most common point mutation in PDAC in which glycine is replaced by aspartic acid in the twelfth codon. Mutation results in constitutional activation of Kras activity which further leads to accelerated proliferation, differentiation and survival via downstream signalling cascades (Campbell et al., 1998). Oncogenic Kras stimulates cell proliferation by activating serine/threonine protein kinase B-Raf (BRAF) and thus by simultaneous activation of mitogen-activated protein kinase kinase1/2 (MEK1/2), extracellular signal-regulated kinase (ERK) and ETS domain- containing protein Elk-1 (Elk-1). It mediates survival by concomitantly activating phosphoinositide 3 kinase (PI3K) – protein kinase B (AKT) and mammalian target of rapamycin complex 1 (mTORC1) pathway (Carpeño and Belda-iniesta, 2013). Oncogenic Kras is also known to stimulate cytokine production by activating serine/threonine protein kinase TBK1 (TBK1) which leads to nuclear translocation of nuclear factor kappa-light-chain-enhancer of activated B-cells (NF-KB) by releasing it from its inhibitory protein NFKBIA (NF-KB inhibitor α) (Carpeño and Belda-iniesta, 2013). Nuclear translocation of NF-KB ultimately leads to transcription of various cytokine including IL-6 (Ancrile, 2009; Ancrile et al., 2007; Leslie et al., 2010), IL-8 (Sparmann and Bar-Sagi, 2004) and Granulocyte-macrophage colony-stimulating factor (GM-CSF) (Pylayeva-Gupta et al., 2012). However, $Kras^{G12D}$ alone is not sufficient to initiate PDAC, and additional genetic events such as deletion or mutations

in tumor suppressor genes P53, INK4a, SMAD4, PTEN, Mist and transforming growth factor ß (TGF-ß) are required for progression to frank carcinoma (Guerra et al., 2007; Hahn et al., 1996; Hingorani et al., 2003; Morris et al., 2010). Moreover, inflammation induced by chronic pancreatitis in conjunction with Kras mutations also gives rise to pancreatic cancer as shown in genetically engineered mouse models (GEMMs) (Guerra et al., 2011).

Upon activation of oncogenic Kras signaling, acinar cells undergo a transition process called "acinar to ductal metaplasia" (ADM) in which the normal acinar cells lose the morphological and functional acinar characteristics (e.g. expression of amylase) and start to acquire the phenotypic and molecular properties of ductal cells. Subsequently, ADM further progress to pre-neoplastic lesions of PDAC - Pancreatic Intra epithelial Neoplasm (PanIN) (Morris et al., 2010). PanINs are by far the most common precursor to PDAC (Matthaei et al., 2011). The initial classification and nomenclature of PanINs as precursors for PDAC was established in 1999 (Klimstra and Longnecker, 1994).

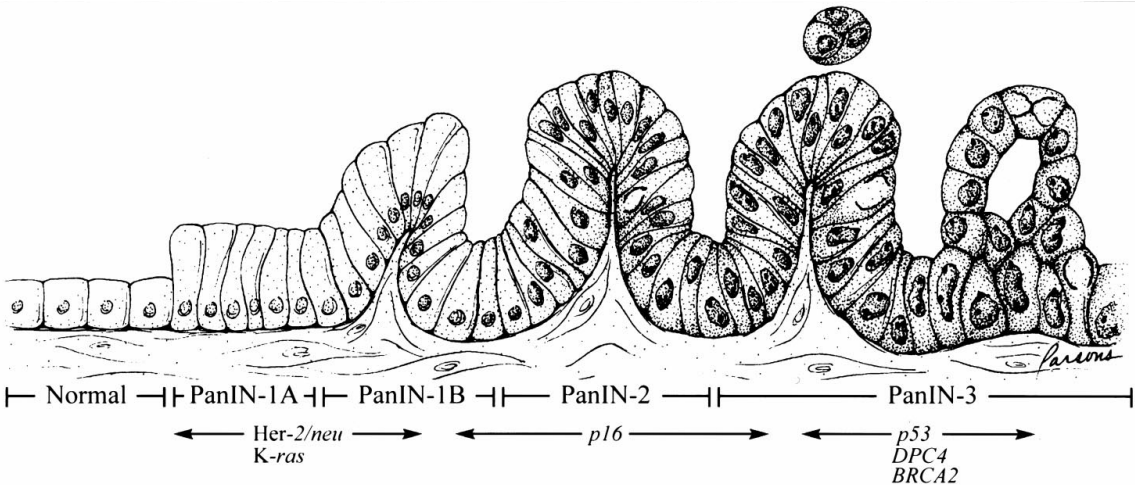

Figure 1: **Initiation and progression of PDAC.** Normal cuboidal (ductal) epithelial cells transform into tall columnar epithelium with basal nuclei which further attains pseudostratification and other cellular abnormalities. Based on the degree of atypia the pre-neoplastic lesions are classified from PanIN1-PanIN3. Throughout the progression multiple mutations are accumulated at various stages. (Figure adapted from Hruban et al., 2000).

During the progression of ADMs to PanINs, cells accumulate various cytological abnormalities including loss of polarity, nuclear crowding, mucinous cytoplasm and atypia. Based on the degree of cellular abnormalities, PanINs are further classified into three categories from PanIN1-3 (Hruban et al., 2004). PanINs cannot be detected in

patients by currently available imaging methods, and up to now it is not clear at which frequency PanIN lesions eventually progress to PDAC.

1.2 Significance of stroma in PDAC

Notably, pancreatic stellate cells (PSCs) are already activated during early PanIN progression resulting in a pronounced accumulation of extracellular matrix components such as collagen and hyaluronic acid (Neesse et al., 2011, 2015).

Invasive PDAC harbors a pronounced desmoplastic reaction, and the tumor stroma comprises more than 90% of the entire tumor mass. The acellular compartment of stroma is made up of dense extracellular matrix components and various secreted growth factors. The cellular compartment of the stroma is comprised of abundant infiltrating inflammatory cells, activated fibroblasts, and altered endothelial cells (Chu et al., 2007; Neesse et al., 2011). Conflicting results have been published regarding the role of the tumor stroma in PDAC. Though different components of stroma have been shown to confer progression, invasion and chemoresistance of PDAC, there are few studies suggesting that stroma plays a tumor-suppressive role in PDAC (Chu et al., 2007; Ellenrieder et al., 2000; Hessmann et al., 2018; Hidalgo and Eckhardt, 2001; Mccleary-Wheeler et al., 2012; Rhim et al., 2014). Recently, it was attempted to classify PDAC into subtypes based on stromal phenotypes (Collisson et al., 2011; Knudsen et al., 2017; Moffitt et al., 2015). Moffitt and colleagues have classified PDAC into basal (no stroma), normal and activated stromal subtypes and further assessed the survival of the respective subtypes using high throughput gene expression microarray analysis. In this study, the normal and activated stromal subtypes were differentiated by the expression of specific markers. The normal stroma expressed markers such as α- Smooth Muscle Actin (α-SMA), vimentin and desmin while the activated stroma was shown to express markers including secreted protein acidic and rich in cysteine (SPARC), chemokine (C-C motif) ligand 13, 18 (CCL13 and 18), gelatinase B and stromelysin 3. Additionally, there was a significant survival difference reported between these two stromal subtypes, in which the normal stromal subtype had a median survival of 24 months while the activated stromal subtype had a median survival of only 15 months (Moffitt et al., 2015).

1.2.1 Acellular compartment of stroma

The abundant extra cellular matrix (ECM) is composed of various soluble and non-soluble factors. The most abundant non-soluble constituents of the ECM are collagen

(type I, III and IV), laminin, fibronectin and hyaluronic acid (Thompson et al., 2010). Besides these solid components there are substantial number of soluble secreted factors such as connective tissue growth factor (CTGF), fibroblast growth factor (FGF), vascular endothelial growth factor (VEGF), platelet derived growth factor (PDGF) and TGF-ß (Apte et al., 2013; Feig et al., 2012; Gress et al., 1998; Lohr et al., 2001; Neesse et al., 2015; Ozawa et al., 2001). Apart from the above mentioned growth factors certain secreted proteins, which are collectively known as modulators of tumor - stroma interaction, are also abundantly found in the stromal compartment such as SPARC, periostin, thrombospondin and tenascin C (Baril et al., 2007; Esposito et al., 2006; Infante et al., 2007; Kanno et al., 2008; Lohr et al., 2001; Mantoni et al., 2008). The matrix metalloproteinases (MMPs) are a family proteolytic enzymes involved in multiple physiological functions including embryo implantation, development, angiogenesis, wound healing and tissue regeneration (Jabłońska-Trypuć et al., 2016). Among the big family of MMPs, MMP-2, MMP-9 and MMP-11 are known to be the crucial members of ECM composition (Iacobuzio-Donahue et al., 2003; Määttä et al., 2000; Qian et al., 2001; Shek et al., 2002; Vonlaufen et al., 2008a). Initially, MMPs were not only reported to facilitate metastatic spread by degrading the ECM barrier but also contributed to carcinogenesis (Chambers and Matrisian, 1997). The inflammatory cytokines (interleukin-1 (IL-1), interleukin-6 (IL-6) and tumor necrosis factor α (TNF-α)) and various growth factors (TGF-ß, FGF, EGF and PDGF) are reported to increase the expression of MMPs. Thus by secreting the above mentioned inflammatory growth factors, tumor cells influence stromal cells in a paracrine manner to secrete more MMPs (Noël et al., 2008).

1.2.2 Cellular compartment of stroma

During the development of PDAC, there are various cell populations which are either activated within the pancreas or recruited from distant sites. Among them, inflammatory cells, activated fibroblasts and PSCs, endothelial cells and neurons are pivotal elements (Ceyhan et al., 2008; Demir et al., 2015; Neesse et al., 2011).

Tumor associated macrophages (TAMs), myeloid derived suppressor cells (MDSC) and regulatory T cells are found to be the most abundantly recruited immune cell population in PDAC. The dynamics of immune cell recruitment from PanIN to PDAC has been investigated in GEMMs of PDAC and showed abundant immunosuppressive MDSC already during early PanIN stages (Clark et al., 2007). These immune populations

suppress T cell proliferation and response and were also shown to play a crucial role in tumor invasion by promoting ECM remodelling (Condeelis and Pollard, 2006; Hao et al., 2012; Pollard, 2004).

Activated fibroblasts or cancer associated fibroblasts (CAFs) are one of the most prominent cell populations within the tumor stroma. The majority of activated fibroblasts originate from PSCs. The resident fibroblasts of the pancreas are a sparse population which accounts for only 4% of total cells of the healthy pancreas (Apte et al., 1998; Bachem et al., 1998). PSCs are normally found in a quiescent state and are activated upon inflammatory or oncogenic stimuli from the pre- neoplastic or neoplastic cells. In turn, the activated PSCs produce abundant ECM and other growth factors to aid the neoplastic growth (Apte et al., 2004; Habisch et al., 2010; Kalluri and Zeisberg, 2006; Schäfer et al., 2012). Studies have reported that CAFs can also be derived from bone marrow (Direkze et al., 2004; Ishii et al., 2003). Additionally, tumor cells were also shown to mimic the phenotypic and molecular properties of activated fibroblasts in certain conditions (Kalluri and Zeisberg, 2006). Several studies have emerged that reveal the contribution of PSCs regarding ECM production, angiogenesis, invasion, metastasis and chemoresistance of PDAC (Erkan et al., 2009; Hessmann et al., 2018; Lohr et al., 2001; Schneiderhan et al., 2007).

1.3 Genetically engineered mouse models of PDAC

The development of GEMMs is a breakthrough in PDAC research. GEMMs are particularly useful for the investigation of the tumor stroma since tumorigenesis occurs within the normal pancreatic microenvironment. Compared to xenograft and orthotopic models, GEMMs are particularly useful to investigate the desmoplastic reaction and study the crosstalk between stromal- and tumor cells.

GEMMs are generated by genetic mutations in oncogenes and tumor suppressor genes that also occur in human PDAC. To this end, activating mutations of the Kras oncogene occurs most frequently in PDAC and is critical for tumor development. Therefore, GEMMs of PDAC are generated by introducing a $Kras^{G12D}$ mutation that is flanked by lox-stop-lox (LSL) sites and excised by Cre-recombinases that are driven under a pancreas-specific promoter such as Pdx or Ptf1a (p48) that are expressed early during embryogenesis. Additional inactivating mutations in various tumor suppressor genes

such as p53, SMAD4 or p16 can be combined to accelerate tumorigenesis (Aguirre et al., 2003; Ahmed et al., 2017; Bardeesy et al., 2006; Ijichi et al., 2006; Tuveson et al., 2006).

The LSL-Kras^{G12D}; Pdx or P48 Cre (KC) model was initially established by Hingorani et al., 2003 (Hingorani et al., 2003; Jackson et al., 2001). The KC model is considered as a slow progression model as mice develop ADM and PanIN lesions over the course of several months. These PanIN lesions highly resemble the precursor lesions found in the patients. Around 60% of mice develop invasive carcinoma between 10-15 months of age. Therefore, the KC model is best suited to study the disease initiation and progression.

The LSL-Kras^{G12D};Trp53^{172H};PdxCre (KPC) harbors an additional inactivating mutation of the p53 tumor suppressor gene that dramatically accelerates pancreatic tumorigenesis. Mice develop invasive pancreatic tumors between 3-6 months of age, and median survival is about 150 days (Hingorani et al 2005). Notably, KPC mice develop the full spectrum of PDAC including desmoplastic, locally invasive carcinoma, bile duct obstruction, ascites, cachexia and liver and lung metastasis. Therefore, the KPC model is appropriate to test response to novel therapies in preclinical studies and is currently the most frequently used GEMM of PDAC.

1.4 Stromal targeting in PDAC

Many preclinical studies and clinical trials have attempted to target different components and pathways of the tumor stroma as a therapeutic option. Though these anti-stromal approaches have shown promising results at the experimental level, they all failed in clinical trials (Bramhall et al., 2001, 2002), and there is currently no approved anti-stromal treatment for PDAC patients. For instance, Hedgehog (Hh) signalling is one of the central regulators of tumor-stroma crosstalk which is shown to contribute to desmoplasia in various tumor entities (Thayer et al., 2003). Following an inflammatory or oncogenic stimuli, pancreatic epithelial cells express Hedgehog ligands (Fendrich et al., 2008; Thayer et al., 2003). In PDAC, Hh signalling has been shown to work in a paracrine manner in which Hh-ligands released by epithelial tumor cells affect the surrounding stromal cells and thus mediates desmoplasia (Lauth et al., 2010; Lee et al., 2014; Yauch et al., 2008). In 2009, Olive and colleagues have successfully depleted stromal deposition in a GEMM of PDAC by inhibiting Hh-signalling using a pharmacological inhibitor (IPI-926). The authors reported that co-administration of IPI-926 and gemcitabine led to a significant increase of intra- tumoral gemcitabine

accumulation and increased vascular density, and thus reduced the tumor growth. In contrast, four years later Rhim and colleagues showed that genetic inhibition of sonic hedgehog in a GEMM resulted in accelerated tumor growth with more aggressive tumor biology including undifferentiated histology, increased vascularity and proliferation of the tumors (Rhim et al., 2014).The data by Rhim et al explain the clinical failure of Hh-inhibitors such as IPI-929. In the same year, Özdemir et al. depleted α-SMA positive myofibroblasts in a GEMM of PDAC. In line with Rhim et al, this preclinical study revealed increased tumor invasiveness and aggressiveness upon myofibroblast depletion. Furthermore, myofibroblast depleted tumor showed pronounced epithelial to mesenchymal transition (EMT) features and an increased amount of cancer stem cells. Additionally, the authors also showed a correlation between decreased myofibroblast content and reduced survival in the patients (Özdemir et al., 2014).

Hyaluronic acid (HA) is one of the major stromal components of PDAC which has been shown to be correlated with poor survival (Whatcott et al., 2015). In preclinical experiments, HA depletion by the hyaluronidase PEGPH20 was shown to increase drug delivery and therapeutic efficacy of gemcitabine (Jacobetz et al., 2013; Provenzano et al., 2012; Singha et al., 2015). In a phase II clinical trial (HALO 202) PEGPH20 was combined with nab-paclitaxel/gemcitabine compared to the standard therapy nab-paclitaxel/gemcitabine to assess the therapeutic efficacy of HA depletion in PDAC patients (Hingorani et al., 2018). The results have shown that the highest benefit was achieved in PDAC patients with high intratumoral HA levels where an objective response rate of 45% vs 31%, and overall survival of 11.5 vs 8.5 months was achieved compared to the control group (Hingorani et al., 2018). Currently, PDAC patients with high HA-expression are enrolled in a phase III trial to confirm the therapeutic potential of HA-depletion in PDAC patients (NCT02715804).

1.5 Secreted Protein Acidic Rich in Cysteine (SPARC)

SPARC, also known as osteonectin or BM-40 is a 32kDa, albumin and calcium binding matricellular protein (Sage et al., 1984), and belongs to a family of eight proteins (Bradshaw, 2012). Secreted modular calcium binding protein (SMOC) 1 and 2 (Vannahme et al., 2002, 2003), hevin (SPARC like 1) (Hambrock et al., 2003), testican 1, 2 and 3 (commonly known as SPOCK) (Alliel et al., 1993; Charbonnier et al., 1998; Schnepp et al., 2005; Vannahme et al., 1999) and folistatin like protein 1 (Hambrock et al., 2004) are the other members of the family.

Originally, SPARC has been identified as a bone specific protein which is reported to aid in mineralization of collagen (Termine et al., 1981). Unlike the typical structural proteins of the ECM (collagen, fibronectin and laminin), SPARC plays a non-structural role by serving as a mediator of cell-matix interaction (Brekken and Sage, 2000; Lane and Sage, 1994).

1.5.1 Structure and biochemistry

Human SPARC protein is encoded by a single copy gene located on chromosome 5q33.1. SPARC protein consists of three modular domains which are the acidic NH_2-terminal domain (amino acid (aa) 1-52), the follistatin like domain (aa 53-137), and the C-terminal calcium binding domain (aa 138-286) (Hohenester et al., 1996; Lane and Sage, 1994; Martinek et al., 2002).

The NH_2-terminal domain (domain I) includes a 17aa signal peptide rich in aspartic and glutamic acid residues. Domain I of SPARC has been shown to bind Calcium^{2+} ions with low affinity and also to interact with hydroxyapatite (bone mineral) (Maurer et al., 1992; Romberg et al., 1985). Depending on the availability of Ca^{2+}, this domain has been shown to bind a maximum of 8 Ca^{2+} ions (Maurer and Hohenester, 1997). However, functions of the domain I are not completely calcium dependant (Lane et al., 1992). Specific sequences of domain I distinguish SPARC from other members of the SPARC like protein family.

Domain II of SPARC is rich in cysteine and is named as follistatin-like (FS) domain due its high homology with follistatin (a peptide which inhibits the secretion of follicle stimulating hormone) (Esch et al., 1987; Patthy, 1991). However, SPARC does not mimic the inhibitory function of follistatin against avtivin-A (Maurer et al., 1992). A synthetic peptide derived from follistatin-like domain (domain II) termed as peptide 2.1

(aa 55-74) has exhibited an inhibitory effect on cell cycle progression similar to original SPARC protein in specific cell type such as bovine aortic endothelial cells (Funk and Sage, 1991). Another synthetic peptide derived from domain II (peptide 2.3-aa 113-130) has exhibited copper binding property due to the presence of Gly-His-Lys (GHL) residues (Funk and Sage, 1993; Lane T. F and Sage Helene., 1994; Vernon and Sage, 1989). Peptide 2.3 has been also shown to promote proliferation (in fibroblasts), angiogenesis and wound healing (Pickart and Lovejoy, 1987; Pickart et al., 1980).

The extracellular domain (EC domain or domain III) is highly conserved in SPARC of different species and among other members of the SPARC protein family. The EC domain of SPARC possesses the binding site for collagen type I and IV, and the two EF-hands of the EC domain exhibit high affinity to calcium (Engel et al., 1987; Hohenester et al., 1997). Peptide 4.2 belongs to domain III (aa 254-273) and has been reported to impede the proliferation of endothelial cells (Kupprion et al., 1998; Motamed and Sage, 1998). The structure and domains of SPARC are depicted in **Figure 2.**

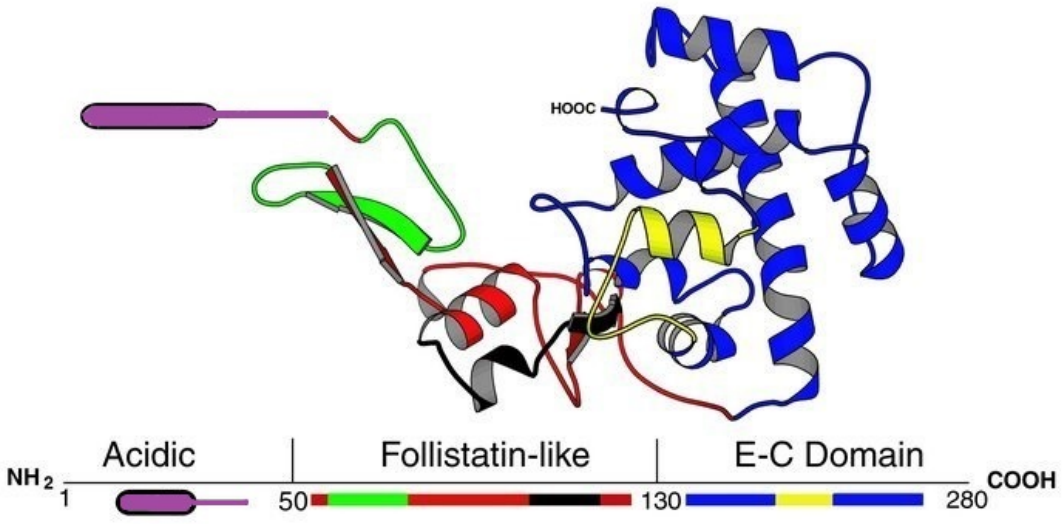

Figure 2: **Structure of SPARC protein.** Three domains of the SPARC protein, NH_2 domain I, follistatin like domain and the extracellular Ca^{2+} binding domain are shown in purple, red and blue,respectively.Peptide2.1, peptide2.3 and peptide 4.2 are shown in green, black and yellow, respectively. Picture adapted from Brekken and Sage, 2000.

There are certain domain and tissue specific post translational modifications such as glycosylation (Asn 99-domain II), crosslinking between transglutaminases or disulfide crosslinking between SPARC that give rise to structural heterogeneity of SPARC.

The heterogeneity in the protein structure allows SPARC to bind a wide range of proteins including different collagen subtypes (Kelm and Mann, 1991; Zhou et al., 1998). Additionally, certain structural similarities between SPARC family proteins explain their similar physiological roles (Bornstein, 1995).

1.5.2 SPARC and ECM

SPARC is a modulator of ECM whose expression is reported to be associated with increased ECM deposition (Framson and Sage, 2004). SPARC binds to various structural and non-structural proteins of the ECM including collagen (type I, II, III, IV, V and VIII) (Maurer et al., 1992; Sage et al., 1989; Termine et al., 1981), vitronectin (Rosenblatt et al., 1997) and thrombospondin (Clezardin et al., 1988). Collagen is one of the predominant components of the ECM which plays a significant role during embryonic development. The proper assembly and folding of collagen is mandatory for the biophysical and biochemical functions maintaining the homeostasis of the basal lamina and various connective tissues (Martinek et al., 2006). There are various molecular chaperons that are involved in the folding, assembling and maturation of collagen. Among them, heat-shock protein 47 (HSP47) is one of the best studied molecular chaperons of collagen whose homozygous deletion results in prenatal lethality in mice (Poschl, 2004). SPARC is a molecular chaperon of collagen due to its ability to bind to the triple helical domains of collagen. In concert with HSP47, SPARC mediates stability of collagen before its secretion from the endoplasmic reticulum (Martinek et al., 2006; Wang et al., 2005). Consistently, Fisher et al., have shown co-expression of HSP47 and SPARC during high collagen synthesis. However, unlike HSP47, homozygous SPARC knock out is not lethal in mice. It has been reported that the type I collagen fibrils of SPARC null mice are smaller than that of SPARC wildtype mice fibrils confirming the participation of SPARC in collagen folding and maturation (Bradshaw et al., 2003). Unlike HSP47, SPARC is thought to be still bound to procollagen during post endoplasmic reticulum (ER) events thus preventing side-to-side aggregation of procollagen (Martinek et al., 2006). The contribution of SPARC in collagen folding, fibrillogenesis and deposition is shown in Fig. 3.

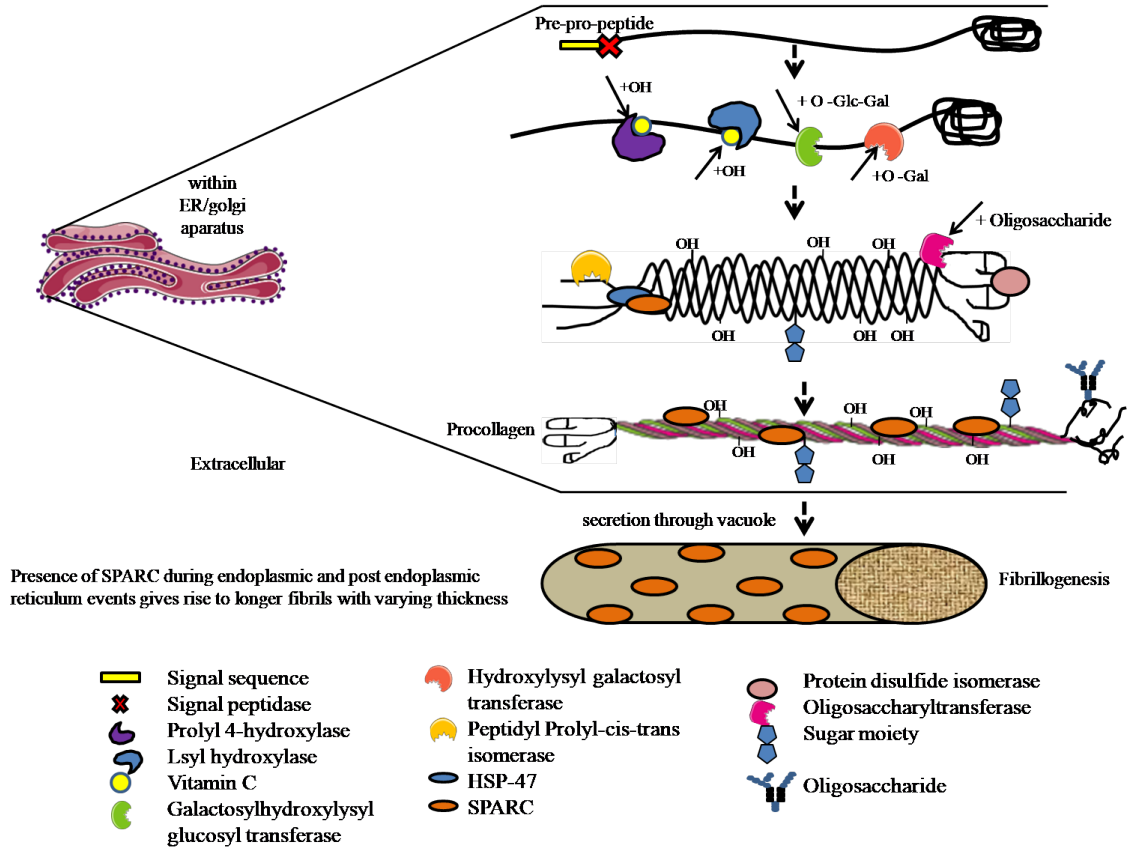

Figure 3: **A model showing the contribution of SPARC during endoplasmic and post-endoplasmic events in collagen fibrillogenesis.** SPARC mediates proper folding of collagen together with HSP47, a known molecular chaperon of collagen. Unlike HSP47, SPARC is still bound to procollagen upon secretion and thus prevents self-aggregation of premature collagen which ultimately leads to the formation of mature and thicker collagen fibrils.

Studies have also discussed various other possibilities by which SPARC maintains collagen homeostasis by interacting with intracellular components like Integrin linked protein kinase (ILK) or by regulating the activity matrix metalloproteinases and certain growth factors (Martinek et al., 2006). Studies have also shown the significance of fibronectin assembly at the cell surface in collagen fibrillogenesis (Robinson et al., 2004). There are certain ligands and receptors such as α2β1 integrin ligand, fibronectin and discoidin domain receptor 2 (DDR2) which are reported to share their binding site on collagen (aa 600-800) with SPARC (Carafoli et al., 2009; Ingham et al., 2002; Wang et al., 2005; Xu et al., 2000). In 2005, Barker and colleagues have shown a direct interaction between SPARC and ILK and they further claimed that SPARC modulates many signaling pathways including TGF-ß by acting as a counter-adhesive molecule. Additionally, SPARC has also been shown to regulate collagen fibrillogenesis by

regulating the activity of decorin, an important proteoglycan involved in collagen fibrillogenesis (Barker et al., 2005).

1.5.3 SPARC and growth factor signalling

SPARC has been reported to interact with various secreted growth factors such as PDGF, VEGF, TGF-ß and basic fibroblast growth factor (bFGF) (Francki et al., 1999b; Hasselaar and Sage, 1992; Kupprion et al., 1998; Raines et al., 1992). Thus, SPARC mediates a wide range of physiological functions by altering ECM organization and by interacting with intracellular growth factor signalling (Funk and Sage, 1991; Tremble et al., 1993; Yan and Sage., 1999). SPARC has been shown to bind PDGF and VEGF directly and thus preventing the ligand binding which further results in inactivation of the respective receptors and receptor mediated cellular functions. SPARC reduced the PDGF and VEGF mediated proliferation in human arterial vascular smooth muscle cells and microvascular endothelial cells, respectively (Kupprion et al., 1998; Raines et al., 1992). SPARC has been also described to regulate the TGF-ß signalling pathway (Francki et al., 1999a; Schiemann et al., 2003). There is a mutual regulatory feedback loop that was identified between SPARC and TGF-ß due to the ability to regulate each other's expression (Bassuk et al., 2000; WRANA et al., 1991). Unlike the direct interaction of SPARC with other growth factors, SPARC does not directly bind bEGF. However, an inhibitory effect against bFGF mediated migration of endothelial cell was reported (Hasselaar and Sage, 1992).

1.5.4 SPARC in cancer

Overexpression or loss of SPARC has been reported in many human tumor entities including breast, colon, oesophageal cancers and melanoma (Sato et al., 2003). SPARC seems to play pro-tumorigenic role in certain cancers such as non-small cell lung cancer, melanoma, glioblastoma while it has been ascribed a tumor suppressive role in other cancers such as colorectal, ovarian, acute myelogenous leukemia and prostate cancers (Chlenski et al., 2002; Dhanesuan et al., 2002; Fernanda Ledda et al., 1997; Koblinski et al., 2005; Koukourakis et al., 2003; Said et al., 2013; Shin et al., 2013; Suzuki et al., 2005; Yiu et al., 2001).

1.5.5 SPARC in PDAC

In PDAC, SPARC is highly expressed by peritumoral fibroblasts, while there is merely any expression in the tumor cell itself. Furthermore, high expression of SPARC in the stromal compartment was correlated with poor prognosis in PDAC patients (Infante et al., 2007; Mantoni et al., 2008). The loss of SPARC in epithelial tumor cells is associated with hypermethylation of the SPARC promoter. In particular, hypermethylation of the CPG-2 region is closely associated with pathophysiological conditions of the pancreas such as pancreatitis and PDAC (Gao et al., 2010; Sato et al., 2003). Different *in vitro* and *in vivo* studies have reported both tumor suppressive and tumor promoting roles of SPARC in PDAC. For instance, the tumor suppressive role of SPARC was shown by the study of Chen and colleagues, in which the authors reported a reduced growth and migration of PDAC cell lines in the presence of exogenous SPARC. Furthermore, a correlation between endogenous SPARC expression and reduced tumor aggressiveness was reported in a xenograft mouse model (Chen et al., 2010). In 2004, a study performed by Puolakkainen et al. revealed the complex nature of SPARC in tumorigenesis. Using subcutaneously implanted tumors in SPARC deficient mice, the authors reported an accelerated tumor growth which was associated with reduced ECM deposition and reduced apoptosis of tumor cells (Puolakkainen et al., 2004).

Contradicting the above studies, SPARC also has been shown to play a protumorigenic role. Guweidhi et al., provided evidence that upon exogenous SPARC treatment Colo-357 (low endogenous SPARC expression) cells exhibited an increased invasiveness *in vitro*. Similarly, inhibition of endogenous SPARC in PANC-1 (high endogenous SPARC expression) resulted in diminished invasion. Moreover, exogeneous SPARC treatment resulted in increased invasiveness of PDAC cell lines with parallel overexpression of MMP-2 (Guweidhi et al., 2005). Another study has revealed a negative correlation between stromal SPARC expression and overall survival of PDAC patients (Mantoni et al., 2008).

Importantly, the role of peritumoral SPARC has not been assessed in appropriate experimental models that recapitulate the pronounced tumor microenvironment. To this end, GEMMs of PDAC seem to be particularly suited to investigate the role of stromal derived SPARC in PDAC.

1.6 Aim of the study

Abundant collagen and HA deposition is a hallmark feature of the tumor microenvironment in PDAC. Several preclinical studies suggest that pharmacological depletion of collagen (e.g. by losartan) and HA (by PEGPH20) relieves vessel compression thus improving drug delivery and therapeutic response (Chauhan et al., 2013; Diop-Frimpong et al., 2011; Jacobetz et al., 2013; Provenzano et al., 2012). In contrast, recent evidence in several GEMMs casted serious doubt on the stromal depletion strategy since preclinical results have shown that pancreatic tumors become more aggressive, invasive and undifferentiated upon genetic or pharmacological inhibition of pro-stromal signaling pathways such as the SHH-pathway (Özdemir et al., 2014; Rhim et al., 2014). Therefore, stromal reprogramming rather depletion has become a novel approach to attempt to normalize tumor stroma rather than deplete it (Neesse et al., 2013; Sherman et al., 2014). To achieve this, a detailed knowledge of pro-tumorigenic and tumor-suppressive properties of the tumor stroma is required. Indeed, detailed molecular studies have identified first features of CAFs that distinguish between tumor promoting and tumor suppressive functions (Öhlund et al., 2017).

In my thesis, I aim to examine the role of SPARC in PDAC. SPARC is overexpressed in human and murine CAFs in the tumor stroma of PDAC, whereas it is hardly expressed in preneoplastic and neoplastic cells. A recent study by Moffitt et al. provided first evidence that SPARC is an important marker of the activated tumor stroma in PDAC patients that is associated with a significantly shortened survival (Moffitt et al., 2015). However, it is not known whether and how peritumoral SPARC contributes to disease progression in PDAC. Furthermore, as SPARC is part of the activated tumor stroma and has been implicated in collagen deposition and remodelling, I hypothesize that genetic ablation of SPARC in a GEMM of PDAC may reprogram the tumor stroma, slowing down tumor progression and increasing drug accumulation and efficacy by collagen remodelling.

To address this hypothesis, I crossed the KC model with a germ-line SPARC knock-out mouse. This mouse model allowed me to address the impact of SPARC during different stages of PanIN and tumor development, as well as metastasis formation. Furthermore, this model allows to conduct preclinical assays to investigate the role of SPARC dependent collagen remodelling on drug delivery and efficacy.

2. Materials

2.1 Technical instruments

Equipment	Company
Agarose gel electrophoresis chamber-Model 40-0911	Peqlab Biotechnologie GmbH, Erlangen, Germany
Arium®pro ultrapure water system	Sartorius, Göttingen, Germany
Aspirator with trap flask	Grant Instruments Ltd, Cambs, England
Autoclave	TecnomaraIntegraBiosciences, Deutschland GmbH
Autoclave (heat sterilization)	SHP Steritechnik AG, Haldensleben, Germany
Centrifuge (Universal 320R)	Hettich lab technology, Tuttlingen, Germany
Centrifuge - Perfect spin 24 plus (Prism R)	Peqlab Biotechnologie GmbH, Erlangen, Germany
Centrifuge (HeraeusMultifuge X1R)	Thermo Fisher scientific, Waltham, USA
Cellometer®Auto 1000 cell counter	Nexcelom Bioscience, Lawrence, MA
Class II safety cabinet (S2020 -1.2)	Thermo Fisher scientific, Waltham, USA
Cold plate (Histocore Arcadia c)	Leica Biosystem, Wetzlar, Germany
Flex cycler block	Analytikjena Germany
Molecular Imager®Chemidoc™XRS System	Bio-rad Hercules USA
Heating plate	Leica Biosystem, Wetzlar, Germany
HERAcell 240i CO_2 incubator	Thermo Scientific, Waltham, USA
Ice flaker (AF80)	Scotsman, Edinburgh, UK
INTAS- ECL Chemocam imager	INTAS Science Imaging Instruments GmbH, Göttingen, Germany
Inverted live cell microscope DMi8 automated	Leica Microsystems GmbH, Wetzlar, Germany
Inverted microscope (CKX53SF)	Olympus, Tokyo, Japan
Light microscope "BX43"	Olympus, Tokyo, Japan
Magnetic stirrer (RH B S000)	IKA®Laboratory equipment, Germany
Microplate Luminometer "LUMO"	Autobiolabtec Instruments Co.,Ltd, Zhengzhou, China
Microplate reader "PHOmo"	Autobiolabtec Instruments Co.,Ltd, Zhengzhou, China
Microwave (NN-E209W)	Panasonic; Japan
Microtome (Leica RM2265)	Leica Biosystems, Wetzlar, Germany
Mini centrifuge (SPROUT ™)	HealthrowScientific®LLC, Illinois, USA
Mini gel tank (A25977)	Invitrogen Thermo Fisher scientific, Waltham, USA
Mini-water bath	Bodo Schmidt GmbH, Göttingen, Germany
Multi-functional orbital shaker (PSu-20i)	Grant Instruments Ltd., Cambs, England
Multipipette®plus	Eppendorf AG Hamburg, Germany
Paraffin Tissue embedder (EG1150H)	Leica Biosystems, Wetzlar, Germany

pH meter (FiveEasy™ Plus FEP20)	Mettler-Toledo AG, Schwerzenbach, Switzerland
Pipetus®Akku	Hischmann, Laborgerate, Eberstadt, Germany
Pipetor – pipetboyacu 2	Integra Biosciences, Zizers, Switzerland
Pipettes Research series	Eppendorf AG Hamburg, Germany
PowerPac™ HC	Bio-rad Hercules USA
Refrigerator 4°C (Comfort)	Liebherr, Bulle, Switzerland
Shandon coverplate™ (cadenza system)	Thermo Scientific, Waltham, USA
Sequenza™slide rack(cadenza system)	TED PELLA,INC, Redding, CA
T100™Thermal cycler	Bio-rad Hercules USA
Thermo mixer compact	Eppendorf AG Hamburg, Germany
Universal oven UF260	MemmertGmbH+Co. KG, Schwabach, Germany
Universal oven UF55 pa	MemmertGmbH+Co. KG, Schwabach, Germany
Vacuum pump	VacuubrandGmbH+Co. KG, Wertheim, Germany
Vortex (MS1)	IKA®works do BrasilLtda, Taquara, Brazil
Vortex (REAX1)	HeidolphInstruments GmbH & Co. KG, Schwabach, Germany
Waterbath (WNB14)	MemmertGmbH+Co. KG, Schwabach, Germany
Weighing balance	Sartorius AG, Göttingen, Germany
-20°C freezer	Liebherr, Bulle, Switzerland
-80°C Ultra low temperature freezer (MDF-U54V)	Sanyo electric Co.,Ltd Japan
Tissue dehydration machine (automated)	Leica Biosystems, Wetzlar, Germany

2.2. General consumables

Goods	Company
Aluminium foil	Carl Roth GmbH Co. KG, Karlsruhe, Germany
Centrifuge tube 15 and 50 ml	Sarstedt, Nümbrecht, Germany
Cell strainer-100µm	Falcon, Durham, USA
Cell scrapper	Sarstedt, Nümbrecht, Germany
Cello meter counting chamber	Nexcelom Bioscience, Lawrence, MA
Cryo pure vial	Sarstedt, Nümbrecht, Germany
Combitips advanced (Multipipette tips)	Starlab International GmbH, Hamburg, Germany
Graduated sterile pipettes (2,10,25 and 50ml)	Greiner bio-one, Frickenhausen, Germany
Glass coverslips (24×32, 24×60)	Menzel Gläser®, Menzel GmbH+Co KG, Braunschweig, Germany
Micropipette filter tips	Starlab International GmbH, Hamburg, Germany

Micropipette tips	Starlab International GmbH, Hamburg, Germany
Microtome blade (S35)	Feather safety Razer Co. Ltd, Osaka, Japan
Microtube (1.5 and 2ml)	Sarstedt, Nümbrecht, Germany
Injection needle (Sterile)	B.Braun, Melsungen, Germany
Nitrocellulose membrane	GE Healthcare lifesciences, Marlborough, USA
Parafilm	Pechiney plastic packaging, Chicago, USA
PCR tubes	Sarstedt, Nümbrecht, Germany
Scalpel	Feather safety Razer Co. Ltd, Osaka, Japan
Serological pipette (2ml)	Greiner bio-one, Frickenhausen, Germany
Sponge Pad ForXCell IITM Blotting	Novex by Life technologies, Carlsbad, CA
Superfrost glass slides (Histology)	Thermo Scientific, Waltham, USA
Syringe (1ml)	BD Plastic, Madrid, Spain
Syringe (5,10,20ml)	B.Braun, Melsungen, Germany
Sterile syringe Filter (0.2µm)	Labsolute, Th.Geyer ingredients GmbH & Co.KG, Höxter, Germany
Tissue culture multiwell plates	Greiner bio-one, Frickenhausen, Germany
Tissue culture flasks	Greiner bio-one, Frickenhausen, Germany
Tissue culture dishes (2cm, 10cm)	Sarstedt, Nümbrecht, Germany
Tissue cassette	Sanowa, Leimen, Germany

2.3 Chemicals

2.3.1 General chemicals

Chemical	Company
Albumin standard	Thermo Scientific, Waltham, USA
Acetic acid	Sigma-Aldrich, St. Louis, USA
Agarose	Biozym Scientific GmbH, Oldendorf, Germany
Aqua	B.Braun, Melsungen, Germany
BSA	Serva, Heidelberg, Germany
β-Mercaptoethanol	Merck, Darmstadt, Germany
Boric acid	Merck, Darmstadt, Germany
Calcium chloride	Applichem, Darmstadt, Germany
Citric acid monohydrate	Carl Roth GmbH Co. KG, Karlsruhe, Germany
EDTA	Acros organics, Geel, Belgium
EGTA	Sigma-Aldrich, St. Louis, USA
Ethanol	ChemSolute®, Th.Geyer ingredients GmbH & Co.KG, Höxter, Germany
Eosin	Sigma-Aldrich, St. Louis, USA
Formaldehyde (4%)	Merck, Darmstadt, Germany
HEPES	Carl Roth GmbH Co. KG, Karlsruhe, Germany

Glycerol	Carl Roth GmbH Co. KG, Karlsruhe, Germany
Hematoxylin	Sigma-Aldrich, St. Louis, USA
HCl	Carl Roth GmbH Co. KG, Karlsruhe, Germany
H_2O_2	Carl Roth GmbH Co. KG, Karlsruhe, Germany
Isofluran	AbbVie Deutschland GmbH & Co. KG, Ludwigshafen, Germany
Magnesium chloride	Applichem, Darmstadt, Germany
Methanol	Carl Roth GmbH Co. KG, Karlsruhe, Germany
Non-fat milk powder	Carl Roth GmbH Co. KG, Karlsruhe, Germany
PBS (Dulbecco's)	Biochrom, Berlin, Germany
PMSF	Sigma-Aldrich, St. Louis, USA
Roticlear	Carl Roth GmbH Co. KG, Karlsruhe, Germany
Rotimount	Carl Roth GmbH Co. KG, Karlsruhe, Germany
Saline (0,9% NaCl)	B.Braun, Melsungen, Germany
Sodium chloride	Merck, Darmstadt, Germany
Sodium citrate	Sigma-Aldrich, St. Louis, USA
Sodium fluoride	Sigma-Aldrich, St. Louis, USA
Sodium hydroxide	Acros organics, Geel, Belgium
Sodium Orthovanadate	Sigma-Aldrich, St. Louis, USA
Sodium pyrophosphate	Sigma-Aldrich, St. Louis, USA
Sodium pyruvate	Gibco® Thermo scientific, Waltham, USA
Tris-HCl	Carl Roth GmbH Co. KG, Karlsruhe, Germany
Tris-base	Carl Roth GmbH Co. KG, Karlsruhe, Germany
Triton X-100	Sigma-Aldrich, St. Louis, USA
Tween-20	Sigma-Aldrich, St. Louis, USA

2.3.2 Special chemicals and reagents

Chemical or reagent	Company
Coomassie blue G-250	Thermo scientific, Rockford, USA
DAPI mounting medium	Vector laboratories, Burlingame, CA
DMEM	Gibco® by Life technologies ltd, Paisley, UK
Fast SYBR Green Master mix	Thermo scientific, Rockford, USA
FBS	Gibco® by Life technologies ltd, Paisley, UK
Gemcitabine hydrochloride	Sigma Aldrich, St. Louis, USA

HBSS 1x	Gibco® by Life technologies ltd, Paisley, UK
LiberaseTL Research grade	Roche, Basel, Switzerland
MEM AA solution (50x)	Gibco® by Life technologies ltd, Paisley, UK
MEM NEAA solution (50x)	Gibco® by Life technologies ltd, Paisley, UK
Midori green	Nippon genetics Europe GmbH, Germany
MTT reagent	Sigma Aldrich, St. Louis, USA
NuPAGE 4-12% Bis-Tris gel	Invitrogen by Thermo scientific, Carlsbad, CA
Penicillin/streptomycin	Gibco® Thermo scientific, Waltham, USA
RNA later® RNA stabilization reagent	Qiagen GmbH, Hilden, Germany
SBTI	Sigma Aldrich, St. Louis, USA
Trypsin EDTA (0.5%)	Gibco® Thermo scientific, Waltham, USA
Protease inhibitor cocktail (25x complete)	Roche, Basel, Switzerland
Dulbecco's PBS 1x	Gibco® Thermo scientific, Waltham, USA

2.4 Buffers and solutions

2.4.1 Buffers for primary cell isolation

Wash Buffer pH 6

Component	For 1000ml
HBSS	770 ml
HEPES (1M)	3.3 ml
MEM Amino Acids (50x)	20 ml
MEM NEAA (100x)	10 ml
Sodiumpyruvate (100mM)	10 ml
Trisodiumcitrate (0,68M), pH7.6	10 ml
Glycerol	2.1 ml
Magnesium chloride (200mM)	135 µl
Calcium chloride (100mM)	80 µl
H2O	Make up to 1L

Digestion buffer

Component	For 100ml
Wash Buffer pH 6	97.5 ml
Liberase1 (5mg/ml)	2 ml
SBTI (50 mg/ml)	0.5 ml

2.4.2 Buffers for genotyping

Alkaline lysis buffer pH 12

Component	Concentration
NaOH	25 mM
EDTA	0.2mM

Neutralization buffer pH 5

Component	Concentration
Tris. HCl	40mM

TBE buffer (10X) pH 8.0

Component	For 1000ml
Tris	108g
Boric acid	55g
EDTA	7,44G
H_2O	Make up to 1L

2.4.3 Buffers for Western blot

Protein lysis buffer

Component	Concentration
HEPES pH 7.5-7.9	50mM
NaF	100mM
$Na_4O_7P_2 \times 10\ H_2O$	10mM
NaCl	150mM
EGTA	1mM
Glycerin	10%
Triton X-100	1%

Readymade Buffers

Stock	Working solution	Company
NuPAGE® LDS Sample buffer (4x)	1:4 dilution+10% β-ME	Invitrogen by Life Technologies, Carlsbad, CA
NuPAGE®MOPS SDS Running buffer (20x)	1:20 dilution in distilled water	Invitrogen by Life Technologies, Carlsbad, CA
NuPAGE®Transfer buffer (20x)	1:20 dilution in distilled water+10% methanol	Invitrogen by Life Technologies, Carlsbad, CA

Wash Buffer

PBS+0.1% Tween-20 (PBS-T)

Blocking solution

Component	Concentration
PBS-T	1x
Non-fat milk	5%

2.4.4 Buffers for Immunohistochemistry

Citrate buffer pH 6.0

Component	Concentration
Citric acid monohydrate	2.1g
H_2O	Make up to 1L

TE buffer pH 9.0

Component	Concentration
EDTA (1mM)	0.372g
Tris	1.211g
H_2O	Make up to 1L

TBS

Component	Concentration
Tris-HCl pH 7.4	50mM
NaCl	150 mM

TBS-T

TBS+0.1% Tween-20

Blocking solution

10% Goat serum+1% BSA in TBS-T

2.5 Kits

Name	Company
DNeasy® Blood and Tissue kit	Qiagen, Hilden, Germany
ImmPACT™DAB Peroxidase Substrate kit (SK4105)	Vector laboratories, Burlingame, CA
KAPA 2G fast HS	KAPA Biosystems, MA, USA
Masson trichrome staining kit	Polysciences

M.O.M™ Kit (BMK-2202)	Vector laboratories, Burlingame, CA
Picrosirius red stain kit	Polysciences, Germany
Peroxidase Goat IgG kit (PK-4005)vectastain ABC kit	Vector laboratories, Burlingame, CA
Peroxidase Mouse IgG kit (PK- 4002)vectastain ABC kit	Vector laboratories, Burlingame, CA
Peroxidase Rabbit IgG kit (PK- 4001)vectastain ABC kit	Vector laboratories, Burlingame, CA
Peroxidase Rat IgG kit (PK-4004)vectastain ABC kit	Vector laboratories, Burlingame, CA
Western Lighting®Plus-ECL	PerkinElmer, Inc., Waltham, USA

2.6 Primers

Genotype primers

Gene name	Sequence (5'-3')
Cre (p48) forward	TGCTGTTTCACTGGTTATGCGG
Cre (p48) reverse	TTGCCCCTGTTTCACTATCCAG
K-ras mut forward	AGCTAGCCACCATGGCTTGAGTAAGTCTGCG
K-ras mut reverse	CCTTTACAAGCGCACGCAGACTGTAGA
SPARC Common forward	TTCTTCCTTGCAACCCTCTC
SPARC wild type reverse	TGTGGAGCTTCCTCTGTCCT
SPARC Mutant reverse	GGGGTTTGCTCGACATTG
1lox <K-ras> G12D forward	GGG TAG GTG TTG GGA TAG CTG
1lox <K-ras> G12D reverse	TCCGAATTCAGTGACTACAGATGTACAGAG

2.7 Antibodies

2.7.1 Primary antibodies

Antibody	Company	Ref. Number	Clone	Dilution	
				IHC	WB
α-SMA	Dako	M0851	Clone 1A4	1:100	
Cytidine deaminase	Abcam	Ab82346		1:100	
CD31	BD Pharmingen	553370		1:100	
CD45	BD Biosciences	550539		1:20	
Cleaved Caspase-3	Cell signaling	#9664L	(D175)(5A1E)	1:100	
Collagen I	Abcam	ab21286		1:100	
CollagenIV	Abcam	ab19808		1:800	1:1000
E-Cadherin	BD Biosciences	BD610181			1:1000
HSP-90	Cell signaling	48755	E289		1:1000
Hyaluronic acid	Calbiochem	385911		1:100	

binding protein					
Ki-67	Thermo scientific	RM-9106-50	SP 6	1:200	
NT5c1A	Assay biotech company.Inc	C15296		1:100	
Pan-cytokeratin	Abcam	ab6401	PCK-26	1:700	
SPARC	R&D Systems	AF942		1:200	1:2000

2.7.2 Secondary antibodies for western blot

Name	Company	Ref. Number	WB	IHC
Rabbit anti-Goat (IgG)-HRP	Dako	P0449	1:2000	
Rabbit anti-Mouse (IgG)-HRP	Dako	P0161	1:2000	
Rabbit anti-Rat (IgG)-HRP	Dako	P0450	1:2000	
Swine anti-Rabbit (IgG)-HRP	Dako	P0217	1:2000	
Biotinylated anti-Goat IgG	Vectastain ABC kit	PK-4005		1:200
Biotinylated anti-Mouse IgG	Vectastain ABC kit	PK-4002		1:200
Biotinylated anti-Rat IgG	Vectastain ABC kit	PK-4001		1:200
Biotinylated anti-Rabbit IgG	Vectastain ABC kit	PK-4004		1:200

2.8 Molecular weight standards

Name	Company
Quick load® 100bp DNA ladder	New England Biolabs, Ipswich, USA
Precision plus protein Dual colour standard	New England Biolabs, Ipswich, USA

2.9 Cell lines

Isolated primary PanIN and fibroblasts from KC-SPARC^{wt} and KC-SPARC$^{-/-}$ were used in *in vitro* experiments of this study.

2.10 Cell culture media

DMEM+10% FBS+1% NEAA+ 1% P/S

DMEM+10% FBS+1% NEAA

DMEM+0.1% FBS+1% NEAA

3. Methods

3.1 Mouse models

SPARC^{wt}, SPARC$^{-/-}$, KC-SPARC^{wt} and KC-SPARC$^{-/-}$ mice with the genetic background of 129SvB6 were used in this study. SPARC^{wt} and SPARC$^{-/-}$ mice were initially purchased from Jackson Laboratory. Generation of KC-SPARC^{wt} and KC-SPARC$^{-/-}$ mice was achieved through multiple breeding steps as previously shown by Hingorani et al., 2003.

Initially SPARC^{wt} and SPARC$^{-/-}$ mice were crossed with mice harbouring conditional LSL-Kras^{G12D} allele in which the expression of oncogenic Kras^{G12D} is inhibited by Lox-STOP-Lox cassette. Further, the expression of mutated oncogenic Kras was achieved by crossing Kras$^{G12D(+/T)}$; SPARC^{wt} and Kras$^{G12D\ (+/T)}$; SPARC$^{-/-}$ mice with mice expressing Cre recombinase under the pancreas specific promoter p48.

Genotyping of the different mouse strains was performed by various genotyping protocols as discussed in part 3.3.3.

3.2 Cell culture

3.2.1 Primary cell isolation

Primary pancreatic cells were isolated from pre neoplastic lesions and tumour bearing KC-SPARC^{wt} and KC-SPARC$^{-/-}$ mice using an established protocol. The protocol involves the dissociation of cells from collagen using Liberase. Liberase is an enzyme mixture in which Collagenase I and Collagenase II are mixed in an appropriate ratio together with Thermolysin at a low concentration. Upon mouse dissection 2-3mm of pancreas tissue was taken and placed on a petri dish with PBS on ice. The following steps were performed under sterile condition in a cell culture safety cabinet. The tissue was then chopped into small pieces using a scalpel as quick as possible and 10 ml of digestion buffer (buffer composition is mentioned in detail in the materials) containing Liberase and trypsin inhibitor was added and mixed well. The mixture was then incubated at 37°C for 10 min. After incubation, the cells were collected in a 50 ml falcon and centrifuged at 1200rpm for 5 min at room temperature (RT). After removing the supernatant carefully, the pellet was resuspended in 5-10 ml of digestion buffer. The mixture was centrifuged at 1200rpm for 5 min followed by incubation in the water bath at 37°C for 10 min. The supernatant was removed carefully and the pellet was resuspended in washing buffer with 50mg/ml of Soy Bean Trypsin Inhibitor (SBTI) to prevent cell lysis

by trypsin. The cell suspension was then filtered through a 100 µm cell strainer and centrifuged at 1200rpm for 5 min. The cell pellet was resuspended in 10 ml of DMEM supplemented with 10% FBS, 1% NEAA and 1% P/S and cultured in a 10 cm petri-dish. Medium change was given the next day and every second day afterwards. The resulting cell population was a mixture of adherent epithelial cells and fibroblasts. The mixed cell population was then subjected to serial trypsinization until it became as homogenous population of epithelial and fibroblasts cells.

3.2.2 Expansion and culturing of primary cells

When the isolated primary cells reached 70-80% of growth confluence, the medium was removed and the cells were washed with PBS once. Then 2 ml of 0.5% trypsin EDTA per T75 culture flask was added and incubated at 37°C for 30 sec-60sec. As the fibroblasts are sensitive for trypsin treatment, they detach from plastic in a very short time of about 30 sec. The detached fibroblasts were cultured in a new culture flask with DMEM supplemented with 10% FBS, 1% NEAA.

The original flask was washed once with PBS to get rid any left detached fibroblasts and then fresh DMEM supplemented with 10% FBS, and 1% NEAA was added. This process of serial trypsinization was done until the epithelial and fibroblast cell populations reached homogeneity. The homogeneity of the culture was confirmed by microscopic observation, genotyping and western blot.

3.2.3 Wound healing assay

Wound healing assays are used to assess the migration of the cells in 2D based culture. The cells were grown in a 6 well plate until they reached 70-80% confluence. Subsequently, the cells were subjected to serum starvation for 24h (serum concentration 0.1%). The next day, the wound was introduced by making a precise scratch using a sterile 100µl micro tip across the middle of the wells. The migration was assessed by live cell imaging microscope (Leica DMi8) equipped with CO_2 and 37°C temperature maintenance. The pictures were taken every 6h till the wounds were completely closed.

3.3. Molecular biology techniques

3.3.1 DNA isolation from cultured cells

DNA isolation from cultured cells was performed using DNeasy® Blood & Tissue Kit from Qiagen. The protocol given by the manufacturer was followed. Maximum of 5×10^6 cells were collected from the culture flask and centrifuged at 190rpm for 5 min. The supernatant was removed and cells were resuspended in 200µl of PBS, and 20 µl proteinase K was added to this mixture. Then, 200 µl of buffer AL (lysis buffer) was added to this and mixed thoroughly by vortexing. The mix was then incubated at 56°C for 10 min. After the incubation 200 µl of 96-100% of ethanol was added to this and mixed well by vortexing. The whole mixture was then transferred to a DNeasy Mini spin column placed on a 2 ml collection tube provided in the kit. The column was then briefly centrifuged at 8000rpm for 1 min. The collection tube with the flow through was discarded and the column was placed on a new 2 ml collection tube. The column was then briefly washed with 500 µl of AW1 buffer (wash buffer with low concentration of quanidine) and centrifuged at 8000rpm. The flow through and the collection tube was discarded. The column was placed in a new 2 ml collection tube and washed with 500 µl of AW2 buffer (Tris- based wash buffer) and centrifuged at 14000rpm for 3 min. The flow through and the collection tube was discarded. The column was then placed in a new 1.5 ml mini centrifuge tube and 200 µl AE buffer (elution buffer) was added and incubated for 1 min at RT. The DNA was eluted by centrifuging the column at 8000 rpm and stored at -20°C.

3.3.2 DNA isolation from mouse tails for genotyping

DNA extraction was done from tail tips of 3-4 weeks old mice for genotyping. 2-3 mm of mouse tail tips were collected and the tissue lysis was achieved by heating the tail biopsy in 100 µl of alkaline lysis buffer for 30 min at 95°C. The lysates were then brought to RT and 100 µl of neutralization buffer was added. At this step, the tail tips look visibly intact but the DNA will be released into the supernatant.

3.3.3 Genotyping

The protocols for SPARC, $Kras^{G12D}$ and Cre-genotyping were obtained from the Jackson laboratory.

3.3.3.1 SPARC genotyping

The reaction mix was prepared as given in the original protocol from the Jackson Laboratory by mixing 12.5 µl of KAPA 2G Fast HS with 8.5 µl H_2O and 20pM of a common forward, a wild type reverse and a mutant reverse primer each. The triple primer system was used in order to detect WT, heterozygous and homozygous genotypes. 2 µl of DNA isolated from tail tip was added to the reaction mix and the following steps were performed in the thermal cycler.

Step	Temperature profile	Time	Note
1	94°C	3 min	
2	94°C	20 sec	35 cycles
3	65°C	15 sec	
4	72°C	15 sec	
5	72°C	2 min	
6	10°C	Infinite hold	

3.3.3.2 $Kras^{G12D}$ and Cre genotyping

Similar protocols for the reaction mix preparation and the thermal profile were used in $Kras^{G12D}$ and Cre genotyping. For $Kras^{G12D}$ genotyping the primers specific for mutated $Kras^{G12D}$ were used. The reaction mix was prepared as given in the original protocol by adding 12.5 µl of KAPA 2G Fast HS with 8.5 µl H_2O and 10µM of forward and reverse primers each. The reaction mix was then subjected to the following thermal profile using a thermal cycler.

Step	Temperature profile	Time	Note
1	95°C	2min	
2	95°C	30sec	34 cycles
3	60°C	30sec	
4	72°C	1min	
5	72°C	5min	
6	4°C	Infinite hold	

3.3.3.3 1lox-<K-ras> G12D genotyping

1lox <K-ras> G^{12D} genotyping was used to validate the homogeneity of isolated primary epithelial and fibroblast cells. The reaction mix was prepared by mixing 2 µl 5X advantage GC melt mix, 0.4 µl of 50X advantage GC-2 polymerase mix, 4 µl of 5X GC2 PCR buffer, 24pM of each forward and reverse primers, 4 µl of 25mM d' NTP's and 11.2 µl of H_2O. The PCR reaction was performed in the thermal cycler as shown below.

Step	Temperature profile	Time	Note
1	94°C	3 min	
2	94°C	30 sec	40 cycles
3	68°C	1.5 min	
4	68°C	3 min	

3.3.4 Agarose gel electrophoresis

Agarose gel electrophoresis is a widely used technique in molecular biology laboratories. This technique was originally invented by Oliver Smithies in 1950 and is used to separate the nucleic acids by their length.

Followed by PCR reaction, the amplified PCR product was run in 1.25-1.5% of agarose gel using gel electrophoresis technique with Tris-Borase-EDTA (TBE) buffer at 100V for 20 min. 100bp DNA ladder was used as a control.

3.4 Protein techniques

3.4.1 Protein extraction from cultured cells

Cells were cultured on a 6 well plate and washed with cold 1x PBS twice. Depending on cell density, 30-200 µl of protein lysis buffer containing protease and phosphatase inhibitors was added per well. The cells were scrapped and collected in a micro centrifuge tube and subjected to a short sonication to improve the protein yield. Followed by incubation on ice for 20-30 min, the lysate was then centrifuged at 14000 rpm at 4°C for 15 min. The supernatant was collected in a new micro centrifuge tube and stored at -20°C for a short period, and for longer storage at -80°C.

3.4.2 Sample preparation

The protein concentration was determined by Bradford method using Coomassie Blue G-250 protein assay reagent and known concentration of albumin as standard curve. Then 1µg/µl of protein lysate was mixed with 4xNuPAGE® LDS sample buffer with 10% β-Mercaptoethanol and boiled at 95°C for 5 min.

3.4.3 SDS-PAGE

The samples were then subjected to poly acrylamide gel electrophoresis (PAGE) using NuPAGE 4-12% Bis-Tris gel and Invitrogen mini gel tank. Minimum concentration of 20 µg of protein was loaded per well.The separation of proteins was achieved by running the samples at160V for 1h in 1x running buffer containing Sodium dodecyl sulphate (SDS) as a denaturing agent.

3.4.4 Western blot analysis

Followed by the separation of protein by SDS-PAGE, the proteins were blotted on a nitrocellulose membrane using 1xNuPAGE transfer buffer with 10% methanol. The resolved proteins from the gel were transferred to the nitrocellulose membrane using a transfer apparatus at 10V for 1.5h. The membrane was blocked with 5% non-fatty milk for 1h at RT to avoid unspecific binding of the primary antibody. Both primary and secondary antibodies were diluted in 5% non-fat milk in PBS containing 0.1% Tween-20. The membrane was incubated with the appropriate concentration of primary antibodies (concentrations of antibodies are mentioned in materials section) at 4°C overnight. The following day, the membrane was washed 3 times with 1X PBS and then incubated with1:2000 dilution of secondary antibody conjugated with horseradish peroxidase for 1h at RT. The membrane was washed 3 times with PBS-T to get rid of unbound secondary antibody. The proteins on the membrane were detected using Enhanced Chemi Luminescence (ECL). ECL is a technique which detects the reactivity of horseradish peroxidase with its substrate luminol as light emission and thus detects immobilized proteins on the membrane. The imaging was done using INTAS- ECL Chemocam imager and analysed using the software provided by the equipment provider.

3.5 Histology

3.5.1 Tissue collection and processing

Upon mouse biopsy, tissues such as pancreas, liver, spleen and intestines were collected in a glass vial containing 4% formaldehyde. The tissue samples were fixed with 4% formaldehyde overnight at RT. Fixation is the process which enhances the tissue stability by cross linking macromolecules and thus inhibiting the disintegration of biological materials. Following overnight fixation, the tissues were subjected to a dehydration process by treating them with a gradually increasing concentration of ethanol from 70-99% at regular time intervals. The dehydration process was achieved using automated dehydration machine provided by Leica. After the dehydration process, the tissues were embedded in paraffin using tissue embedder system. The tissues in paraffin blocks were sectioned with the thickness of 4µm using a microtome (Leica RM2265) and fixed on SUPERFROST® microscope glass slides and used for various histological staining protocols.

3.5.2 Haematoxylin and Eosin stain

Haematoxylin and Eosin (H&E) stain is one of the most commonly used dyes to study the basic histology of the tissues. The tissue sections were immersed in roticlear for 10 min two times in order to de-mask the paraffin. The tissue slides were subsequently subjected to rehydration process by treating them with gradually decreasing concentration of ethanol from 99-50% each for 3 min. The tissue slides were then washed briefly in tap water 2-3 times and stained with haematoxylin for 5-7 min. Haematoxylin is a chemical compound which specifically stains cell nuclei in purple colour. The slides were washed with running tap water for 5 min until the colour turns purple. Then the slides were counterstained with eosin, a red stain specific for cytoplasm of the cell for 7 min. The slides were washed three times with tap water and the tissue was dehydrated by treating them with increasing concentration of ethanol from 70-99% each for 3 min. Finally, the slides were treated with roticlear 4 times each for 10 min and mounted using rotimount solution.

3.5.3 Immunohistochemistry

For immunohistochemical analysis, the tissue slides were deparaffinized and rehydrated as mentioned above in the H&E staining protocol. Antigen retrieval was achieved by boiling the slides with appropriate buffer solutions (Tris-EDTA-pH 9.0 or Citrate buffer-pH 6.0) for 10 min in the microwave at maximum power (700 watts). The slides were then cooled down on ice for 20 min and washed briefly with tap water. Then the slides were treated with freshly prepared 3% $H_2O_2$for 20 min to quench the endogenous peroxidase activity. Subsequently, the slides were rinsed in tap water for 5 min and aligned in a Cadenza slide holder system and washed thrice with TBS containing 0.1% Tween-20. Tween is a mild detergent used in many washing buffers. The tissues were then blocked with 10% of appropriate serum and 1% BSA in TBS-T for 1 hour at RT. Both primary and secondary antibodies were diluted in the blocking solutions. The tissues were then incubated with appropriate concentration (antibody concentration was given in materials) of primary antibody at 4°C overnight. The following day, the slides were washed thrice with TBS-T before incubating them with biotinylated secondary antibody provided in a species specific ABC vectastain kit for 1 hour at RT. Afterwards, the slides were washed thrice with TBS-T and incubated with AB complex prepared by mixing equal volumes of Solution A and Solution B containing peroxidase (i.e. 10µl of Solution A and 10µl of Solution B) provided in the same kit. The slides were washed

thrice with TBS-T before removing them from Cadenza system and once with tap water before treating them with 3,3'-Diaminobenzidine (DAB) a substrate of the peroxidase enzyme. The positive staining was observed as a brown chromogen development upon incubation with DAB.

3.5.4 DAPI staining

After de-waxing and rehydration of the tissue slides, the antigen retrieval was achieved by boiling the slides with appropriate buffer solutions (Tris-EDTA-pH 9.0 or Citrate buffer-pH 6.0) for 10 min in the microwave at maximum power (700 watts). The slides were cooled down on ice for 20 min and washed briefly with tap water 2-3 times. The slides were then aligned in a Cadenza system and washed thrice with TBS containing 0.1% Tween-20. Afterwards, the tissues were blocked with 10% of appropriate serum and 1% BSA in TBS-T for 1h at RT before incubation with the appropriate concentration of primary antibody at 4°C overnight. For immunofluorescence the appropriate secondary antibodies coupled with fluorochromes were used and the detection was achieved by using a fluorescence microscope.

3.5.5 Masson trichrome staining

Masson trichrome is a chemical staining used to detect the collagen fibers in tissue specimen embedded in paraffin. For masson trichrome staining, different compartments of tissues were stained in three different colours. The collagen fibers are recognized from other compartments by a prominent blue colour stain, while the nucleus is stained in black and the muscle and other parts stained in red. The Masson trichrome staining kit from Polysciences, Inc was used. The protocol was performed under the fume hood in order to avoid health hazards. The de-waxing and rehydration of slides was done as mentioned above. The fixation was achieved by incubating the slides overnight with Bouin's solution at RT. The slides were washed with running tap water for 5 min to remove picric acid. Subsequently, the slides were stained with Weigert's iron haematoxylin working solution (prepared by mixing 1:1 ratio of Weigert's haematoxylin A and Weigert's haematoxylin B) for 15 min and washed in running tap water for 5 min and rinsed once with distilled water. The slides were further incubated with Biebrich Scarlet - Acid Fuchsin Solution for 5 min and rinsed in distilled water. The slides were then treated with phosphomolybdic acid for 10 minutes, and directly transferred into a glass beaker containing aniline blue for 5 min. Followed by rinsing with distilled water; the slides were treated with 1% acetic acid for 1 min and rinsed in distilled water.

Subsequently, the slides were dehydrated with 95% and 99% of ethanol each for 30 sec and cover slipped.

3.5.5 Herovici staining

Herovici is a chemical staining method used to distinguish young (pro) collagen from mature dense collagen (Friend, 1963). Herovici is a defined combination of methyl blue (aniline blue) and picro acid fuchsin. When the prestained sections are treated acetic acid or acidic water, the red stain is retained by the mature collagen while procollagen loses the red stain and turns into blue (Lillie et al., 1980). The cytoplasm and nucleus are counter stained yellow and black in colour respectively. The protocol provided by the Histopathology/ISH core facility, Cambridge research Institute was followed. The tissue slides were de-waxed and rehydrated as mentioned before and washed briefly in tap water before treating them with Weigert's hematoxylin solution for 5 min. The slides were then briefly rinsed with tap water for 45 sec and treated with Herovici's working solution (1:1 Herovici's solution A and Herovici's solution B) for 2 min. The slides were then directly kept in 1% acetic acid solution for 2 min without rinsing. Finally, the slides were dehydrated, and coverslipped.

3.5.6 Picrosirius Red stain

Picrosirius red stain is a chemical staining used to detect the total collagen in the given tissue. The Picrosirius red stain kit and the protocol from Polysciences, Inc was used. The slides were subjected to de-waxing and dehydration as mentioned before and treated with Weigert's haematoxylin solution for 5 min. The slides were rinsed with tap water once and agitated with 2% acid ethanol for 10 sec. The slides were again rinsed with tap water and washed once with distilled water before counter staining with solution A (phosphomolybdic acid) provided in the kit for 2 min. Subsequently, the slides were washed with distilled water and placed in solution B (picrosirius red F3BA stain) provided in the kit for 110 min without rinsing the slides. Afterwards, the slides were treated with solution C (0.1N HCl) for 2 min. Then the slides were treated with 70% ethanol for 45 sec and further dehydrated and mounted.

3.6. *In vivo* experiments

The animal breeding and survival study (animal allowance application number -TVA-14/1634) and other *in vivo* experiments (gemcitabine treatment- TVA15/2056) of our study have met the ethical requirements of the institute and the federal government. The

animals were bred and maintained in Central animal experimental facility, University Medical Center Göttingen (ZTE-UMG). The animals were subjected to 12/12h day/night cycles. The newly born pups were separated from mother after three weeks of birth.

A clear score sheet with specific parameters (severity level 1-3) was followed to define the end point criteria. Severity level 1 includes isolation of animal in the cage, rough fur, narrowed ocular margins, slightly increased breathing, and alteration in the fecal /urine quantity, color and consistency. These animals were observed closely for recovery, and they are sacrificed if were found with persistent symptoms. Severity level 2 parameters include conditions such as persistant pain (facial expression, bent position), open wounds, severe breathing and diarrhea, notable weight loss (10%). Animals with severity level 2 were sacrificed upon veterinarian's advice. While animals with severity level 3 symptoms (paralysis, any other terminal illness and significant weight loss (20%) were immediately sacrificed. The animals that died of any symptoms mentioned above are considered as end point criteria. If the animals presented no symptoms at the age of 20 months, they were sacrificed and considered as end point.

3.6.1 Study design and sample collection

KC-SPARC^{wt} and KC-SPARC$^{-/-}$ mice were categorized into three different age groups: 3 months, 7-8 months and 12-20 months in order to study the role of SPARC during different stages of PDAC progression. Tissue samples such as pancreas, liver, spleen and intestine were harvested in 4% formaldehyde for histological analysis. For protein extraction, tissues such as pancreas, liver and intestine were snap frozen using liquid nitrogen. For RNA isolation pancreas and liver were collected in a vial containing RNA later, a stabilizing reagent.

3.6.2 Gemcitabine treatment and the sample preparation for Mass Spectrometry analysis

PanIN lesions bearing (7-8 months old) and tumor bearing KC-SPARC^{wt} and KC-SPARC$^{-/-}$ mice and 3 months old SPARC^{wt} and SPARC$^{-/-}$ (as control) cohorts were treated with 100mg/kg of Gemcitabine for 2h by an intraperitoneal injection. After 2 h, the mice were sacrificed and the pancreas was harvested and instantly frozen by immersing the tissue in liquid nitrogen. The drug injections and sample collection were done by Ms. M. Patzak with the assistance of technical assistants. The pancreas tissue was processed and subjected to liquid chromatography-mass spectrometry/ mass spectrometry (LC-MS/MS)

to analyse the concentration of native 2′,2′-difluorodeoxycytidine (dFdC) and its metabolites such as 2′,2′-difluorodeoxycytidine-5′-triphosphate (dFdCTP) and 2′,2′-difluorodeoxyuridine (dFdU) as previously described (Bapiro et al., 2011). The LC-MS/MS analysis was performed in CRUK-Pharmacokinetics & Bioanalytics (PKB) Core Facility, Cancer Research UK Cambridge Institute.

4. Results

In this study, we explored the expression of SPARC in normal murine pancreas and during various stages of disease initiation and progression to PDAC in the context of oncogenic $Kras^{G12D}$. To experimentally address the above mentioned issues, I employed KC-$SPARC^{-/-}$ and KC-$SPARC^{wt}$ GEMMs in this study. $SPARC^{wt}$ and $SPARC^{-/-}$ mice were used as controls.

4.1 Characterization of mouse models

The mouse models were successfully generated as mentioned previously in the methods section and observed closely for any noticeable phenotypes. Genetic ablation of SPARC has been reported to be lethal in the lower organisms such as C. elegans and Drosophila (Fitzgerald and Schwarzbauer, 1998; Martinek et al., 2011). Nevertheless, embryonic SPARC knockout is not lethal in mice according to the previous studies. In the absence of SPARC in higher animals, the functions of SPARC are partly accomplished by other members of the SPARC protein family (Liu et al., 2008; Sullivan and Sage, 2004).

$SPARC^{-/-}$ mice showed certain specific non-lethal phenotypes such as fragile bones, cataract and curled tail tips. These phenotypic changes are caused by impairment in collagen maturity and deposition. SPARC has been reported to aid the folding and deposition of collagen through various mechanisms, and thus the lack of SPARC resulted in low bone density (Bradshaw, 2009). SPARC has also been shown to maintain the lens fiber and fluid transport, thus the absence of SPARC affects the lens homeostasis (Greiling et al., 2009; Norose et al., 1998a).

3 months old $SPARC^{-/-}$ (n=6) and WT (n=6) mice were sacrificed and organs such as pancreas, liver, kidney and spleen were harvested and weighed. The whole body weight was measured prior to necropsy. The study results show that $SPARC^{-/-}$ mice have a trend towards reduced overall body weight compared to WT mice (Fig. 4A) (p=0.06). Additionally, the weight of internal organs such as pancreas (Fig.4B) (p=0.11), liver (Fig.4C) (p=0.13), kidney (Fig.4D) (p=0.02) and spleen (Fig.4E) (p=0.02) of $SPARC^{-/-}$ mice were relatively lower than of WT mice. Though the difference was not statistically significant, the trend was obvious in terms of body weight, pancreas and liver weight between $SPARC^{-/-}$ and WT.

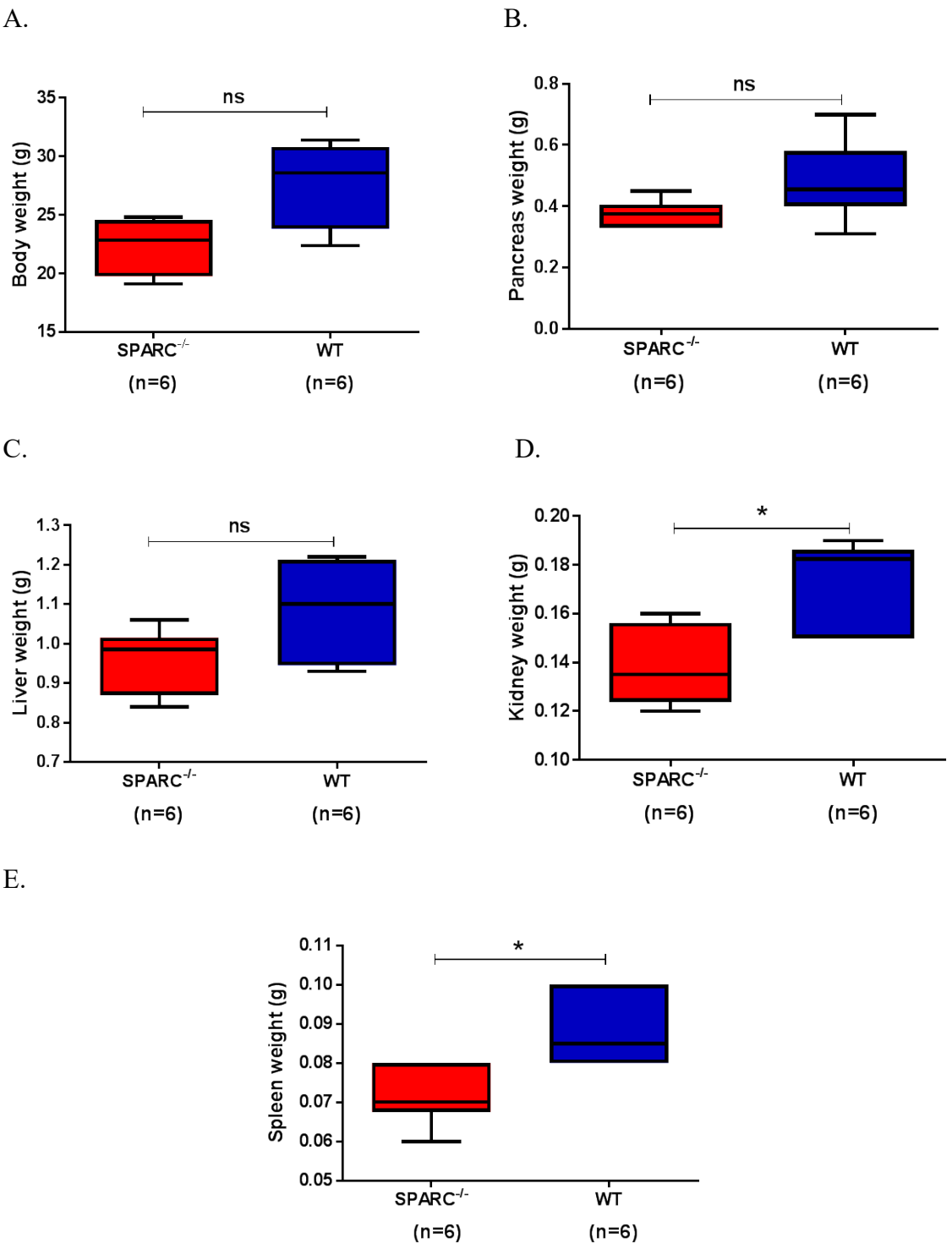

Figure 4: (A) Graph shows that SPARC$^{-/-}$ mice have a trend towards reduced overall body weight (p=0.06) compared with WT mice. (B, C, D & E) Graphs showing that the weight of the internal organs such as pancreas (p=0.11), liver (p=0.13), kidney (p=0.02) and spleen (p=0.02) are also lower in SPARC$^{-/-}$ mice compared to WT mice. Mann-Whitney test was used to assess the statistical significance. * p≤0.05.

4.1.1 SPARC knock out does not affect murine pancreas development

Histology of pancreas assessed by H&E staining confirmed that the murine pancreas development was not affected by genetic SPARC ablation. Pancreas tissue sections from 3 months old SPARC$^{-/-}$ and WT mice stained with H&E (Fig. 5) show the tissue integrity of the organ. Different compartments of the pancreas such as acinar cells (*) and islets (arrow) are found to be structurally intact.

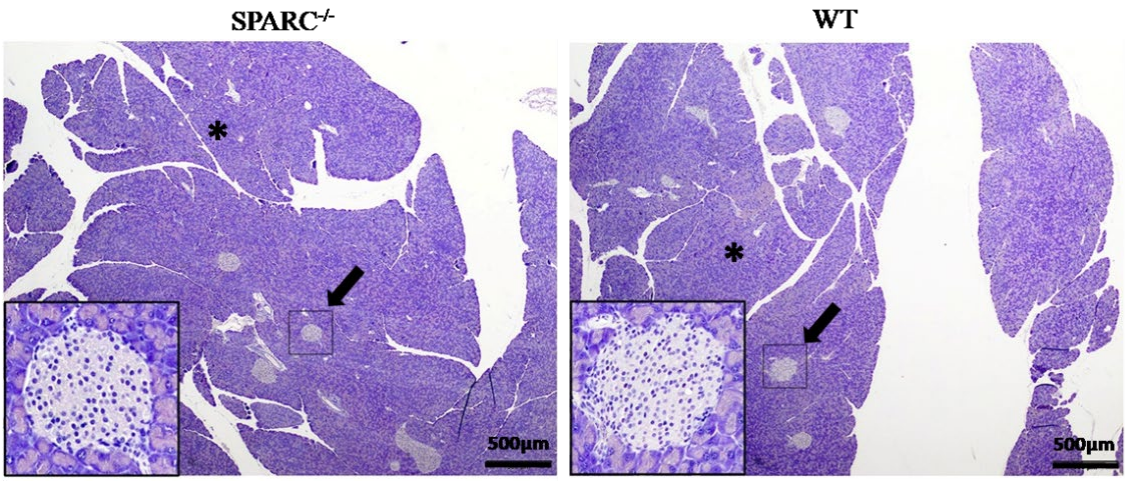

Figure 5: Representative images of H&E staining of 3 months old SPARC$^{-/-}$ and WT mice pancreata. The inset shows higher magnification of islets.

4.1.2 Oncogenic Kras^{G12D} activation results in disease initiation

Upon oncogenic Kras^{G12D} expression both KC-SPARC$^{-/-}$ and KC-SPARC^{wt} mice developed ADMs and low grade PanIN lesions at the age of 3 months (Fig. 6A) which further progressed to advanced PanIN lesions (Fig. 6B). Based on the anticipated progression stage, mice have been categorized under three age groups: 3-5 months (early prenneoplasia), 7-8 months (late preneoplasia and more than 12 months (tumors, end point cohort) in order to study the effect of SPARC on different stages of PDAC progression.

A.

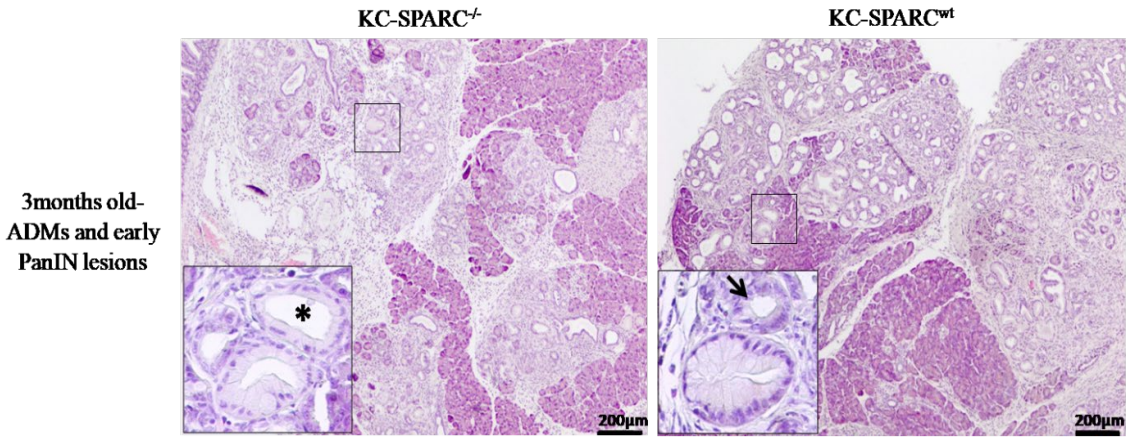

B.

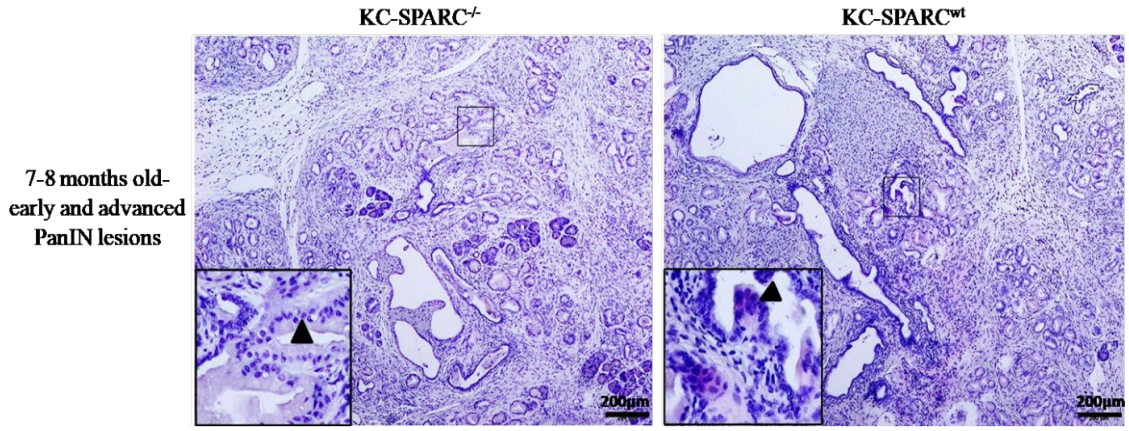

Figure 6: (A) Representative images of H&E staining of 3 months old and (B) 7-8 months old KC-SPARC$^{-/-}$ and KC-SPARC^{wt} mice pancreata show ADMs (down arrow), low grade PanINs (*) and high grade PanINs (thick arrow head) respectively. The inset shows 40x magnification of ADMs and low PanINs and advanced PanIN lesion.

4.2 Primary cell isolation and characterization

Primary PanIN associated fibroblasts (PAFs) and PanIN (epithelial) cells were successfully isolated from 3-5 months old KC-SPARC^{wt} and KC-SPARC$^{-/-}$and established in cell culture. Microscopic observation of the cells was performed to investigate the phenotypic characteristics of the isolated cells. Isolated fibroblasts exhibited spindle shaped elongated structure while the PanIN cells were growing in patches indicating the morphological fibroblast and epithelial properties respectively.

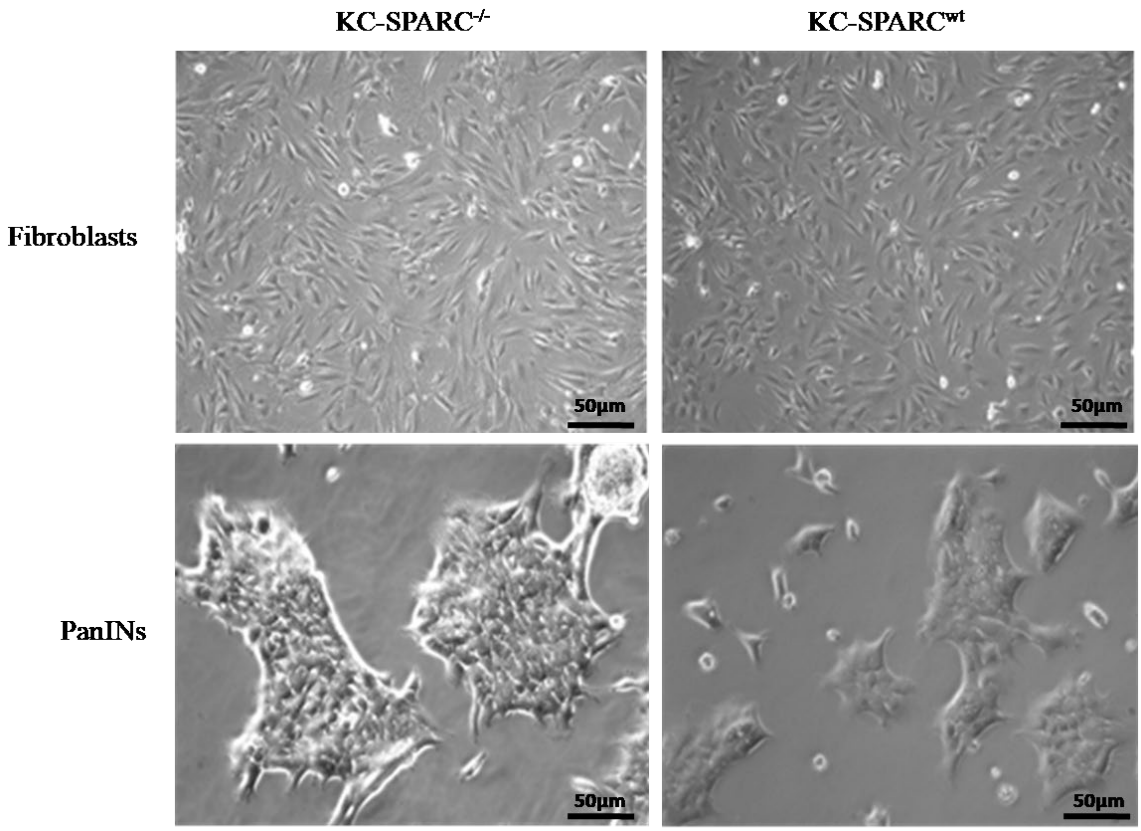

Figure 7: Representative bright field pictures of PAFs and PanINs cultures confirm the homogeneity of the population. Pictures were taken at 20x magnification.

4.2.1 Characterization of PAF cells by 1LoxP Kras genotype

Having confirmed the homogeneity of the cultured PAF cells by microscopic observation, we further employed 1LoxP Kras PCR to ensure the purity of the culture at DNA level. In KC mice Cre mediated recombination results in one WT allele and one mutated allele with a LoxP site. 1LoxP Kras PCR specifically targets the single LoxP site left after the Cre recombination. PCR results showed clear bands at 285bp (WT allele) in the lanes of fibroblasts (no Cre expression) while in the positive control (DNA from PanIN cells) there are two bands at 285bp (WT allele) and 325bp (mutated allele with loxp-site). This confirms the purity of PAF cells at DNA level with no detectable contamination with PanIN cells.

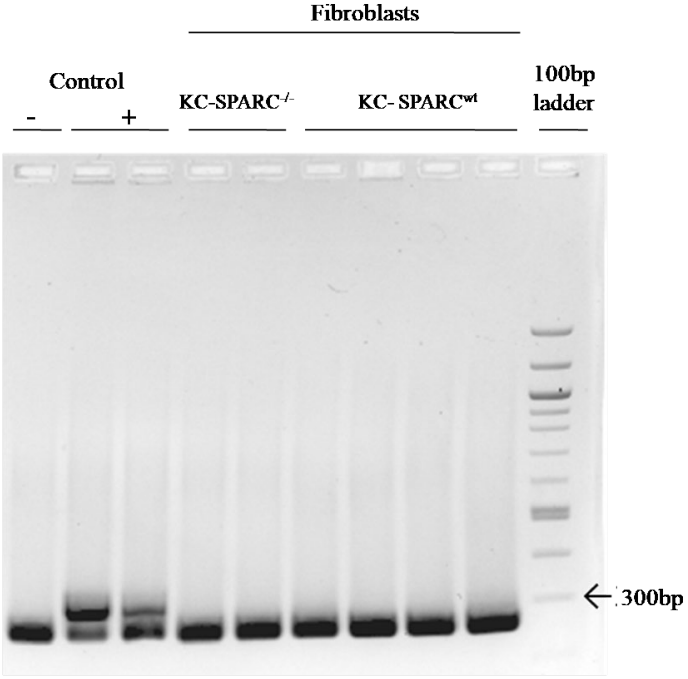

Figure 8: Agarose gel electrophoresis of 1LoxP Kras PCR product shows clear single band at 285bp (Kras WT allele) in fibroblast lanes. DNA from PanIN cells was used as a positive control showing a 285bp (WT allele) and 325bp (mutated allele with loxp site) as the result of Cre recombination. 100bp DNA ladder was used as a marker.

4.2.2 Characterization of PanIN cells by western blot

In order to further confirm the homogeneity of cultured primary PanIN cells, western blot analysis was performed for E-Cadherin (epithelial marker) and α-SMA (fibroblast marker) in protein lysates of cultured PanIN cells. As shown in Fig. 9, E-Cadherin was strongly expressed by PanIN cells while there was no α-SMA expression (except two clones) by PanIN cells. The slight bands for α-SMA in two clones of KC-SPARC$^{-/-}$

PanINs show that there is a contamination of fibroblasts. Therefore, those two clones were not used for further experiments.

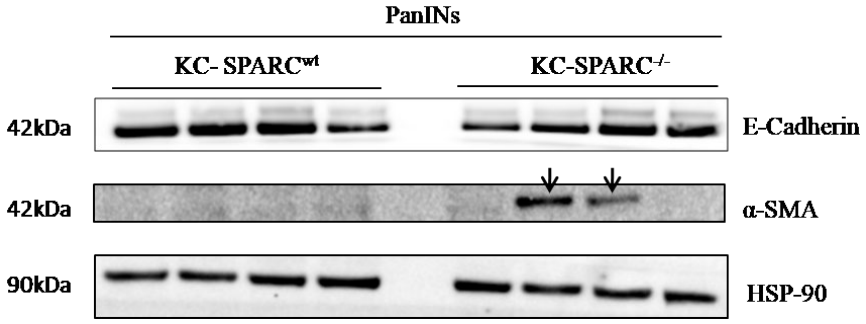

Figure 9: Western blot analysis shows strong expression of E-Cadherin by primary PanIN cells isolated from 3 months old KC-SPARC^{wt} and KC-SPARC$^{-/-}$ pancreata. In two clones of KC-SPARC$^{-/-}$PanINs (down arrow) there was expression of α-SMA which shows contamination with fibroblasts. HSP-90 was used as a loading control.

4.3 *In vitro and in vivo* expression of SPARC

The expression of SPARC by isolated primary fibroblast and PanIN cells was assessed by western blot analysis. Furthermore, IHC for SPARC in KC-SPARC^{wt} and KC-SPARC$^{-/-}$ mice pancreata with PanIN lesions and tumor was performed to investigate the *in vivo* expression of SPARC during different stages of PDAC progression. SPARC is not expressed in healthy pancreas. However, SPARC is overexpressed by CAFs during tumorigenesis of PDAC (Chen et al., 2010; Mantoni et al., 2008; Sato et al., 2003).

The western blot analysis performed in cell lysates of cultured primary fibroblasts (KC-SPARC^{wt} and KC-SPARC$^{-/-}$) and PanIN cells (KC-SPARC^{wt} and KC-SPARC$^{-/-}$) show strong expression of SPARC by fibroblasts of KC-SPARC^{wt} (n=4), while there is nearly no expression in PanIN cells of KC-SPARC^{wt} (n=3).The lack of SPARC expression in fibroblasts (n=3) and PanINs (n=4) of KC-SPARC$^{-/-}$ further confirms the genetic knock out of SPARC (Fig. 10A). Similarly, IHC analysis for SPARC in pre-neoplastic and tumor tissues of KC-SPARC^{wt} and KC-SPARC$^{-/-}$ mice shows that there was no expression in the normal acinar cells and strong expression by PAFs and CAFs. Interestingly, SPARC is hardly expressed by tumor cells. The absence of positive staining in pre-neoplastic and tumor tissue of KC-SPARC$^{-/-}$ mice confirms the genetic ablation of SPARC *in vivo* (Fig. 10B).

A.

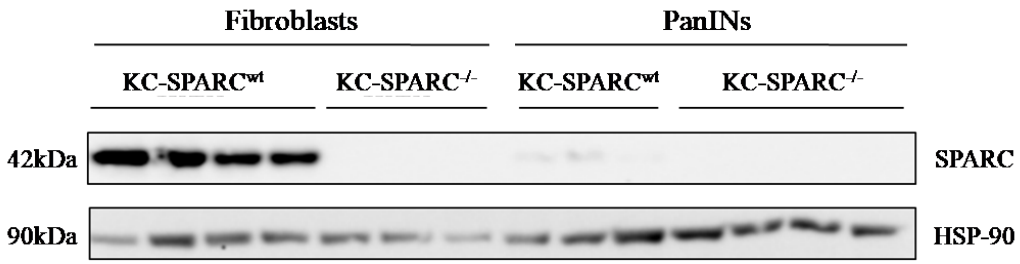

B.

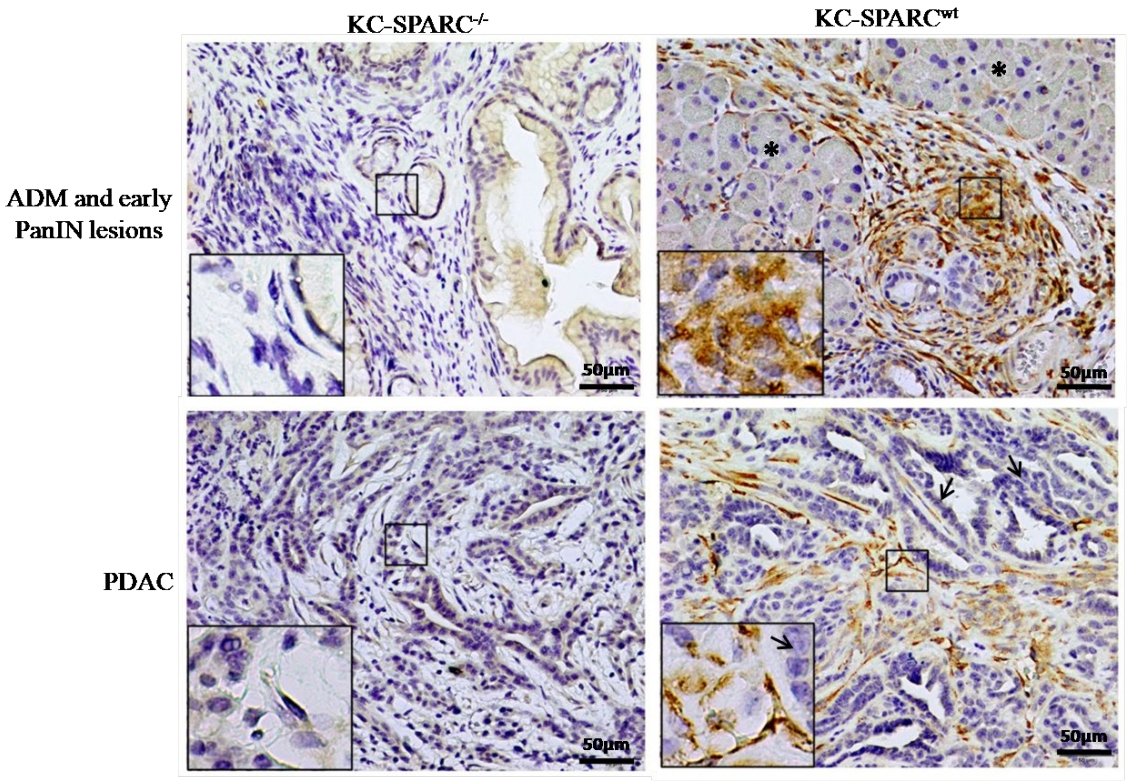

Figure 10: (A) Western blot analysis of cultured PAFs and PanIN cell lysates showing expression of SPARC in PAFs and hardly any expression in PanIN cells of KC-SPARC^{wt} mice. Absence of SPARC in PAFs and PanINs of KC-SPARC$^{-/-}$ confirms genetic knock out. HSP-90 was used as a loading control. (B) Representative pictures of IHC-SPARC in precursor lesions and PDAC of KC-SPARC^{wt} and KC-SPARC$^{-/-}$ shows that SPARC is not expressed in the normal acinar cells (*) and highly expressed by PAFs and CAFs of KC-SPARC^{wt}, while there is nearly no expression in PanIN and tumor cells (arrow). Images were taken at 20x magnification and the inset shows 40x magnification.

4.4 Early tumorigenesis

4.4.1 SPARC depletion does not affect ADMs, PanIN development and inflammation

Having confirmed the elevated expression of SPARC during early tumorigenesis, we further elucidated whether ablation of SPARC promotes disease initiation and progression by performing a semi quantitative histological scoring of H&E stained pancreata from 3 months and 7-8 months old KC-SPARC$^{-/-}$and KC-SPARC^{wt} mice. Histological scores from 1-3 were given based on the extent of ADMs and PanIN development as well as the immune cell infiltration. The scoring was performed by Prof. Dr. med. B. Sipos, Pathology, Universitätsklinikum, Tübingen. The semi-quantitative histological scoring shows that both KC-SPARC^{wt} and KC-SPARC$^{-/-}$(3 months and 7-8 months old) mice have comparable scoring of ADMs, PanIN1, PanIN2 and immune infiltration (Fig. 11A &B). This finding indicates that expression of SPARC neither influences the disease initiation nor the disease progression in KC-SPARC^{wt}.

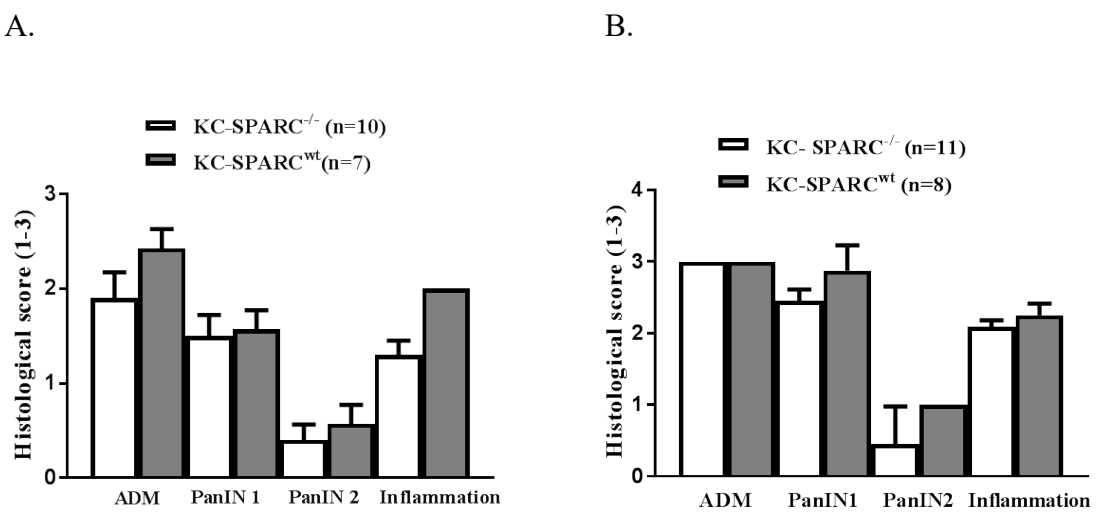

Figure 11: (A&B) Semi-quantitative histological scoring of ADMs, PanIN1, PanIN2 and inflammation in 3 months and 7-8 months old KC-SPARC$^{-/-}$ and KC-SPARC^{wt} pancreas tissues show that stromal SPARC expression has no influence on disease progression.

4.4.2 Collagen deposition is significantly reduced upon SPARC depletion

The abundant extra cellular matrix (e.g. collagen and hyaluronic acid) deposition has been reported to be associated with disease progression and poor clinical efficacy of drugs (Minchinton and Tannock, 2006; Netti et al., 2000). Furthermore, SPARC has been reported as a modulator of desmoplasia (Bradshaw, 2009; Tremble et al., 1993).

Therefore, to see if SPARC affects ECM deposition, two chemical stainings for collagen such as masson trichrome (total collagen) and Herovici (mature collagen) were performed in pre-neoplastic pancreatic tissues of 3 months old KC-SPARC$^{-/-}$ and KC-SPARC^{wt} mice. Masson trichrome staining analysis of 3 months old pancreatic tissue revealed that the total collagen deposition was significantly reduced in pre-neoplastic pancreatic tissues of KC-SPARC$^{-/-}$(n=10) mice compared to that of KC-SPARC^{wt} (n=7) mice (p=0.0001) (Fig 12A&B).Masson trichrome staining analysis in 7-8 months old cohort (late tumorigenesis) exhibited similar trend though it did not reach statistical significance (p=0.08) (Fig. 12C). These results show that depletion of SPARC affects collagen deposition regardless of disease progression stage, with the most pronounced effect during early PanIN development. Furthermore, herovici staining was performed to quantify the mature dense collagen deposition (Fig. 12D). Consistent with the total collagen deposition, the mature collagen deposition was also found to be reduced upon SPARC ablation. The mature dense collagen deposition was less in KC-SPARC$^{-/-}$ mice from both early (3 months) (p=0.1) and late tumorigenesis (7-8 months) (p=0.0002) cohort compared to that of KC-SPARC^{wt} mice (Fig12 E& F).

A.

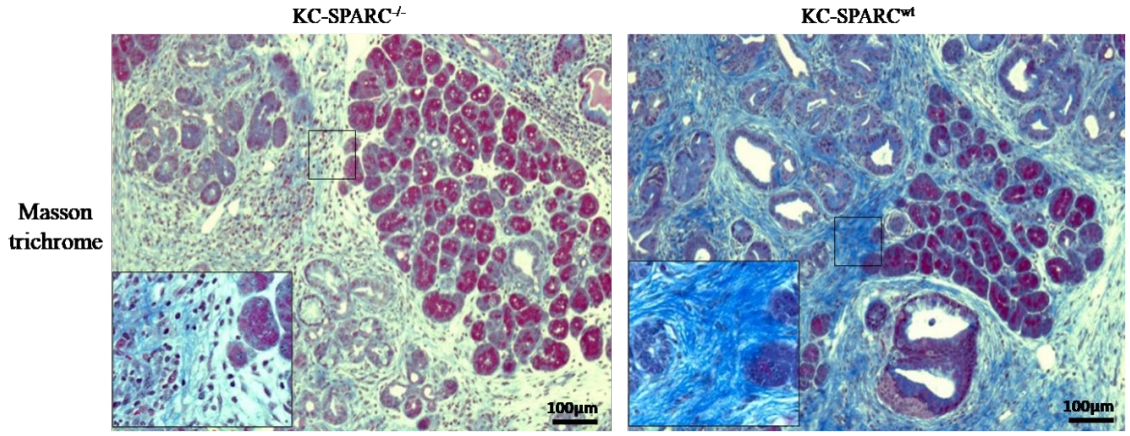

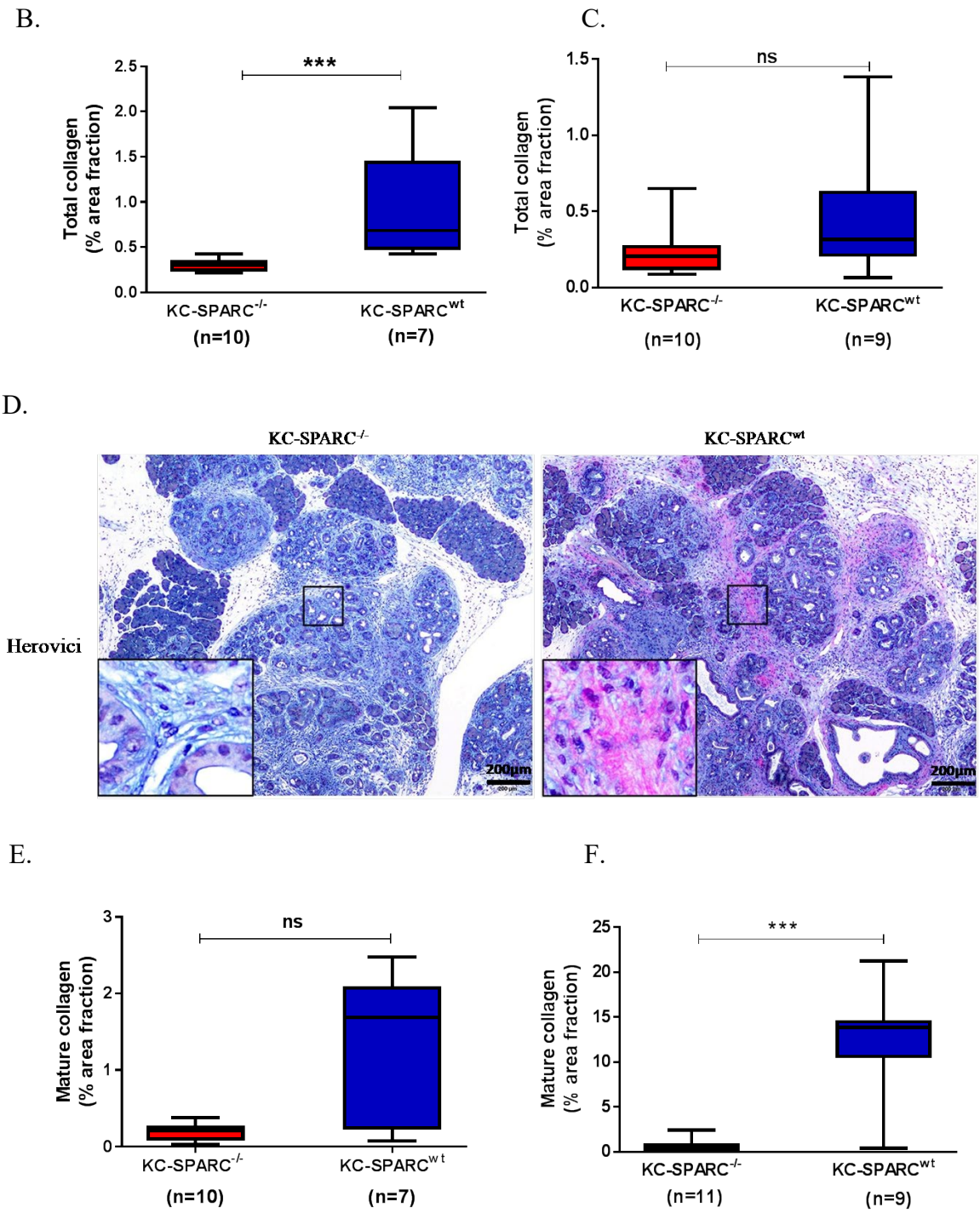

(B&C) Quantification of masson trichrome staining in 3 months old (p=0.0001) and 7-8 months old (p=0.08) KC-SPARC$^{-/-}$ and KC-SPARC^{wt} mice pancreata. (D) Representative images of herovici staining in pancreas tissues of 3 months old KC-SPARC$^{-/-}$ and KC-SPARC^{wt} mice. (E&F) Quantification of herovici staining in 3 months old (p=0.11) and 7-8 months old (p=0.0002) KC-SPARC$^{-/-}$ and KC-SPARC^{wt} mice pancreata. Statistical analysis was performed using Mann-Whitney test. *** $p \leq 0.005$.

4.4.3 SPARC depletion does not affect fibroblast population

Activated PSCs are the major source of ECM components production (Apte et al., 1998; Bachem et al., 1998). Having confirmed the significant reduction of collagen deposition upon SPARC depletion, we assessed if depletion of SPARC directly affects the PSC population. To achieve this, IHC was performed for α-SMA in pre-neoplastic pancreatic tissues of 3 months old KC-SPARC$^{-/-}$ (n=9) and KC-SPARC^{wt} (n=6) mice. α-SMA positive fibroblasts were specifically stained while the ductal and other cell population were devoid of positive staining as shown in Fig. 13A. The quantification of this staining was performed by measuring the α-SMA positive area using color deconvolution tool, ImageJ software. The quantification of IHC-α-SMA revealed that both KC-SPARC$^{-/-}$and KC-SPARC^{wt} mice have comparable α-SMA positive area (4.16% vs 5.71%) (p=0.38). This result shows that SPARC ablation does not affect the fibroblast population during early tumorigenesis.

A.

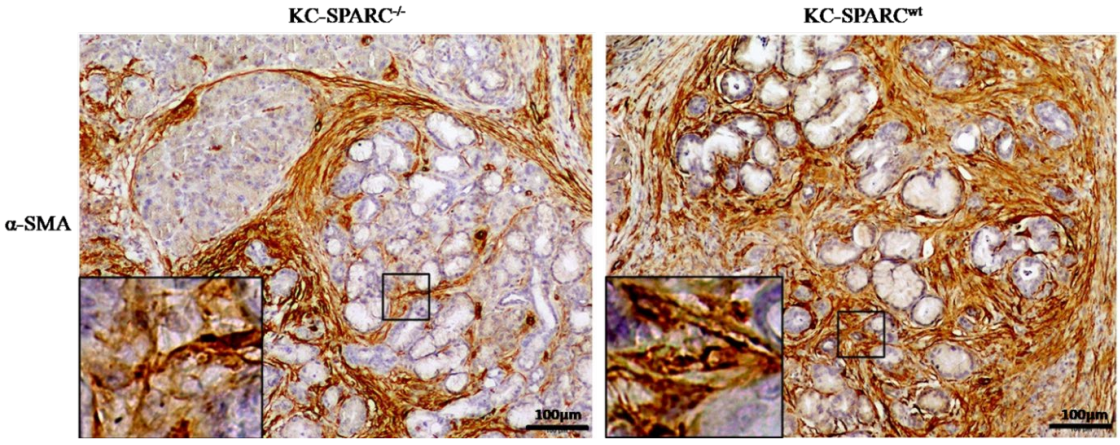

Figure 13: (A) Representative pictures of IHC-α-SMA in pancreata of 3 months old KC-SPARC$^{-/-}$KC-SPARC^{wt} mice. Images were taken at 10x magnification, and the inset shows 40x magnification.

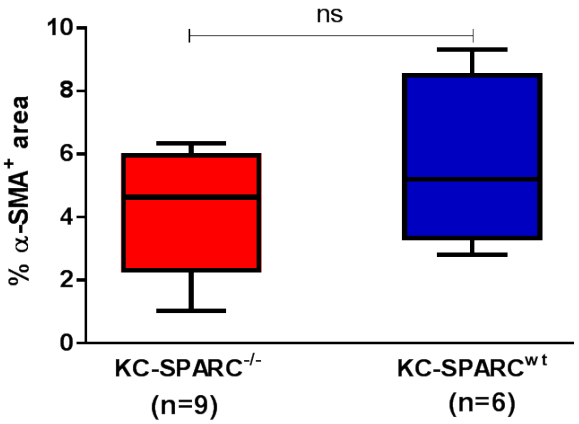

Figure 13: (B) Graph shows that KC- KC-SPARC$^{-/-}$ and SPARC^{wt} mice have comparable positive areas of α-SMA (p=0.38). Statistical analysis was performed using Mann-Whitney test.

4.4.4 SPARC depletion does not affect overall proliferation *in vivo*

The role of SPARC in proliferation has been reported in several tumor entities such as ovarian, melanoma, head and neck cancers. For instance, SPARC has been shown to act as key regulator of proliferation in ovarian cancer (Chen et al., 2012). In melanoma, SPARC seems to promote proliferation of stromal cells but not tumor cells in a context dependent manner (Haber et al., 2008). Therefore, to investigate whether SPARC depletion affects overall proliferation *in vivo*, IHC for Ki67was performed in pre-neoplastic pancreatic tissues (3 months old) in a SPARC dependent manner. Proliferation index (% of proliferating cells) was calculated by dividing the number of Ki67 positive nuclei by total number of nuclei. The result was expressed in percentage. IHC- Ki67 specifically stained the nuclei of proliferating cells as shown in Fig. 14A. Quantification of the staining revealed that SPARC status does not affect the overall proliferation of pre-neoplastic lesions as PanIN lesions of both KC-SPARC$^{-/-}$ (n=10) and KC-SPARC^{wt} (n=7) mice have similar proliferation rate (5 vs 6% proliferating nuclei) (p=0.08).

A.

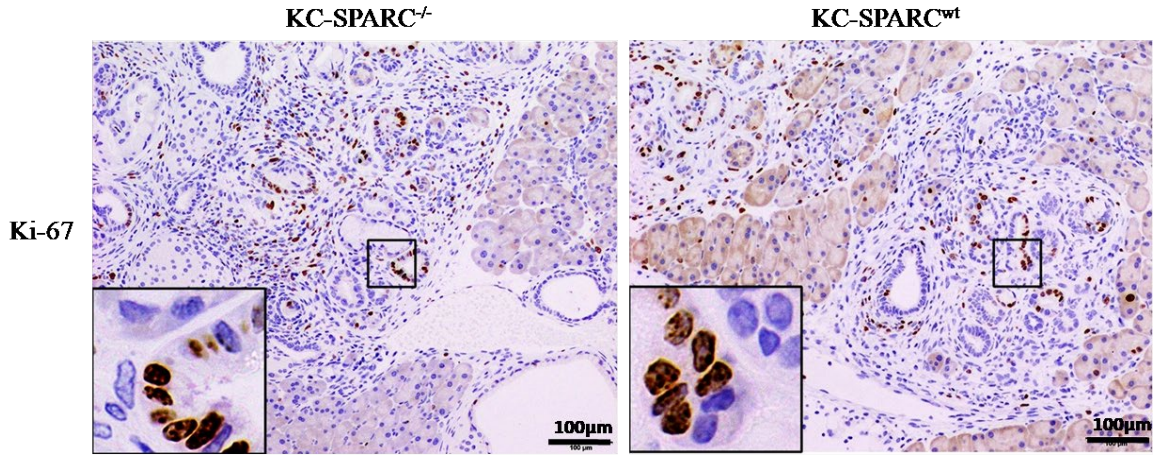

B.

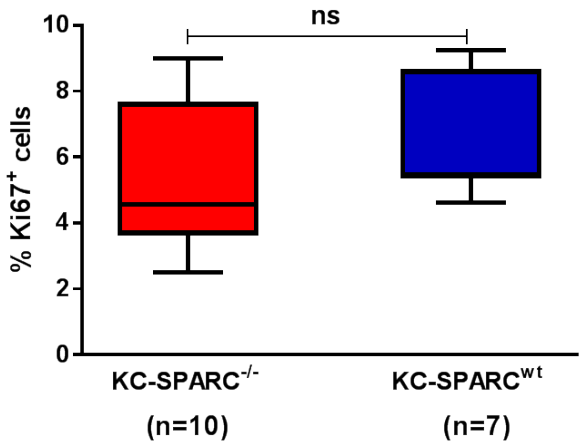

Figure 14: (A) Representative pictures of IHC-Ki67 in the PanIN lesions of KC-SPARC$^{-/-}$ (n=10) and KC-SPARC^{wt} (n=7) mice. Images were taken at 10x magnification and the inset shows 40x magnification. (B) Graph shows that SPARC ablation did not affect the overall proliferation the PanIN lesions (p=0.08). Statistical analysis was performed using Mann-Whitney test.

4.4.5 Stroma derived SPARC does not affect migration of PanIN cells

The role SPARC on tumor cell migration and invasion has been investigated in many tumor entities and was reported to play pro- and anti-invasive role in different cancers. Overexpression of SPARC has been shown to increase the risk of metastasis in various tumors such as melanoma, glioblastoma, clear-cell renal carcinoma, prostate carcinoma, breast and pancreatic ductal adenocarcinoma (Arnold and Brekken, 2009; Arnold et al., 2012; Nagaraju et al., 2014).

To investigate whether SPARC influences the migration of cells *in vitro*, PanIN and PAFs cells derived from KC-SPARC$^{-/-}$ and KC-SPARC^{wt} cells were subjected to wound healing assays without any exogenous stimulation. Wound healing assays were performed with KC-SPARC$^{-/-}$ (n=3) and KC-SPARC^{wt} (n=3) PAF cells showed no difference in terms of migration regardless of SPARC status (Fig. 15A). Similar results were obtained in wound healing assays performed with PanIN cells (Fig 15B). However, SPARC is predominantly secreted by activated fibroblast while there is almost no protein expression in the epithelial compartment as shown in Fig. 10. Therefore, to investigate if exogenous SPARC has any effect on wound healing properties of KC-SPARC$^{-/-}$PanIN cells, we performed wound healing assay upon stimulation with the conditioned media (culture supernatant) prepared from KC-SPARC$^{-/-}$ and KC-SPARC^{wt} PAFs. Result show that stimulation with PAF conditioned media did not influence the wound healing properties of KC-SPARC$^{-/-}$ PanIN cells (Fig. 15C).

A.

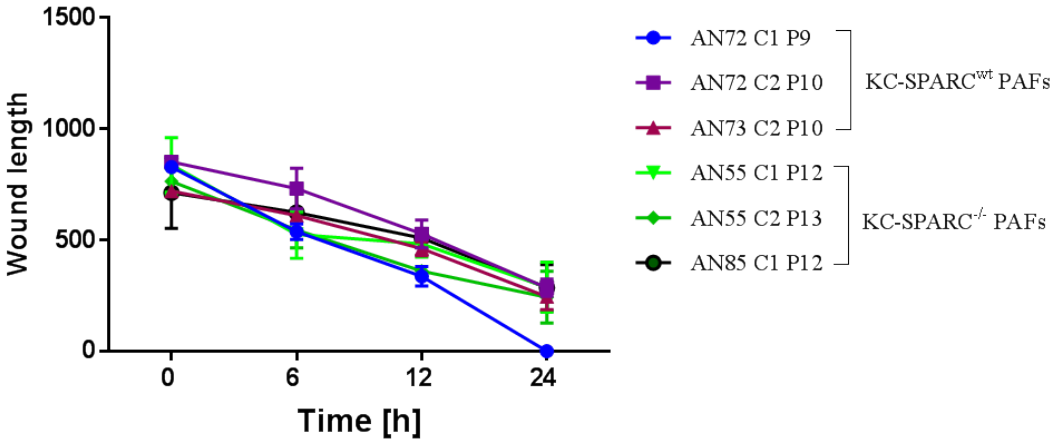

B.

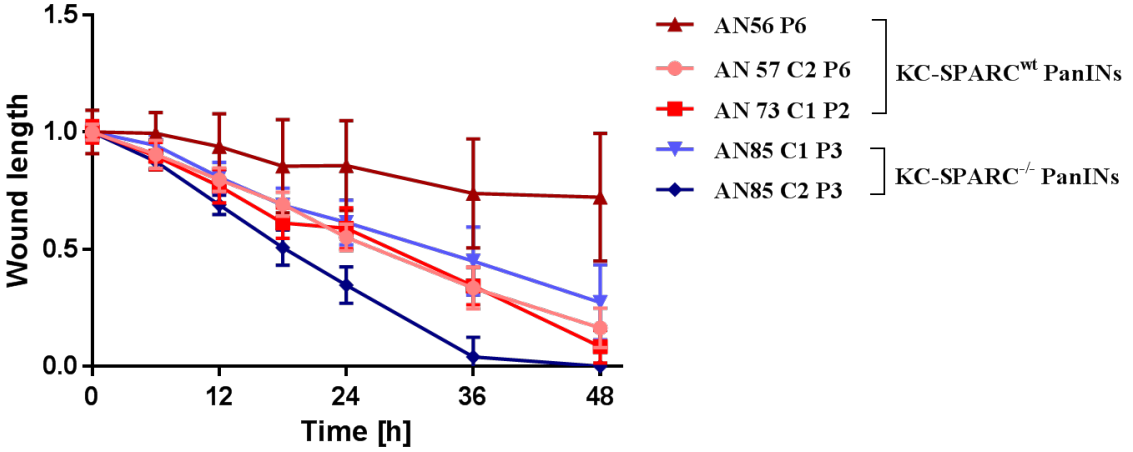

C.

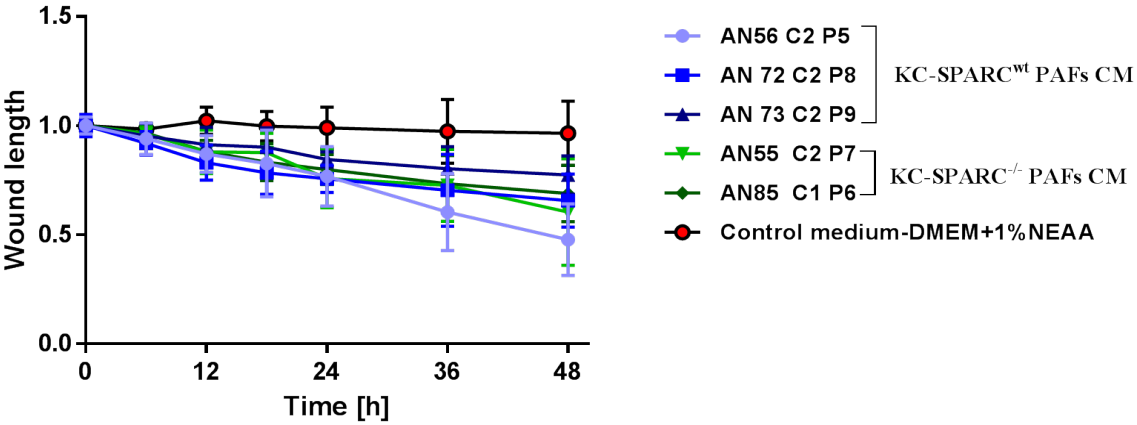

Figure 15: Wound healing assays performed in isolated primary (A) PAF cells and (B) PanIN cells from KC-SPARC^{wt} and KC-SPARC$^{-/-}$ mice shows that SPARC depletion does not affect the migration of both cell types in 2D based wound healing assays. (C) PanIN cells from KC-SPARC$^{-/-}$ were treated with conditioned media from PAFs derived from KC-SPARC^{wt} and KC-SPARC$^{-/-}$ mice and wound healing assays were performed showing no difference upon stromal derived SPARC.

4.4.6 SPARC and angiogenesis during early and late tumorigenesis

Angiogenesis is the process of forming blood vessels and it is important for tumor growth and to enhance metastatic spread. Angiogenesis is achieved through proliferation of endothelial cells. SPARC has been shown to play an anti-angiogenic role in various tumor entities such as gastric cancer and neuroblastoma (Chlenski et al., 2010; Zhang et al., 2012). To investigate whether stromal derived SPARC plays a pro- or anti-angiogenic role during tumorigenesis, immunohistochemistry was performed for CD31 in 3-4 months and 7-8 months old KC-SPARC$^{-/-}$ (n=10 and 11) and KC-SPARC^{wt} (n=7 and 9) pancreata bearing early and advanced PanIN lesions respectively. Interestingly, there was no significant difference between KC-SPARC^{wt} and KC-SPARC$^{-/-}$mice regarding mean vessel density in both the 3 months old cohort (p=0.66) and the 7-8 months old cohort (p=0.15).

A.

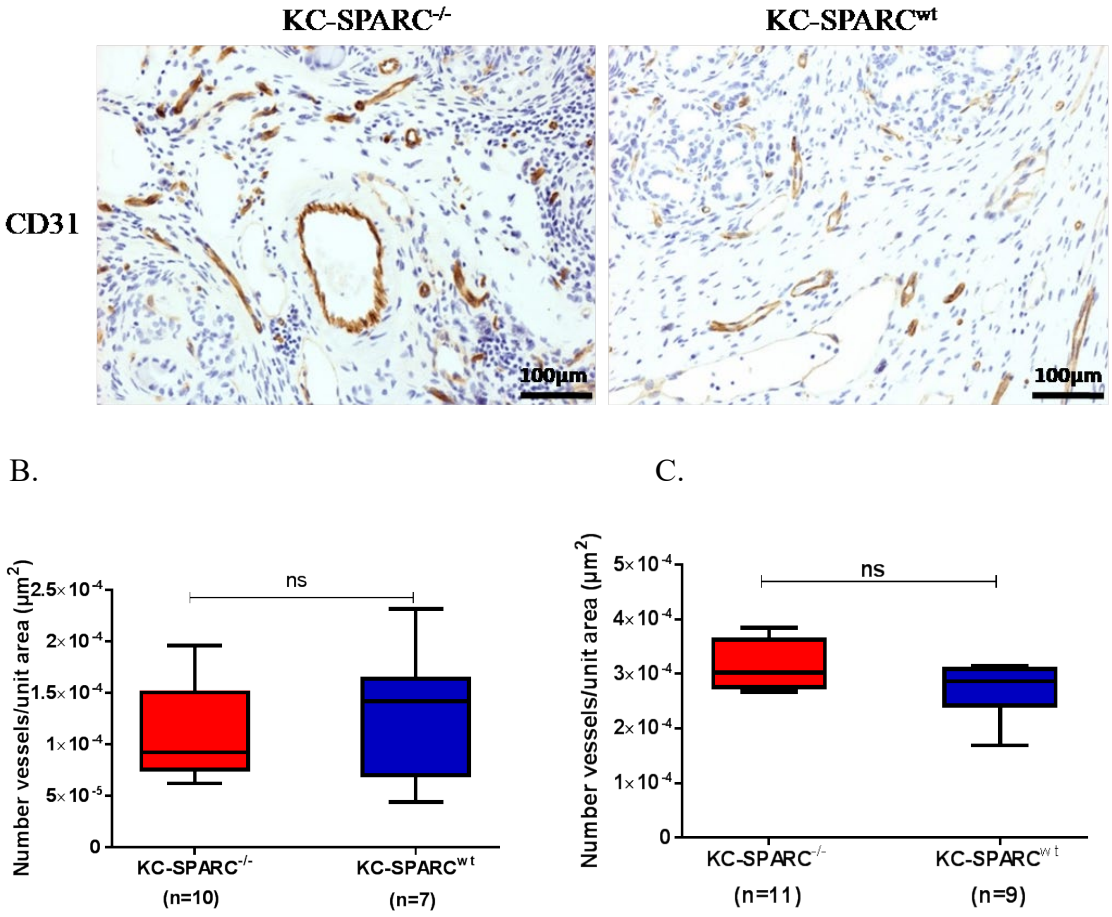

Figure 16: (A) Representative pictures of IHC-CD-31 in 3 months old pancreas tissues of KC-SPARC^{wt} and KC-SPARC$^{-/-}$ mice taken at10x magnification. (B&C) Graphs show no statistical significance in terms

of number of vessels between 3 months and 7-8 months old KC-SPARC^{wt} and KC-SPARC$^{-/-}$ mice (p=0.66) (p=0.15) respectively. Statistical analysis was performed using Mann-Whitney test.

4.5 SPARC in invasive adenocarcinoma

4.5.1 SPARC status does not affect the tumor incidence and the tumor weight

Both KC-SPARC$^{-/-}$ and KC-SPARC^{wt} mice developed invasive adenocarcinoma at about 12 or more months. The tumor incidence was calculated by dividing the number of mice that developed tumors by the total number of mice in the cohort. Tumor incidence analysis (Fig. 17A) revealed that both KC-SPARC$^{-/-}$and KC-SPARC^{wt} cohorts have comparable tumor incidences. In the KC-SPARC$^{-/-}$ cohort 26 mice out of 53 mice (49%) developed tumors while in the SPARC^{wt} cohort 19 mice out of 29 mice developed tumors (66%). Chi-square (Fisher's exact test) was used to assess the statistical significance (p=0.17). The weight of the whole tumors was recorded during the sample collection and the relative tumor weight was calculated by normalizing the tumor weight with body weight. The relative tumor weight analysis (Fig. 17B) showed that the tumors of KC-SPARC$^{-/-}$ (n=15) and KC-SPARC^{wt} (n=11) were of similar size (p=0.75). Mann Whitney test was used for statistical analysis.

A. B.

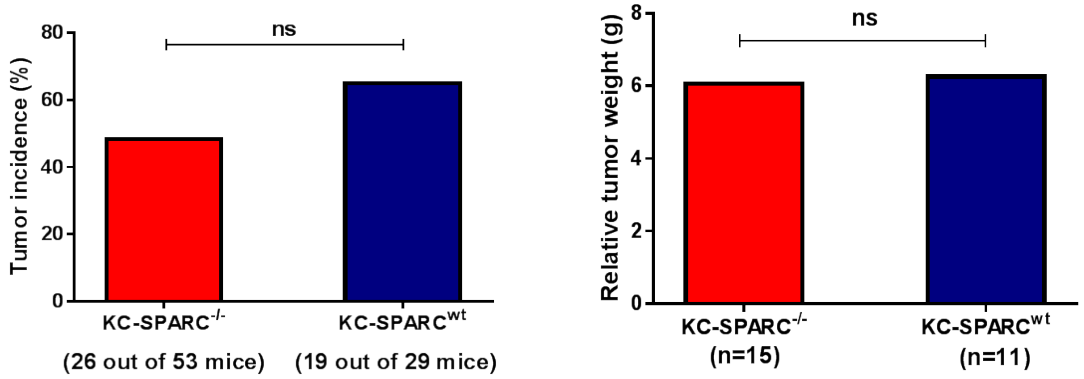

Figure: (A) Graph of tumor incidence in KC-SPARC$^{-/-}$(49%) and KC-SPARC^{wt} (66%) cohort. Statistical analysis was performed using Chi-square (Fisher's exact test) (p=0.17). (B) Graph of relative tumor weight of KC-SPARC$^{-/-}$ and KC-SPARC^{wt} mice tumors. Mann-Whitney test shows no statistical significance (p=0.75).

4.5.2 Collagen deposition was impaired upon SPARC depletion in established tumors

To explore the effect of SPARC depletion on collagen deposition in established murine pancreatic tumors we performed chemical stainings for collagen such as masson trichrome and picrosirius in tumor tissues of KC-SPARC^{wt} (n≥7) and KC-SPARC$^{-/-}$ (n≥17) mice. Consistent with the results in PanIN lesions (Figure 12), loss of SPARC resulted in a significant reduction of collagen deposition in established tumors (Fig. 20A). Quantification of masson trichrome and picrosirius staining was performed using an area based analysis in ImageJ software. The results of masson trichrome and picrosirius were expressed as % area fraction and % of picrosirius red positive area, respectively. Quantification of masson trichrome staining in tumor tissues of KC-SPARC$^{-/-}$ (13%) and KC-SPARC^{wt} (22%) mice revealed that the total collagen deposition was significantly reduced in KC-SPARC$^{-/-}$ tumors (p=0.04) (Fig. 20B). The significant reduction in collagen deposition was further confirmed by picrosirius staining analysis (p=0.01) (Fig. 20C).

A.

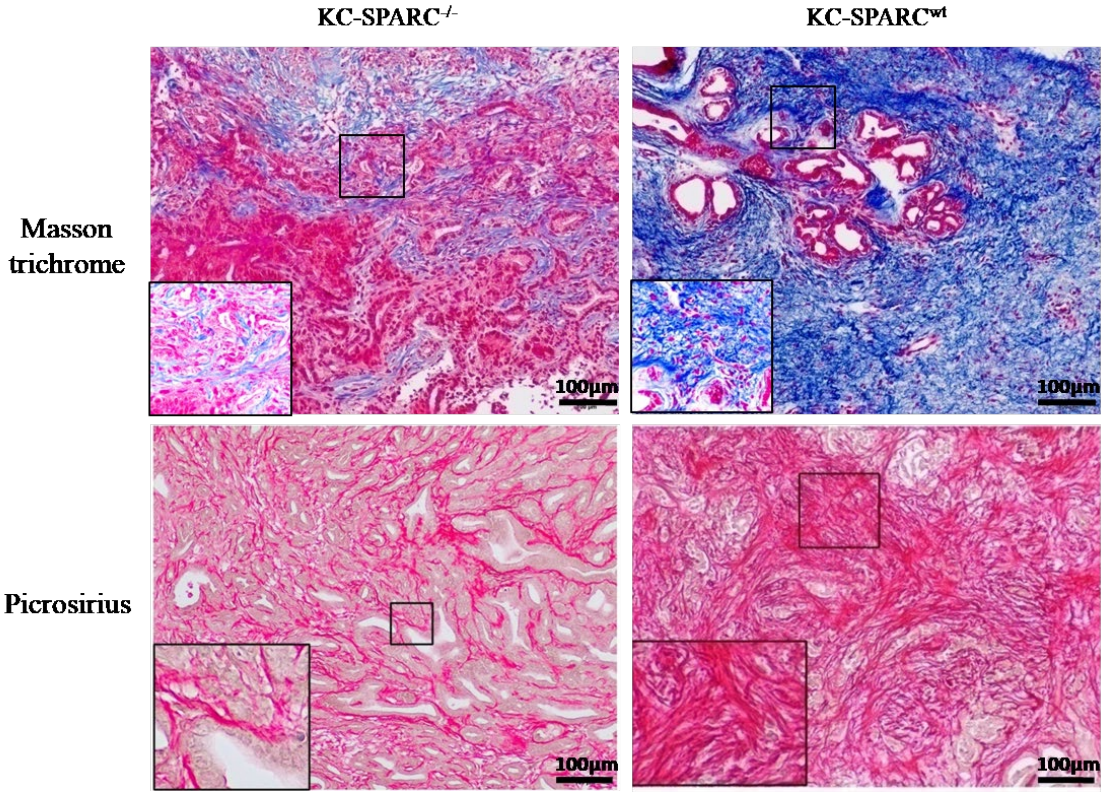

Figure 20: (A) Representative pictures of masson trichrome and picrosirius red stain in established tumor tissues of KC-SPARC$^{-/-}$ and KC-SPARC^{wt} mice. The images were taken at 10x magnification (inset40x magnification).

B.

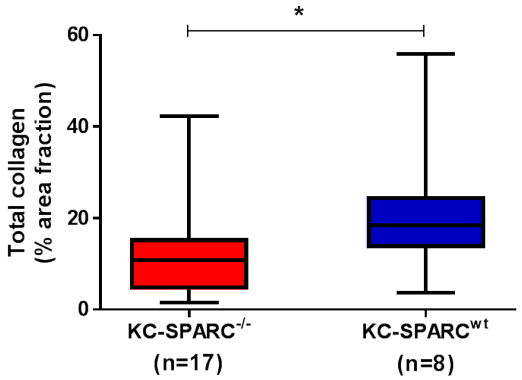

C.

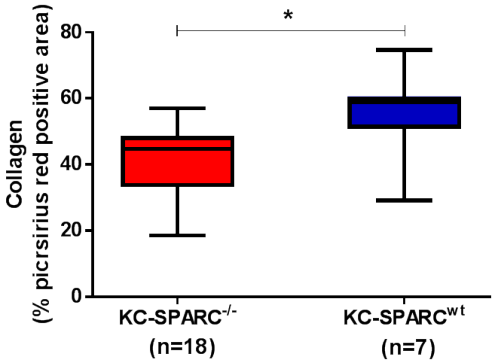

(B) Quantification of masson trichrome staining (p=0.04) and picrosirius red (p=0.01) shows significant reduction of collagen deposition in established tumors of KC-SPARC$^{-/-}$ mice. Mann-Whitney test was used to assess the statistical significance.*p≤0.05.

4.5.3 SPARC and hyaluronic acid deposition in tumor

HA is an abundant ECM component which has been shown to modulate the tumor microenvironment. HA is overexpressed in many tumors and the amount of HA is directly correlated with a poor prognosis in patients (Chanmee et al., 2016). The significance of HA expression and deposition has been described in many tumor entities such as breast, bladder and pancreatic cancer (Mahlbacher et al., 1992)(Lokeshwar et al., 1997; Yahya et al., 2014). In pancreatic cancer, HA has been shown to promote tumor growth (Sato et al., 2003, 2016).

Therefore, to investigate whether SPARC affects HA deposition in established KC tumors, chemical staining for HA in established tumors of KC-SPARC$^{-/-}$ (n=17) and KC-SPARC^{wt} (n=8) mice was performed. Quantification of HA staining showed similar amount of accumulation of HA in the tumors of KC-SPARC$^{-/-}$ and KC-SPARC^{wt} mice (p=0.97) and thus revealed that SPARC status does not affect HA accumulation in established tumors (Fig. 21A & B).

A.

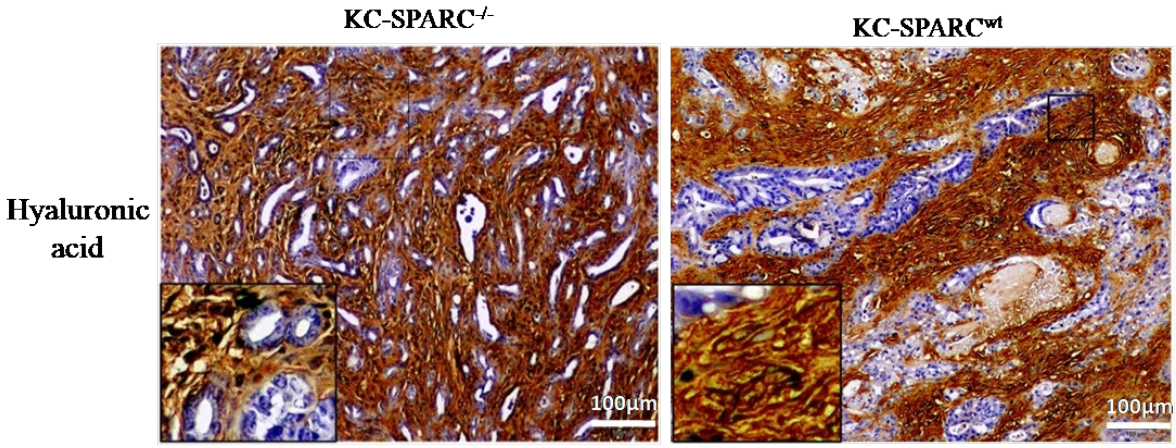

B.

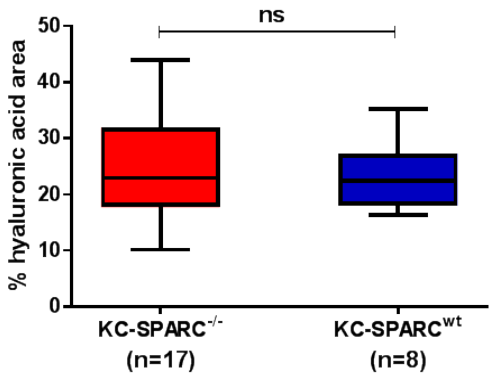

Figure 21: (A) Representative pictures of HA stainings in KC-SPARC$^{-/-}$ and KC-SPARC^{wt} tumors. Both KC-SPARC$^{-/-}$ and KC-SPARC^{wt} tumors show extensive accumulation of HA. (B) Quantification of HA staining shows that SPARC depletion does not affect HA accumulation in tumors (p=0.97).Mann-Whitney test shows no statistical significance.

4.5.4 SPARC depletion does not affect fibroblast density in established tumor

As shown in the early tumorigenesis cohort, we investigated if SPARC affected the fibroblast population in established tumor by performing IHC for α-SMA in the tumor tissue sections of KC-SPARC$^{-/-}$(n=16) and KC-SPARC^{wt} (n=8) mice. Consistent with the results shown in the early PanIN cohort (Fig. 13A &B), the fibroblast density was not altered in established tumors upon SPARC depletion (16% vs 15% KC-SPARC$^{-/-}$and KC-SPARC^{wt} tumors) (p=0.78) (Fig. 22).

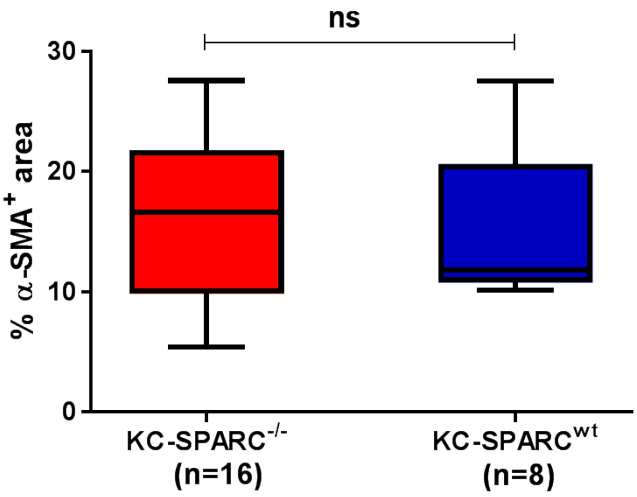

Figure 22: Graph shows that α-SMA positive fibroblast density was not altered upon SPARC depletion (p=0.78). Mann-Whitney test shows no statistical significance.

4.5.5 Tumor proliferation and apoptosis were not affected by stromal SPARC

Uncontrolled proliferation and decreased apoptosis are the hallmark features of tumors. An increased number of proliferating cells and decreased rate of cell death result in tumor growth and aggressiveness. To assess the proliferation index of tumors in KC-SPARC$^{-/-}$ (n=6) and KC-SPARC^{wt} (n=7) mice, IHC for Ki67 was performed (Fig 23A- top images). The proliferation index was determined by dividing the number of Ki67 positive nuclei by the total number of nuclei and was expressed as % of Ki67 positive cells. To assess the apoptotic rate of the tumor, IHC for Cleaved Caspase 3 (CC3) was performed in tumor tissues of KC-SPARC$^{-/-}$ (n=12) and KC-SPARC^{wt} (n=7) mice (Fig 23A-bottom images). Percentage of apoptotic nuclei was assessed using similar formula as mentioned above.

Analysis of IHC-Ki67 shows that both KC-SPARC$^{-/-}$ and KC-SPARC^{wt} tumors have similar proliferation index and thus revealed that stromal SPARC does not affect overall proliferation (Fig. 23B). The mean proliferation index of KC-SPARC$^{-/-}$ and KC-SPARC^{wt} tumors were 24% and 29% respectively (p=0.44). In line with the proliferation index, IHC-CC3 analysis showed no difference in apoptotic cells between the tumors of KC-SPARC$^{-/-}$ and KC-SPARC^{wt} mice (0.82% vs 0.86%; p=0.85) (Fig. 23C).

A.

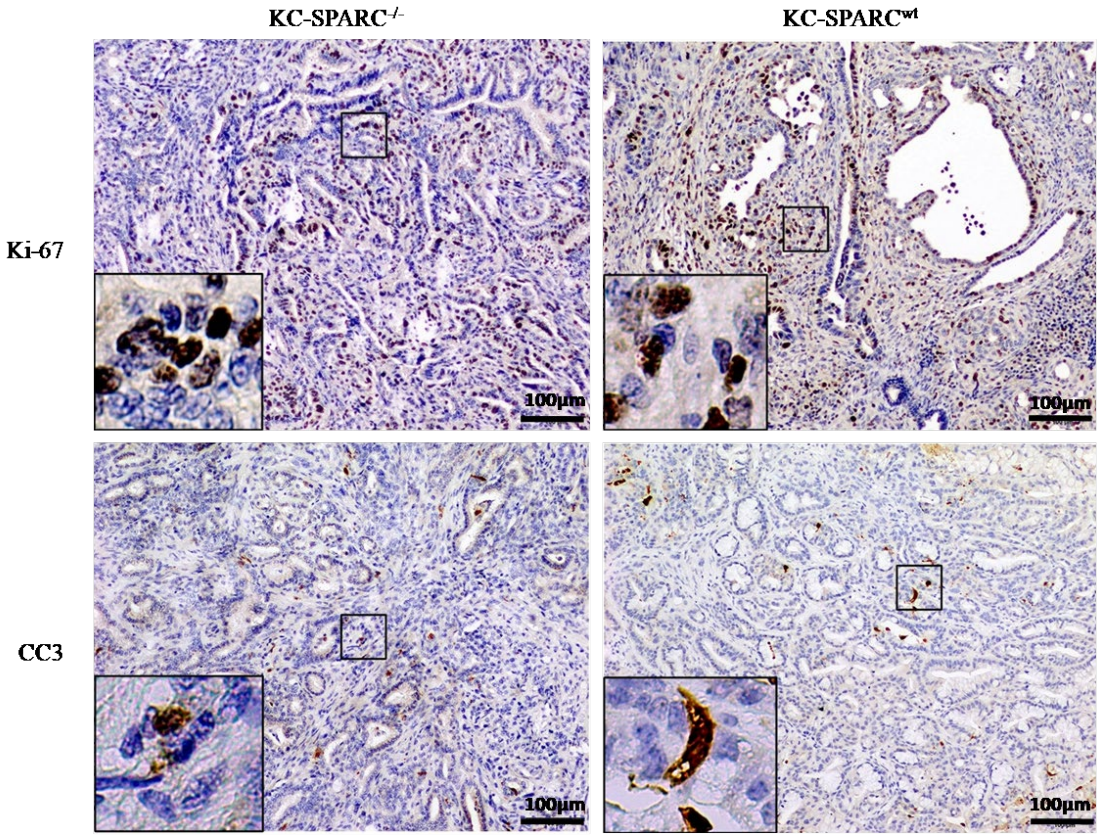

B.

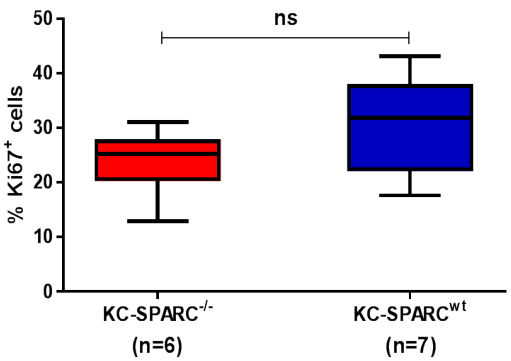

C.

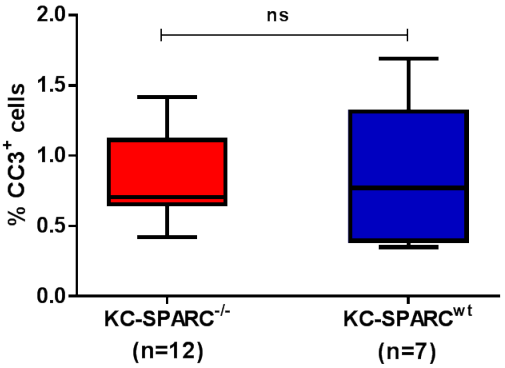

Figure 23: Representative pictures of IHC-Ki-67 and IHC-CC3 in KC-SPARC^{wt} and KC-SPARC$^{-/-}$ tumors. (B) Quantification of IHC-Ki67 (p=0.44) and C) IHC-CC3 (p=0.85) shows that proliferation and apoptosis was not affected by stromal SPARC expression.

4.5.6 SPARC status has no correlation with liver metastasis burden

To see whether SPARC influences metastatic spread, we performed metastatic score analysis in H&E stained liver sections of tumor bearing KC-SPARC$^{-/-}$ (n=15) and KC-SPARC^{wt} (n=10) mice. The average number of liver metastasis per mouse was assessed

by counting the number of liver metastases in H&E stained liver sections. 5 serial sections were used per mouse. Liver metastases ranging from 100-200µm were considered as micro-metastases, and liver metastases with a size larger than 200µm were considered as macro-metastases. Each macro-metastasis was multiplied by 3 for the final count. Finally, the average number of liver metastasis per mouse was calculated by dividing the total number by 5. This analysis revealed that both KC-SPARC$^{-/-}$(n=15) and KC-SPARC^{wt} (n=10) tumor bearing mice cohort have comparable metastatic score (p=0.14).

A.

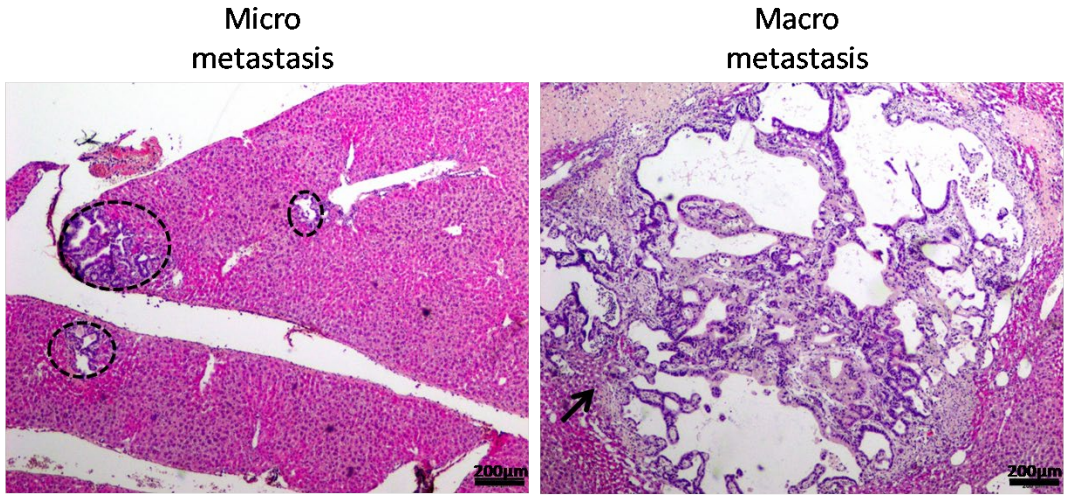

B.

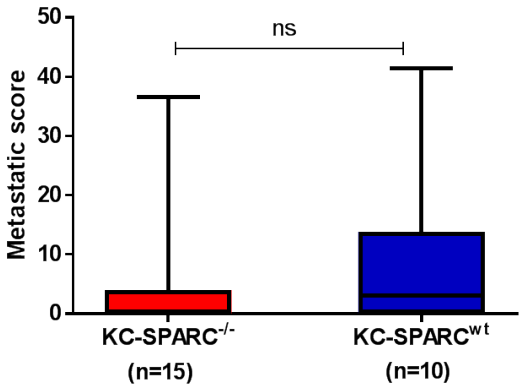

Figure 24: Representative H&E staining pictures show the micro (left) and macro (right) metastasis in the livers of tumor bearing KC-SPARC^{wt}. (B) Metastatic score comparison of KC-SPARC^{wt} and KC-SPARC$^{-/-}$ mice showing similar metastatic burden for both genotypes (p=0.14).

4.6 Survival analysis

4.6.1 Overall survival analysis

Overall survival analysis of KC-SPARC$^{-/-}$ (n=90) and KC-SPARC^{wt} (n=44) mice was performed using Kaplan Meier Curve. Overall survival refers to the survival of all mice that died for tumor related health concerns as well as other reasons. The mice were sacrificed using the endpoint criteria such as persistent pain, open wounds, dyspnea, diarrhea, weight loss>20%, ascites or inactivity. The remaining mice were sacrificed after 20 months. Overall survival analyses revealed that KC-SPARC$^{-/-}$mice had a shorter survival than KC-SPARC^{wt} mice (median survival- 390 vs 471 days). However, the difference was not statistically significant (p=0.77; Fig. 25).

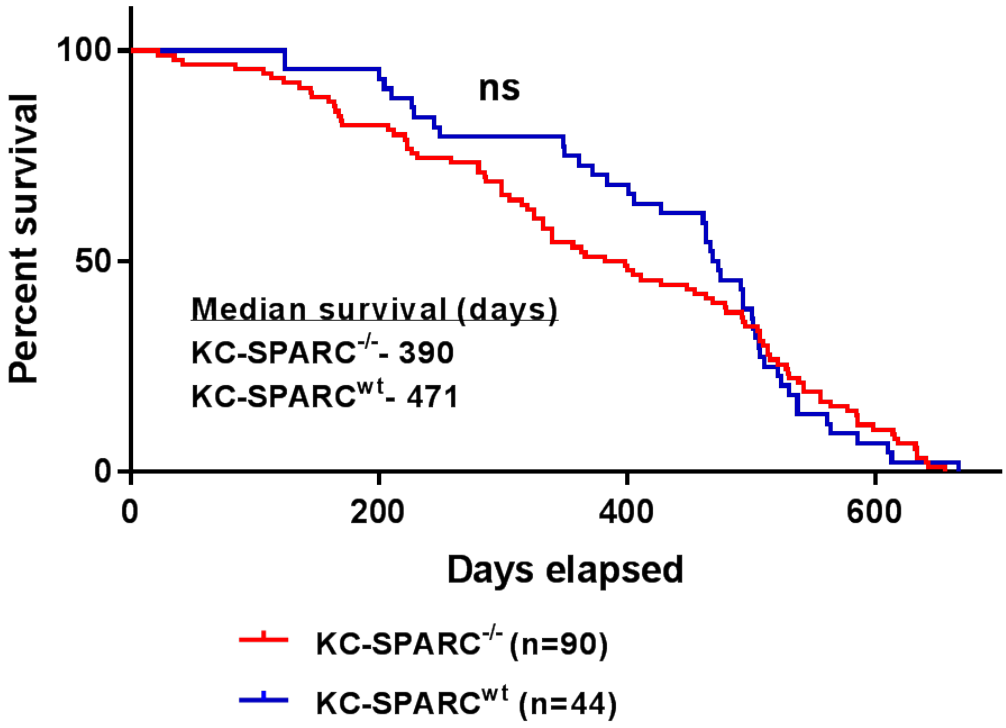

Figure 25: Kaplan Meier curve showing overall survival of KC-SPARC$^{-/-}$(n=90) and KC-SPARC^{wt} (n=44) mice. KC-SPARC^{wt} and KC-SPARC$^{-/-}$ have median survival of 471 and 390 days respectively (p=0.77). Log-rank (Mantel-cox) test was used to assess the statistical significance.

4.6.2 Tumor related survival analysis

Tumor related survival of KC-SPARC$^{-/-}$ (n=25) and KC-SPARC^{wt} (n=16) mice was assessed by comparing the survival days of mice which died from tumor-related health concerns. Tumor status was confirmed by visual observation of tumors upon necropsy and subsequent H&E staining. Tumor related survival analysis shows that tumor bearing KC-SPARC$^{-/-}$ mice live significantly shorter (p=0.02). The median survival of tumor bearing KC-SPARC$^{-/-}$ and KC-SPARC^{wt} mice was 280 and 485 days respectively (Fig. 26).

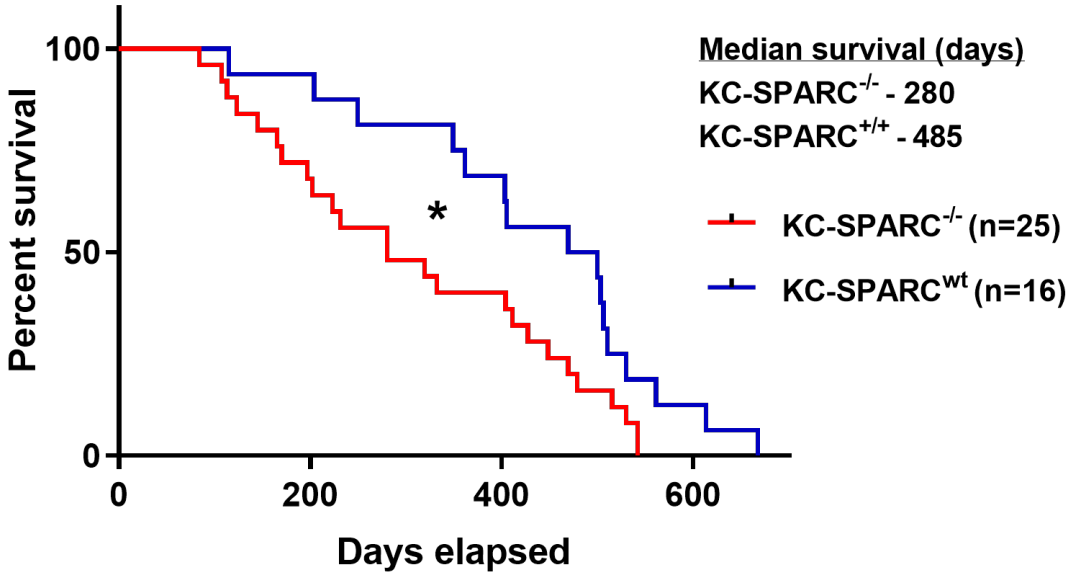

Figure 26: Kaplan Meier Curve of tumor-related survival shows that KC-SPARC^{wt} have a significantly prolonged survival compared to KC-SPARC$^{-/-}$ mice (485 days versus 280 days; p=0.02).

4.6.3 Tumor bearing KC-SPARC$^{-/-}$ mice show severe tumor related complications

Even though KC-SPARC$^{-/-}$and KC-SPARC^{wt} reveal comparable biological characteristics of their primary tumor and metastatic lesions (proliferation, apoptosis and liver metastasis status), stromal SPARC ablation resulted in a significantly shortened survival. One possible reason for this survival difference might be a more severe disease course and a higher and earlier complication rate in KC-SPARC$^{-/-}$ mice upon pancreatic tumor development. Table.1 depicts the recorded clinical complications following tumor development that prompted sacrifice of the mice. Even though the single parameters did not reach statistical significance, the accumulation of several factors such as ascites, biliary obstruction and diarrhea occurred more frequently in KC-SPARC$^{-/-}$ mice and might serve as a feasible explanation for the observed survival difference.

	Tumor				p-value
	KC-SPARC$^{-/-}$ (n=26)		**KC-SPARC^{wt} (n=18)**		
Ascites	4	(15%)	0		p=0.13
Jaundice	4	(15%)	1	(6%)	p=0.63
Cachexia	3	(12%)	2	(11%)	p>0.9
Bowel related complaints (Obstruction, dilation and ischemic)	3	(12%)	2	(11%)	p>0.9
Incidence of macrometastasis	3	(12%)	4	(22%)	p=0.41
Abdominal hemorrhage	2	(8%)	2	(11%)	p>0.9
Spleen enlargement	3	(12%)	1	(6%)	p=0.63
Diarrhea	2	(8%)	0		p=0.50
Hypothermia	1	(4%)	1	(6%)	p>0.9

Figure 27: Table shows the comparison of clinical features of tumor bearing KC-SPARC$^{-/-}$ and KC-SPARC^{wt} at endpoint.

4.7 SPARC does not affect gemcitabine delivery and metabolism

4.7.1 SPARC mediated collagen deposition does not affect gemcitabine delivery and metabolism in murine pancreatic tumors

SPARC is a modulator of desmoplasia. In the presented work, I have shown a significant reduction of collagen deposition upon SPARC depletion in murine pancreatic tumors. Extensive ECM deposition (especially collagen) has been shown to impede drug delivery and drug response (Dangi-Garimella et al., 2011; Khan et al., 2016; Olive et al., 2009). Recently, overexpression of collagen genes were found to associated with drug resistance in ovarian cancer (Januchowski et al., 2016; Sherman-Baust et al., 2003).

To investigate whether SPARC mediated ablation of ECM components such as collagen has any effect on delivery and metabolism of gemcitabine, we have treated tumor bearing KC-SPARC$^{-/-}$ (n=10) and KC-SPARC^{wt} (n=6) mice with gemcitabine (100mg/kg/body weight) and sacrificed animals 2h after the gemcitabine administration. Prior work had shown that peak levels of gemcitabine are detected about 2h after intraperitoneal administration (Neesse et al PNAS 2013). Metabolites of gemcitabine were then analyzed in freshly frozen bulk tumor tissue by LC-MS/MS.

Gemcitabine is a prodrug which has to be further metabolized into a functionally active drug by subsequent phosphorylations. Difluorodeoxycytidine (dFdC) is transported into the cells by human nucleoside transporters (hENTs) and phosphorylated by deoxycytidine kinase (dCK) enzyme to form difluorodeoxycytidine monophosphate (dFdCMP), which is further phosphorylated to form difluorodeoxycytidine diphosphate (dFdCDP) and difluorodeoxycytidine triphosphate (dFdCTP) (Heinemann et al., 1988). dFdCTP is the cytotoxic form of gemcitabine. Upon incorporation into DNA, it inhibits the function of DNA polymerase and thus terminates chain elongation.

In contrast to previously published data on collagen and drug delivery in murine pancreatic cancer, SPARC mediated collagen deposition in established KC-SPARC^{wt} tumors did not impede drug delivery or affect metabolism of gemcitabine compared to collagen-poor tumors in KC-SPARC$^{-/-}$mice. There was no difference in terms prodrug (dFdC) accumulation (p=0.11) (Fig. 28B), the amount of activated metabolite (dFdCTP) (p=0.11) (Fig. 28C), and the amount of inactivated metabolite (dFdU) (p=0.79) between the collagen-rich (KC-SPARC^{wt}) and collagen-poor tumors. This finding is surprising and contradicts previous studies which suggested that the extensive ECM (especially

collagen) deposition could impede drug delivery (Dangi-Garimella et al., 2011; Khan et al., 2016; Olive et al., 2009).

A.

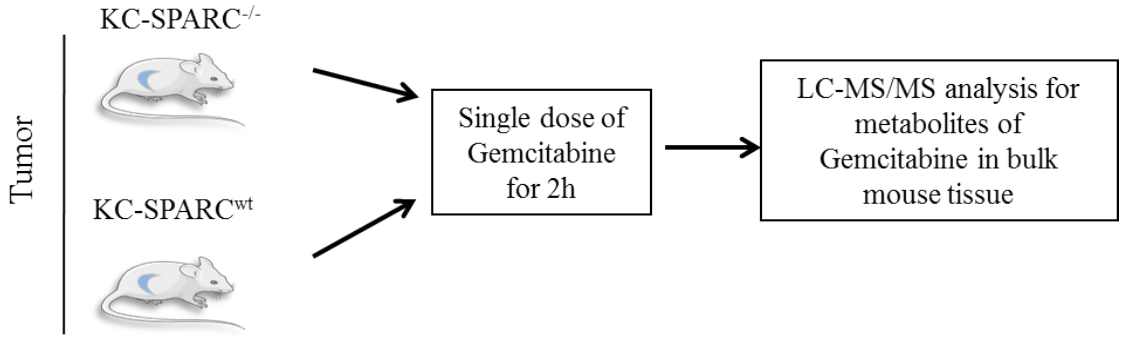

B.

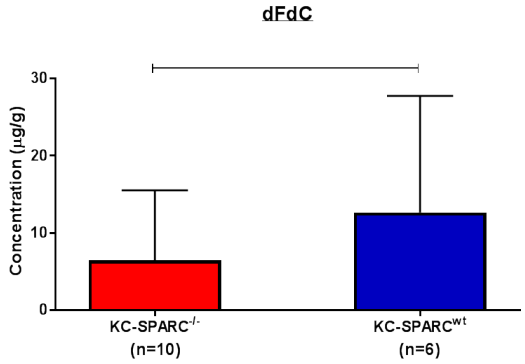

C.

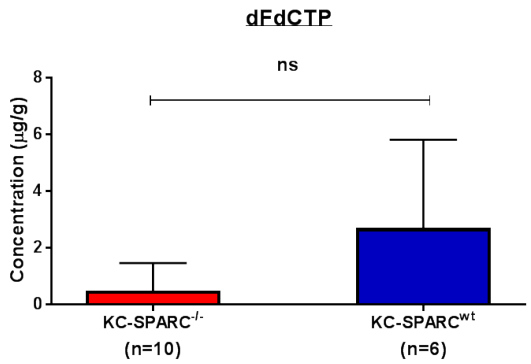

D.

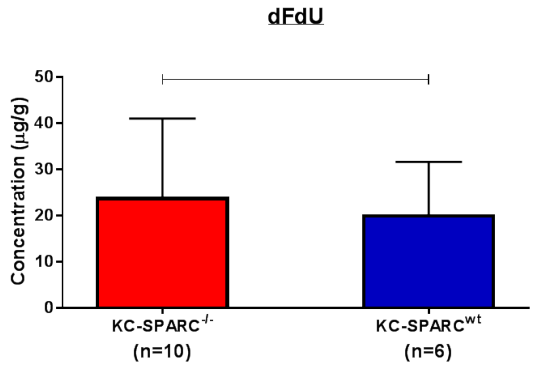

Figure 28: (A) Schematic diagram shows the experimental plan. LC-MS/MS analysis of gemcitabine metabolites (B) dFdC, (C) dFdCTP and (D) dFdU shows that there is no difference in terms of the amount of dFdC (p=0.11), dFdCTP (p=0.11) and dFdU (p=0.79) between collagen-rich tumors (KC-SPARC^{wt}) and collagen-poor tumors (KC-SPARC$^{-/-}$). Mann Whitney test was used to assess the statistical analysis.

4.7.2 Overall cellularity but not the SPARC mediated collagen deposition affects drug accumulation and metabolism

As shown above, SPARC mediated collagen deposition does not affect drug delivery and metabolism of gemcitabine in murine pancreas tumors. Further experiments were aimed to investigate whether drug uptake and metabolism between normal pancreas and different stages of tumorigenesis would differ in order to understand the role of desmoplasia and drug accumulation. In order to achieve this, wildtype mice with healthy pancreata (n=6), mice bearing PanIN lesions (n=8) and tumor bearing KC-SPARC^{wt} mice (n=4) were treated with gemcitabine (100mg/kg/body weight) 2h prior to sacrifice, and gemcitabine metabolites were analyzed in freshly frozen bulk tissues by LC-MS/MS.

The analysis revealed a gradual increase in native gemcitabine metabolite (dFdC) between normal pancreas, PanIN lesions and murine pancreatic tumors derived from KC-SPARC^{wt} mice (Fig. 29A). However, dFdC was rapidly inactivated to dFdU in a significant amount in the tumors (Fig. 29C). Hence, there was no significant difference in the amount of activated gemcitabine metabolites (dFdCTP) between normal pancreas, PanIN lesions and tumors (Fig. 29B).

The accumulation of dFdC was found to be significantly higher in murine tumors (n=4) (15 times more) compared to healthy control pancreas (n=6) (p=0.009). This is surprising due to the fact that the normal pancreas tissue has a much better vascularization than the tumor (Hessmann et al., 2018; Olive et al., 2009). Therefore, one would expect increased accumulation of the pro-drug in normal pancreas compared to hypovascular pancreatic tumors. We hypothesized that the cellularity (both stromal and epithelial cells) might determine LC-MS/MS results for gemcitabine metabolites as an increased number of epithelial and stromal cells might also increase the number of intracellularly measured gemcitabine metabolites. To this end, DAPI staining and IHC for pan-cytokeratin and α-SMA were performed to assess the overall epithelial and stromal cellularity. And indeed, an increased cellularity was detected in PanIN lesions and murine tumors compared to normal pancreas. Analysis of DAPI staining revealed that the total number of nuclei was significantly higher in tumor tissue (average 930 nuclei) compared to normal pancreas (average 503 nuclei) (Fig. D & E) (p=0.002).

Additionally, IHC-pan-cytokeratin and IHC-α-SMA analysis revealed that there is a significant increase in epithelial and mesenchymal cell population in murine tumors compared to PanIN lesions (Fig. 29 F-H) (p=0.04 and p=0.0007 respectively). Normal pancreas tissue sections were not included in the staining panel as it is well known that both epithelial (ductal) and the fibroblast cell populations are significantly lower in the healthy pancreata.

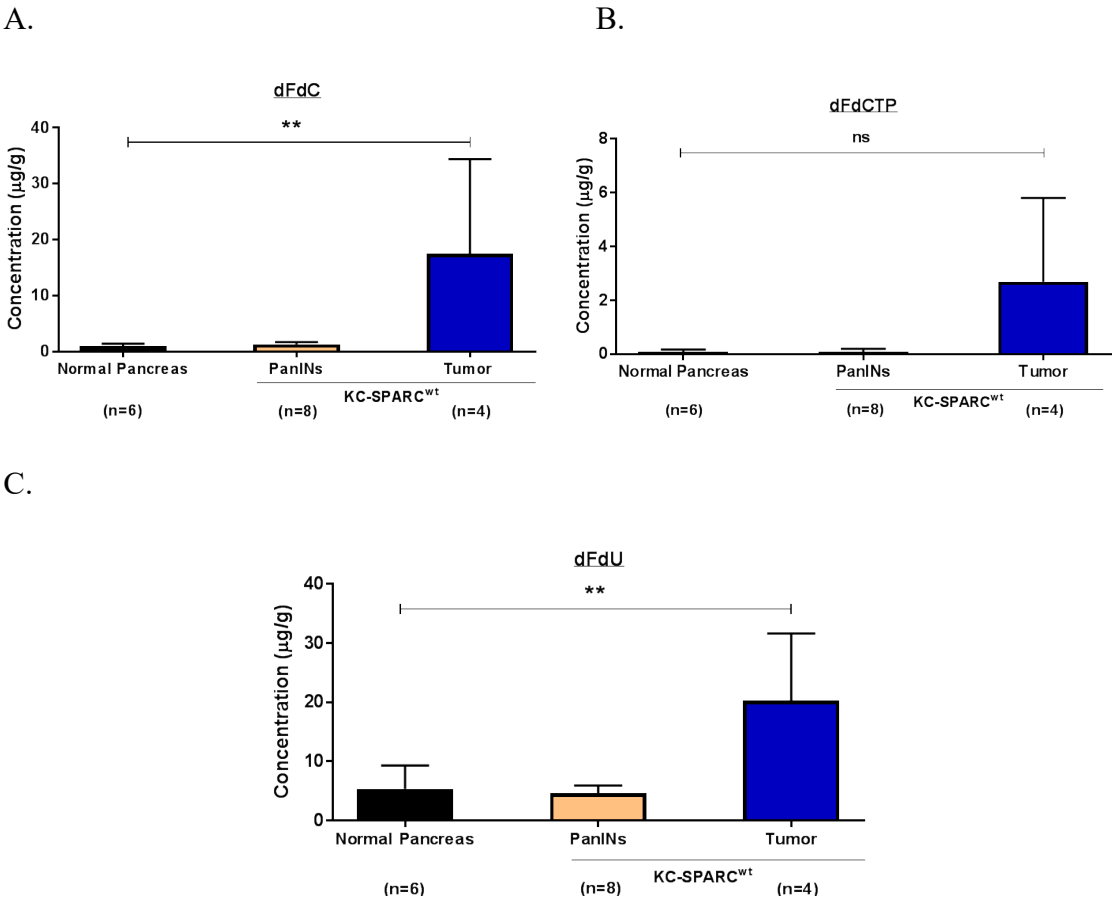

Figure 29: LC-MS/MS analysis of gemcitabine metabolites (A) dFdC, (B) dFdCTP and (C) dFdU in normal pancreas (n=6), PanIN lesions (n=8) and pancreatic tumors (n=4) of KC-SPARC^{wt} mice.

D.

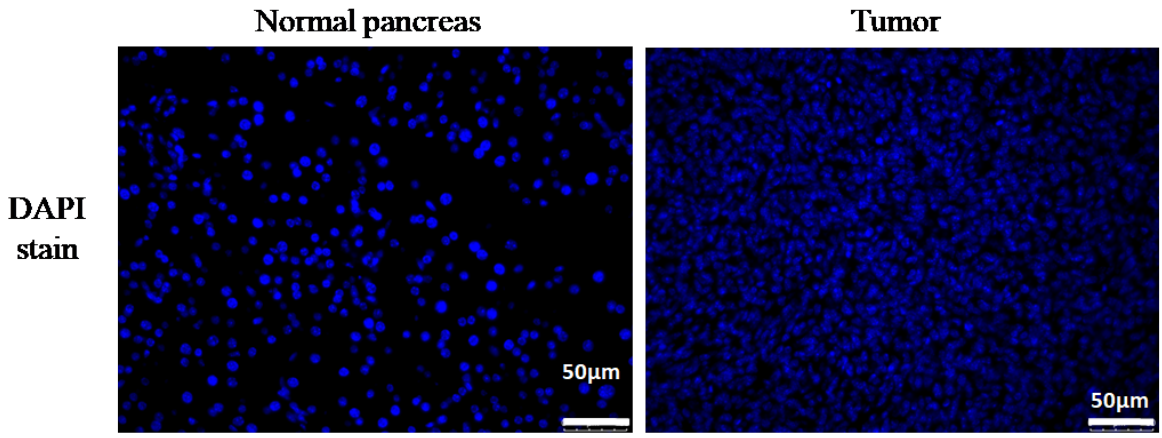

E.

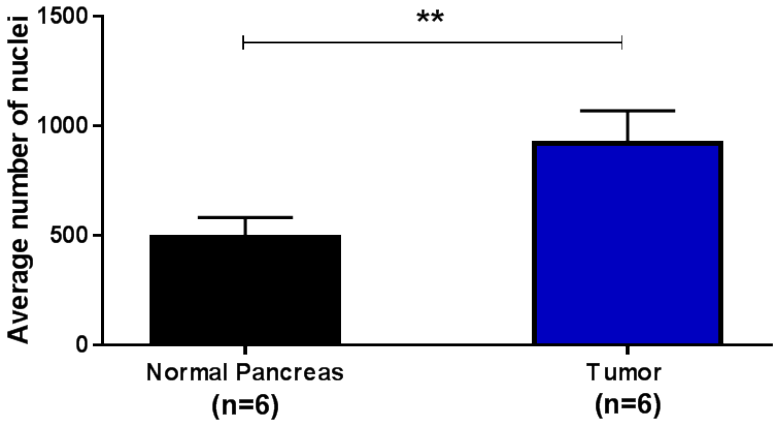

(D) Representative pictures of DAPI staining in control pancreas and KC-SPARC^{wt} tumor tissue. (E) The quantification of total nuclei in normal pancreas and tumor of KC-SPARC^{wt} mice shows a significant increase in overall cellularity in tumors compared to normal pancreas (p=0.002).

F.

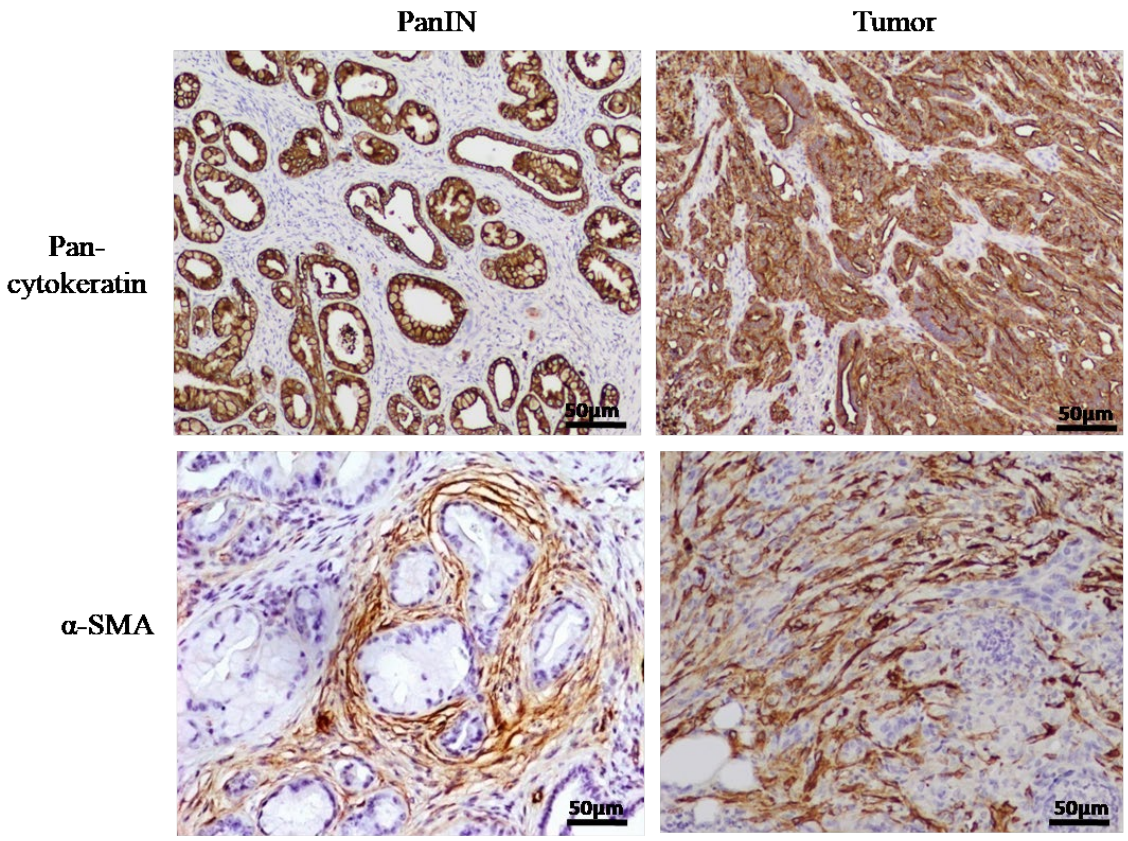

G.

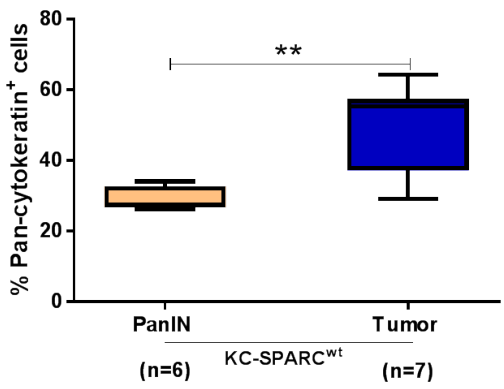

H.

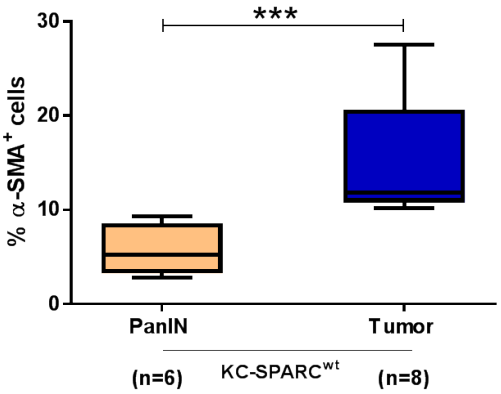

(F) Representative pictures of IHC-pan-cytokeratin and IHC-α-SMA in PanIN lesions and tumor tissue shows the increase in cellularity of epithelial and stromal compartment between PanIN lesions and tumors. (G&H) Quantification of pan-cytokeratin and α-SMA showing the increase in cellularity of epithelial and stromal compartments in PanIN lesions compared to tumors. Mann Whitney test was used to assess the statistical significance. ** $p \leq 0.01$ and *** $p \leq 0.005$.

4.7.3 Gemcitabine is enzymatically inactivated by drug metabolizing enzymes

Overexpression of the inactivating enzymes of gemcitabine is directly associated with drug resistance. Cytidine deaminase (CDA), and Cytosolic 5-Nucleotidase 1A (Nt5c1A) are the two major inactivating enzymes of gemcitabine nucleosides (Mini et al., 2006). In the previous part I had shown that a significant amount of pro-drug accumulated in tumor tissue compared to the normal and pre-neoplastic tissues. Although there was a trend towards more dFdCTP in tumor tissues, no significant difference of dFdCTP between the normal pancreas tissue, PanIN lesions and murine tumors was detected by LC-MS/MS (Fig. 29B). One possible explanation for this could be that rapid inactivation of dFdC occurred through CDA (dFdC to dFdU) and Nt5c1A (dFdCMP to dFdC). Indeed, IHC confirmed the strongest expression of Nt5c1A and CDA in murine tumors compared to PanINs and normal pancreas tissue (Fig. 30).

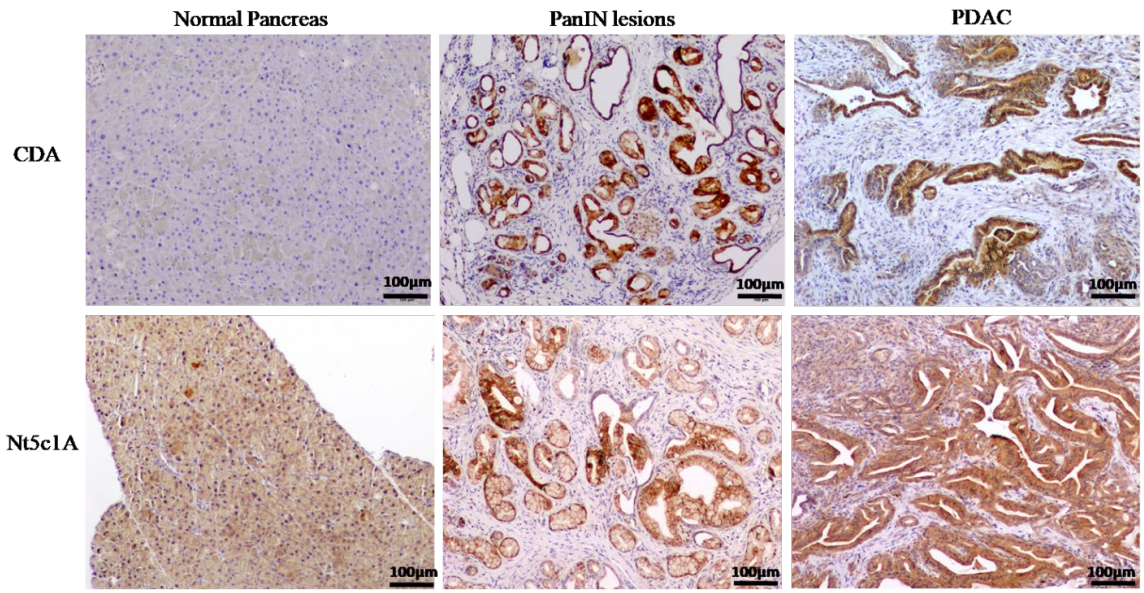

Figure 30: Representative pictures of IHC-CDA and IHC-Nt5c1A in normal pancreas, PanIN lesions and tumors show increased expression in PanIN lesions, and robust overexpression in murine tumor compared to normal pancreas tissue.

5. Discussion

The tumor microenvironment (TME) in PDAC is histologically composed of various components such as acellular and cellular stromal compartments. Each compartment has been shown to contribute to the initiation and progression of the disease. However, depletion of certain cellular components such as CAFs in several GEMMs of PDAC has led to a more aggressive and undifferentiated phenotype suggesting that certain components of the TME are tumor-suppressive whereas others are tumor-promoting (Özdemir et al., 2014; Rhim et al., 2014). SPARC is a matricellular protein that has been shown to be involved in various cellular processes such as development and wound healing. Aberrant SPARC expression is associated with various diseases such as renal fibrosis and arthritis. SPARC expression has also been described in various tumors. In PDAC, SPARC is overexpressed by activated fibroblasts of the tumor stroma and correlates with poor clinical outcome (Infante et al., 2007; Mantoni et al., 2008). Though, extensive research has been done on SPARC, its exact role in PDAC and the mechanism involved are yet a matter of debate. Therefore, analyzing the role of SPARC during different stages of PDAC tumorigenesis using GEMMs may shed light into the role of SPARC in PDAC.

5.1 Advantages and disadvantages of genetically engineered mice used in this study

In our study, we have provided a detailed insight into the phenotypic characterization of the mouse models including SPARC$^{-/-}$, KC-SPARC$^{-/-}$ and KC-SPARC^{wt}. As described previously (Gilmour et al., 1998; Norose et al., 1998b; Yan and Sage, 1999), we have observed SPARC knockout related phenotypes such as fragile bones and cataractogenesis in both SPARC$^{-/-}$and KC-SPARC$^{-/-}$ mice. In addition, we have observed a trend towards reduced overall body weight as well as organ weight in SPARC knockout mice compared to SPARC^{wt}. Though these phenotypes are not lethal, SPARC$^{-/-}$ mice may be more susceptible to tumor related complications such as weight loss, cachexia and ascites. This limitation could be circumvented by using a pancreas specific SPARC knockout mouse instead of a germline SPARC knockout system. Thus, collagen impairment in the muscle, bone and other tissues such as the cornea would not be affected. However, major advantages of the KC mouse model are the slow progression of ADM and PanIN lesions that eventually progress to frank carcinomas only after >8-10 months. In addition, pancreatic precursor lesions are surrounded by a dense

extracellular matrix that resembles the histological features in human preneoplasia. Thus, the KC mouse models allow a detailed histological and molecular characterization at different stages of tumorigenesis, and eventually tumor growth and metastasis upon SPARC depletion. This prompted us to allocate KC mice into different age groups with well characterized preneoplastic lesions. However, a major drawback of p48-Cre driven mouse models is the fact that oncogenic Kras mutations are initiated during embryonic stages at day 8.5, and all p48 expressing cells bear an activating $Kras^{G12D}$ mutation. This is in stark contrast to human PDAC in which the tumor normally develops only at one site in the pancreas (head, body or tail) and from one or very few cell clones.

From a technical and experimental point of view, GEMMs are expensive and time consuming due to multiple crosses and genotyping that is required to obtain the correct genotypes.

5.2 Cancer associated fibroblast in PDAC

The significance of CAFs and their ability to modulate PDAC stroma by secreting extensive amount of ECM proteins, MMPs and tissue inhibitors of MMPs have been unnoticed for decades (Phillips et al., 2003). Later, the contribution of CAFs in PDAC progression and the potential cross talks between neoplastic cells and CAFs have been described by many *in vitro* and *in vivo* studies. *In vitro* co-culture experiments have shown that both CAFs and tumor cells reciprocally contribute to their proliferation and migration which indeed results in tumor progression and metastasis (Kikuta et al., 2010; Vonlaufen et al., 2008b). Studies have also explored the signaling pathways involved in the interaction between these two different compartments. Tumor cells are known to influence the CAFs to produce more ECM through TGFß1, FGF2, and the increased proliferation of CAFs is known to be associated with the secretion of tumor PDGF, respectively (Bachem et al., 2005; Yoshida et al., 2004; Yoshida et al., 2005). The cross-talk between CAFs and tumor cell was further validated by *in vivo* studies using xenograft models in which an increase in tumor growth was reported upon co-injection of CAFs and tumor cells compared to tumors cells alone. It has been also shown that the amount the tumor cells was also significantly increased upon co-injection which is supporting the fact that CAFs contribute to the proliferation of tumor cells (Bachem et al., 2005). Similar results were obtained in an orthotopic model in which co-implantation of human PDAC cells and human PSCs led to significant increase in tumor growth and metastasis (Hwang et al., 2008). Considering the tumor promoting roles of CAFs in PDAC, many groups

have recently attempted to target CAFs to improve therapeutic outcome. Even though few initial studies in preclinical models have shown convincing results (Olive et al 2009), most of those studies failed as the depletion of CAFs resulted in unfavorable tumor characteristics. This might be due to the fact that CAFs also have certain anti-tumorigenic roles (Froeling et al., 2011; Özdemir et al., 2014; Rhim et al., 2014).

Initially, CAFs were considered a homogenous cell population in tumor biology. But later researchers have realized that CAF population express a wide range of molecular markers and were also thought to be functionally divergent. Further studies have explored the subtypes of CAFs based on different parameters including the expression profile, origin (locally recruited versus bone marrow derived), and their subsequent roles in PDAC (Öhlund et al., 2014; Sugimoto et al., 2006). More recently, Öhlund and colleagues have subclassified CAFs into myofibroblasts and inflammatory fibroblasts based on the expression of different markers and their location of distribution. The group distinguished myofibroblasts from inflammatory fibroblasts based on high expression of α-SMA and their proximity with the neoplastic cells (myoCAFs), while the inflammatory fibroblasts (iCAFs) were shown to express mostly inflammatory cytokines such as IL-6 and were located distally from the neoplastic lesions (Öhlund et al., 2017).

We hypothesized that SPARC might indeed determine specific functions in CAFs, as SPARC is predominantly expressed by CAFs during PDAC tumorigenesis. Similar to protumorigenic properties of CAFs, SPARC has been shown to enhance the invasiveness of the tumor cells (Guweidhi et al., 2005). Considering the fact that SPARC is a potent modulator of interaction between tumor and stromal cells, we hypothesized that SPARC may determine the fibroblast's pro or anti-tumorigenic nature. Consequently, we anticipated a direct effect on CAF population upon SPARC depletion in our mouse model.

To differentiate between cell-autonomous and non-cell autonomous effects of SPARC, we first investigated the role of SPARC in epithelial cells. Wound healing assays performed on primary PanIN cells revealed that endogenous SPARC expression has no direct effect on phenotypic properties of pre-neoplastic epithelial cells. This was not surprising due to the fact that there is hardly any expression of SPARC in PanIN cells itself. Similar results were obtained in wound healing assay performed on fibroblasts isolated from KC-SPARC^{wt} and KC-SPARC$^{-/-}$ mice. Therefore, it appears that SPARC

had no autocrine effects on both epithelial as well as stromal cells. To investigate whether CAF derived SPARC has paracrine effects on surrounding epithelial cells, co-culture assays with supernatant from CAFs on epithelial cells were performed. To this end, PanIN cells from KC-SPARC$^{-/-}$ mice were incubated with supernatant from both KC-SPARC^{wt} and KC-SPARC$^{-/-}$ fibroblasts. Both KC-SPARC^{wt} and KC-SPARC$^{-/-}$ fibroblast conditional media showed no measurable phenotypic effect on epithelial cells. However, a potential limitation of our in vitro experiments might be the 2D design. CAFs have been shown to exhibit different expression profile upon mono and co-culturing with tumor cells. In addition, CAFs may also require tumor cells in the proximity in order to achieve their original expression profile as seen *in vivo*. Thus, the stimulation with conditional medium may not fully recapitulate the *in vivo*. 3D organoid co-cultures would be the appropriate model to study this effect.

Still, our *in vitro* results are in line with our *in vivo* findings from KC mice that SPARC has no effect on PanIN and tumor progression. In our model, the disease initiation and progression led to a gradual increase of the number of CAFs regardless of the SPARC expression. Although we did not observe a direct effect on the fibroblast cell population, loss of SPARC significantly changed the ECM composition by reducing the amount of collagen within preneoplastic lesions and murine tumors. Surprisingly, these alterations in ECM composition did not show significant effects on tumor biology.

5.3 SPARC mediated ECM deposition and PDAC progression

The ECM in PDAC is a highly complex network composed of various acellular constituents such as collagen, laminin, fibronectin and proteoglycons which has been shown to regulate various vital cellular functions (Theocharis et al., 2016). SPARC has been shown to modulate the interaction between cellular and acellular (ECM) compartments (Bornstein, 1995; Brekken and Sage, 2000).

In the existing literature, various partly opposing roles of SPARC have been described in different tumor entities. There are certain factors which determine the functions of SPARC in different systems such as the cellular origin of the protein, the amount of secretion and the availability of domains for receptor binding. To this end, SPARC interacts with soluble (i.e growth factors) and insoluble components (collagen, fibronectin etc.,) and is involved in a wide range of cellular functions. In 2003, Brekken et al., have performed a study in which pancreatic tumor cells were implanted

subcutaneously in SPARC$^{-/-}$ and SPARC^{wt} mice. The authors reported that tumor growth, volume and weight was increased in SPARC$^{-/-}$ compared to SPARC^{wt} mice indicating a tumor-suppressive role of SPARC (Brekken et al., 2003). Using a GEMM of PDAC, we first explored the expression pattern of SPARC in the KC model. In the KC mouse model, SPARC was mainly expressed by CAFs that either surrounded PanINs or tumor cells, while there was hardly any expression in epithelial (PanIN or tumor cells) compartment as such. An almost identical expression profile was described in human PDAC where SPARC was found to be expressed by peritumoral fibroblasts (Infante et al., 2007; Mantoni et al., 2008; Sinn et al., 2014). Therefore, we believe that GEMMs of PDAC, in this case Kras^{G12D} driven model is more appropriate to recapitulate the human situation, especially in terms of the tumor microenvironment. Interestingly, SPARC has been characterized as one of the markers of activated stroma and its overexpression by stromal fibroblast is correlated with poor clinical outcome in the patients (Infante et al., 2007; Mantoni et al., 2008; Moffitt et al., 2015). However, overexpression of SPARC in activated fibroblasts in the KC model has not resulted in enhanced tumor progression. Our data is in line with previously published observations in the KPC model, in which SPARC ablation resulted in a similar frequency of liver metastases (Neesse et al., 2014). Comparing our data with the findings of Moffitt et al., we hypothesize that SPARC alone may not contribute to an activated tumor stroma. Rather, the combination of different markers such as CCL13, CCL18, Gelatinase B, Stromelysin 3 and SPARC resulted in the "activated" stroma subtype that was associated with significantly shortened survival in patients. Therefore, clinical and histopathological data that suggest that SPARC is associated with a poor prognosis in PDAC patients might not necessarily reflect pro-tumorigenic functions of SPARC itself but rather SPARC as a marker for desmoplasia.

Mechanistically, SPARC is involved in assembly, folding and secretion of collagen (Martinek et al., 2006). In KC-SPARC$^{-/-}$ mice, collagen deposition was significantly reduced upon SPARC depletion. Different types of collagen have been shown to confer to tumor growth and progression (Aguilera et al., 2014). However, in our model significant reduction in collagen deposition in KC-SPARC$^{-/-}$ mice did not affect both disease initiation and progression. Based on our data, one could hypothesize that collagen serves as a passive bystander during carcinogenesis, at least in the KC mouse model that was used in this study. Alternatively, as collagen deposition was not completely absent in KC-SPARC$^{-/-}$ mice, there might be a critical amount of collagen that drives PanIN and

tumor progression that was still present despite the ablation of SPARC. In addition, HA deposition was not affected by SPARC expression. HA is an important stromal constituent of the ECM in PDAC which was shown to promote disease progression and to contribute to drug resistance (Provenzano et al., 2012). Although we did not observe differences in terms of overall survival between KC-SPARC^{wt} and KC-SPARC$^{-/-}$ mice, tumor bearing KC-SPARC$^{-/-}$ lived significantly shorter than tumor bearing KC- SPARC^{wt} mice. However, the detailed preclinical analysis did not show any meaningful differences in terms of proliferation, apoptosis, angiogenesis and frequency of liver metastasis. Still, it became apparent that KC-SPARC$^{-/-}$ mice showed more severe tumor associated symptoms such as jaundice, ascites and diarrhea. Therefore, we hypothesize that germline SPARC knockout mice tolerate pancreatic tumor burden less due to intrinsic abnormalities such as metabolic disturbances, ascites development and more severe jaundice.

Intriguingly, the association between SPARC and ascites formation has been previously described in experimental ovarian cancer. Here, host specific SPARC plays a tumor suppressing role by normalizing the ovarian tumor stroma through decreasing the pro-tumorigenic and pro-metastatic factors in ascites (Said et al., 2007). Said and colleagues have explored the mechanism by which SPARC modulates the biochemical composition of the ascitic fluid using syngeneic mouse models. In this study, the authors injected either control ID8 cells or ID8 cells overexpressing VEGF in SPARC$^{-/-}$ and SPARC$^{+/+}$ mice. They observed an increased tumor growth, increased incidence of ascites, increased ascites fluid volume and decreased survival in SPARC$^{-/-}$ mice which received ID8+VEGF cells. Furthermore, this study revealed that SPARC reduces the proliferation and invasion of ID8 cells by downregulating the VEGF-MMP levels. Additionally, the ascitic fluid of SPARC$^{-/-}$ mice was reported to have higher amounts of pro-tumorigenic inflammatory factors (Said et al., 2007). The positive feedback loop between MMPs and VEGF has been previously reported (Belotti et al., 2003). Thus quantification of VEGF level using ELISA or mRNA expression analysis in the ascitic fluid of KC-SPARC^{wt} and KC-SPARC$^{-/-}$ mice may provide further insight into mechanisms by which the increased ascites incidence in KC-SPARC$^{-/-}$ mice had occurred. For this study, ascites was unfortunately not routinely collected for further analysis.

Even though there was no obvious evidence showing the relationship between SPARC and increased incidence of jaundice, there is evidence suggesting a strong correlation

between the altered collagen level or mutation in collagen genes and jaundice incidence (Mizuguchi et al., 2005; Tomotaki et al., 2016). However, the exact mechanism has not been elucidated so far.

5.4 SPARC and angiogenesis

In general, PDAC is a highly desmoplastic and hypovascular tumor. This hypovascularity causes reduced tumor perfusion which is further decreased by physical compression of the existing tumor vessel by the ECM matrix and the high colloidal tumor pressure. These observations have led to the hypothesis that the abundant tumor stroma is one of the main reasons for the failure of chemotherapies (Olive et al., 2009). Therefore, various experimental attempts have been made to deplete the tumor stroma and increase vascular perfusion thus allowing drugs to enter the tumor more easily. SPARC has been extensively studied in the field of vascular biology and has been referred to as the regulator of angiogenesis (Sage et al., 1984, 1989). Previous studies have shown the anti-angiogenic role of SPARC in various tumors entities such as ovarian cancer, neuroblastoma and gastric cancer (Chlenski et al., 2010; Said et al., 2007; Zhang et al., 2012). In ovarian cancer, SPARC has been shown to downregulate VEGF and MMPs in order to achieve the anti-angiogenic activity (Said et al., 2007).

SPARC has also been previously shown to interact with VEGF and thus regulate the proliferation and migration of endothelial cells (Kupprion et al., 1998; Raines et al., 1992). Prior to this work, it could be hypothesized that SPARC depletion may result in enhanced angiogenesis and possibly improved perfusion of murine PDAC tumors. Therefore, mean vessel density was assessed by analyzing immunoreactivity of CD31 in tumor tissues of KC-SPARC$^{-/-}$ and KC-SPARC^{wt} mice. Surprisingly, no changes in the number of tumor vessels were observed upon SPARC depletion. However, the finding that SPARC ablation resulted in a higher frequency of malignant ascites in tumor bearing mice may still indicate an anti-angiogenic role of SPARC that was abolished following SPARC depletion. Further experimental studies such as a detailed biochemical work-up of ascites and serum samples for secreted factors such as VEGF may further help to investigate this hypothesis in mice. From a clinical point of view, it is interesting to note that only a fraction of patients with PDAC develop malignant ascites during the end stages of the tumor disease. It remains to be determined whether these patients have any differences in global or tumor-associated SPARC expression. Again, this could be interrogated by a clinical proof of concept study where serum samples from patients with

and without ascites, but comparable tumor stages are analyzed for circulating SPARC, VEGF and other growth factors.

5.5 SPARC mediated desmoplasia and drug delivery

Previous studies have described the association between the extensive amount of ECM deposition and drug resistance in PDAC. Various components of ECM such as collagen and hyaluronan have been thought to impede drug delivery by acting as a physical barrier (Jacobetz et al., 2013; Minchinton and Tannock, 2006; Provenzano et al., 2012). In addition to the extrinsic resistance, the desmoplastic stroma of PDAC also has been shown to confer to intrinsic resistance by differentially regulating the cellular enzymes involved in gemcitabine metabolism pathway (Dangi-Garimella et al., 2011, 2013; Hessmann et al., 2018).

Several investigators have used various GEMMs to assess different compounds that target the tumor stroma. For example, Cilengitide, an angiogenesis inhibitor, and Verapamil, a Ca^{++} channel blocker, were co-administered and resulted in improved vascular function, intratumoral gemcitabine accumulation and therapeutic response. There are a number of additional stromal targets such as TGF-β using the inhibitor LY364947, HA using the enzyme PEGPH20, or collagen maturation using the lysyl oxidase (LOX) inhibitor that have been experimentally probed in various mouse models with success (Jacobetz et al., 2013; Kano et al., 2007; Miller et al., 2015; Provenzano et al., 2012; Thompson et al., 2010). However, none of these findings could be successfully translated in phase III trials in humans, and so far, no approved anti-stromal drug is currently available in the clinical routine for PDAC patients. To this end, PEGPH20 might represent the most promising candidate right now. A phase III study (NCT02715804) has recently been approved, and patients with high intratumoral HA levels are randomized to nab-paclitaxel/gemcitabine ± PEGPH20. This trial will show whether the biophysical drug delivery hypothesis in PDAC will translate to patient care.

Another explanation for the failure of chemotherapies has recently been discovered in the Neesse laboratory. Experimental data from GEMMs indicate that CAFs, compared to epithelial tumor cells, metabolize and intracellularly store large amounts of gemcitabine metabolites that are not available for tumor cells anymore. This phenomenon was termed “drug scavenging” and may explain why tumor cells are very sensitive

towards the chemotherapeutic drug gemcitabine in vitro, but fail to undergo apoptosis when surrounded by a dense, fibroblast-rich environment (Hessmann et al., 2018).

In my thesis, I explored whether SPARC or SPARC mediated desmoplasia affects gemcitabine delivery and metabolism by employing LC-MS/MS analysis in normal pancreas tissue, bulk preneoplastic tissues, and tumor tissues from KC-SPARC$^{-/-}$ and KC-SPARC^{wt} mice upon gemcitabine treatment. These mice models provided an excellent platform to investigate whether collagen content really affected intratumoral gemcitabine accumulation in preneoplastic tissues as well as murine pancreatic tumors. Surprisingly, the results showed that there is no noticeable difference in terms of intrapancreatic gemcitabine accumulation between tumors with high and low collagen content. In fact, the amount of native gemcitabine (dFdC) accumulation was comparable between tumors with high and low collagen content (KC-SPARC^{wt} vs KC-SPARC$^{-/-}$). According to our model, the extensive deposition of collagen in KC-SPARC^{wt} tumor does not affect the delivery and metabolism of gemcitabine. This is contradicting the previous studies which have described collagen as a physical barrier for gemcitabine delivery (Dangi-Garimella et al., 2013; Diop-Frimpong et al., 2011).

We further investigated if the accumulation of gemcitabine is disease stage dependent in order to explore the contribution of desmoplasia for drug accumulation. Completely contradicting the biophysical drug barrier hypothesis, LC-MS/MS results revealed a gradual increase in gemcitabine accumulation dependent from normal pancreas to PanIN lesions and fully developed tumors. Bases on the stromal scavenging theory, we hypothesized that the increase in drug accumulation is rather due to the increase in overall cellularity. And indeed, performing nuclear density analysis (DAPI) and IHC for pan-cytokeratin and α-SMA a significant increase in both epithelial and mesenchymal cells in tumors compared to normal pancreas tissues was detected. The ratio between native gemcitabine (dFdC), inactive gemcitabine (dFdU) and the activated form (dFdCTP) demonstrated that the increased accumulation of native gemcitabine in tumor tissue was eventually not phosphorylated to the active dFdCTP. Instead, the amount of inactive dFdU increased in tumor tissues indicating an increased activity of gemcitabine inactivating enzymes in tumor tissues compared to preneoplastic pancreas tissue and normal pancreas.

5.6 Conclusions

We hypothesized that SPARC is an important matricellular protein in PDAC contributing to disease progression, ECM remodeling and possibly drug delivery. Therefore, genetic abrogation of SPARC in Kras-driven mouse models and cell lines may directly or indirectly affect tumorigenesis and progression, as well as the delivery of chemotherapeutic drugs such as gemcitabine.

5.6.1 SPARC and tumorigenesis

- SPARC depletion lead to significant reduction of collagen deposition in KC-SPARC$^{-/-}$mice regardless of the disease stage
- SPARC depletion did not affect progression of the ADM-PanIN-tumor sequence in GEMMs.
- The tumor incidence and liver metastasis rate were unaffected by genetic abrogation of SPARC in KC mice.
- SPARC depletion did not change hallmark characteristics of murine pancreatic tumors including tumor weight, proliferation, apoptosis and angiogenesis.
- *In vitro*, SPARC abrogation did not affect morphology and proliferation of both epithelial and fibroblast cell lines derived from preneoplastic lesions and murine pancreas tumors.
- The overall median survival of KC-SPARC^{wt} and KC-SPARC$^{-/-}$ mice was similar and was not affected by SPARC abrogation.
- Loss of SPARC significantly shortened survival of tumor bearing KC-SPARC$^{-/-}$ mice compared to KC-SPARC^{wt} mice and was associated with more severe clinical symptoms such as ascites, diarrhea and jaundice.

5.6.2 SPARC and drug delivery

- There was no difference in terms of delivery and metabolism of gemcitabine between collagen-rich and collagen-poor tumors (KC-SPARC^{wt} vs. KC-SPARC$^{-/-}$).
- There was a striking increase in the accumulation of native gemcitabine in murine tumors (high collagen) compared to normal pancreas tissue (no collagen) contradicting several reports that the desmoplastic reaction impedes gemcitabine delivery.

- Interestingly, native gemcitabine was inactivated by enzymes such as CDA and Nt5c1A that were overexpressed in murine tumors but not normal pancreas tissue resulting in comparable levels of activated gemcitabine metabolites in normal pancreas and murine tumors.

6. References

Aguilera, K.Y., Rivera, L.B., Hur, H., Carbon, J.G., Toombs, J.E., Goldstein, C.D., Dellinger, M.T., Castrillon, D.H., and Brekken, R.A. (2014). Collagen signaling enhances tumor progression after anti-VEGF therapy in a murine model of pancreatic ductal adenocarcinoma. Cancer Res. *74*, 1032–1044.

Aguirre, A.J., Bardeesy, N., Sinha, M., Lopez, L., Tuveson, D.A., Horner, J., Redston, M.S., and Depinho, R.A. (2003). Activated Kras and Ink4a/Arf deficiency cooperate to produce metastatic pancreatic ductal adenocarcinoma. Genes Dev. 3112–3126.

Ahmed, S., Bradshaw, A.-D., Gera, S., Dewan, M., and Xu, R. (2017). The TGF-β/Smad4 Signaling Pathway in Pancreatic Carcinogenesis and Its Clinical Significance. J. Clin. Med. *6*, 5.

Albrecht Neesse, Christian Bauer, Daniel Öhlund, Matthias Lauth, Malte Buchholz, Patrick Michl6, D.A.T. and T.M.G. (2018). Stromal biology and therapy in pancreatic cancer- Ready for clinical translation? Gut.

Alliel, P.M., Perin, J. -P, Jolles, P., and Bonnet, F.J. (1993). Testican, a multidomain testicular proteoglycan resembling modulators of cell social behaviour. Eur. J. Biochem.

Ancrile, B.B. (2009). Oncogenic Ras–Induced Expression of Cytokines in Cancer. Mol Interv *8*, 22–27.

Ancrile, B., Lim, K.H., and Counter, C.M. (2007). Oncogenic Ras-induced secretion of IL6 is required for tumorigenesis. Genes Dev.

Anderson, M.W., Reynolds, S.H., You, M., and Maronpot, R.M. (1992). Role of Proto-oncogene activation in carcinogenesis. In Environmental Health Perspectives, pp. 13–24.

Apte, M. V., Haber, P.S., Applegate, T.L., Norton, I.D., McCaughan, G.W., Korsten, M.A., Pirola, R.C., and Wilson, J.S. (1998). Periacinar stellate shaped cells in rat pancreas: Identification, isolation, and culture. Gut *43*, 128–133.

Apte, M. V., Park, S., Phillips, P.A., Santucci, N., Goldstein, D., Kumar, R.K., Ramm, G.A., Buchler, M., Friess, H., McCarroll, J.A., et al. (2004). Desmoplastic reaction in pancreatic cancer: Role of pancreatic stellate cells. Pancreas *29*, 179–187.

Apte, M. V., Wilson, J.S., Lugea, A., and Pandol, S.J. (2013). A starring role for stellate cells in the pancreatic cancer microenvironment. Gastroenterology *144*, 1210–1219.

Arnold, S.A., and Brekken, R.A. (2009). SPARC: A matricellular regulator of tumorigenesis. J. Cell Commun. Signal. *3*, 255–273.

Arnold, S.A., Rivera, L.B., Carbon, J.G., Toombs, J.E., Chang, C.L., Bradshaw, A.D., and Brekken, R.A. (2012). Losartan slows pancreatic tumor progression and extends survival of SPARC-null mice by abrogating aberrant TGFβ activation. PLoS One *7*.

Arslan, A.A., Helzlsouer, K.J., Kooperberg, C., Shu, X., Steplowski, E., Bueno-de-mesquita, H.B., Fuchs, C.S., Myron, D., Jacobs, E.J., Lacroix, A.Z., et al. (2010). Anthropometric Measures, Body Mass Index and Pancreatic Cancer: a Pooled Analysis from the Pancreatic Cancer Cohort Consortium (PanScan). Arch Intern Med *170*, 791–802.

Bachem, M.G., Schneider, E., Groß, H., Weidenbach, H., Schmid, R.M., Menke, A., Siech, M., Beger, H., Grünert, A., and Adler, G. (1998). Identification, culture, and characterization of pancreatic stellate cells in rats and humans. Gastroenterology *115*, 421–432.

Bachem, M.G., Schünemann, M., Ramadani, M., Siech, M., Beger, H., Buck, A., Zhou, S., Schmid-Kotsas, A., and Adler, G. (2005). Pancreatic carcinoma cells induce fibrosis by stimulating proliferation and matrix synthesis of stellate cells. Gastroenterology.

Bapiro, T.E., Richards, F.M., Goldgraben, M.A., Olive, K.P., Madhu, B., Frese, K.K., Cook, N., Jacobetz, M.A., David, D.S., Gri, J.R., et al. (2011). A novel method for quantification of gemcitabine and its metabolites 2',2'-diXuorodeoxyuridine and gemcitabine triphosphate in tumour tissue by LC–MS/MS: comparison with 19F NMR spectroscopy. 1243–1253.

Bardeesy, N., Cheng, K.H., Berger, J.H., Chu, G.C., Pahler, J., Olson, P., Hezel, A.F., Horner, J., Lauwers, G.Y., Hanahan, D., et al. (2006). Smad4 is dispensable for normal pancreas development yet critical in progression and tumor biology of pancreas cancer. Genes Dev. *20*, 3130–3146.

Baril, P., Gangeswaran, R., Mahon, P.C., Caulee, K., Kocher, H.M., Harada, T., Zhu, M., Kalthoff, H., Crnogorac-Jurcevic, T., and Lemoine, N.R. (2007). Periostin promotes invasiveness and resistance of pancreatic cancer cells to hypoxia-induced cell death: Role of the β4 integrin and the PI3k pathway. Oncogene *26*, 2082–2094.

Barker, T.H., Baneyx, G., Cardó-Vila, M., Workman, G.A., Weaver, M., Menon, P.M., Dedhar, S., Rempel, S.A., Arap, W., Pasqualini, R., et al. (2005). SPARC regulates extracellular matrix organization through its modulation of integrin-linked kinase activity. J. Biol. Chem.

Bassuk, J.A., Pichler, R., Rothmier, J.D., Pippen, J., Gordon, K., Meek, R.L., Bradshaw, A.D., Lombardi, D., Strandjord, T.P., Reed, M., et al. (2000). Induction of TGF-β1 by the matricellular protein SPARC in a rat model of glomerulonephritis. Kidney Int.

Belotti, D., Paganoni, P., Manenti, L., Garofalo, A., Marchini, S., Taraboletti, G., and Giavazzi, R. (2003). Matrix metalloproteinases (MMP9 and MMP2) induce the release of vascular endothelial growth factor (VEGF) by ovarian carcinoma cells: Implications for ascites formation. Cancer Res.

Biankin, A. V., Waddell, N., Kassahn, K.S., Gingras, M.C., Muthuswamy, L.B., Johns, A.L., Miller, D.K., Wilson, P.J., Patch, A.M., Wu, J., et al. (2012). Pancreatic cancer genomes reveal aberrations in axon guidance pathway genes. Nature *491*, 399–405.

Boeck, S., Ankerst, D.P., and Heinemann, V. (2008). The role of adjuvant chemotherapy for patients with resected pancreatic cancer: Systematic review of randomized controlled trials and meta-analysis. Oncology *72*, 314–321.

Bornstein, P. (1995). Diversity of function is inherent in matricellular proteins: An appraisal of thrombospondin 1. J. Cell Biol.

Bos, J.L., Fearon, E.R., Hamilton, S.R., Verlaan-de Vries, M., van Boom, J.H., van der Eb, A.J., and Vogelstein, B. (1987). Prevalence of ras gene mutations in human colorectal cancers. Nature *327*, 293–297.

Boyle, P., Hsieh, C.C., Maisonneuve, P., La Vecchia, C., Macfarlane, G.J., Walker, A.M., and Trichopoulos, D. (1989). Epidemiology of pancreas cancer (1988). Int. J. Pancreatol. *5*, 327–346.

Bradshaw, A.D. (2009). The role of SPARC in extracellular matrix assembly. J. Cell Commun. Signal. *3*, 239–246.

Bradshaw, A.D. (2012). Diverse Biological Functions of the SPARC Family of Proteins. *44*, 480–488.

Bradshaw, A.D., Puolakkainen, P., Dasgupta, J., Davidson, J.M., Wight, T.N., and Sage, E.H. (2003). SPARC-null mice display abnormalities in the dermis characterized by decreased collagen fibril diameter and reduced tensile strength. J. Invest. Dermatol.

Bramhall, S.R., Rosemurgy, a, Brown, P.D., Bowry, C., and Buckels, J. a (2001). Marimastat as first-line therapy for patients with unresectable pancreatic cancer: a randomized trial. J. Clin. Oncol.

Bramhall, S.R., Schulz, J., Nemunaitis, J., Brown, P.D., Baillet, M., and Buckels, J.A.C. (2002). A double-blind placebo-controlled, randomised study comparing gemcitabine and marimastat with gemcitabine and placebo as first line therapy in patients with advanced pancreatic cancer. Br. J. Cancer.

Brekken, R.A., and Sage, E.H. (2000). SPARC, a matricellular protein: at the crossroads of cell-matrix communication. Matrix Biol. *19*, 569–580.

Brekken, R.A., Puolakkainen, P., Graves, D.C., Workman, G., Lubkin, S.R., and Sage, E.H. (2003). Enhanced growth of tumors in SPARC null mice is associated with changes in the ECM. J. Clin. Invest. *111*, 487–495.

Burris, H.A., Moore, M.J., Andersen, J., Green, M.R., Rothenberg, M.L., Modiano, M.R., Cripps, M.C., Portenoy, R.K., Storniolo, A.M., Tarassoff, P., et al. (1997). Improvements in survival and clinical benefit with gemcitabine as first-line therapy for patients with advanced pancreas cancer: a randomized trial. J. Clin. Oncol. *15*, 2403–2413.

Campbell, S.L., Khosravi-Far, R., Rossman, K.L., Clark, G.J., and Der, C.J. (1998). Increasing complexity of Ras signaling. Oncogene *17*, 1395–1413.

Carafoli, F., Bihan, D., Stathopoulos, S., Konitsiotis, A.D., Kvansakul, M., Farndale, R.W., Leitinger, B., and Hohenester, E. (2009). Crystallographic Insight into Collagen Recognition by Discoidin Domain Receptor 2. Structure.

Carpelan-Holmstrom, M. (2005). Does anyone survive pancreatic ductal adenocarcinoma? A nationwide study re-evaluating the data of the Finnish Cancer Registry. Gut *54*, 385–387.

Carpeño, J.D.C., and Belda-iniesta, C. (2013). KRAS mutant NSCLC , a new opportunity for the synthetic lethality therapeutic approach. Transl. Lung Cancer Res. *2*, 142–151.

Casper, E.S., Green, M.R., Kelsen, D.P., Heelan, R.T., Brown, T.D., Flombaum, C.D., Trochanowski, B., and Tarassoff, P.G. (1994). Phase II trial of gemcitabine (2,2'-difluorodeoxycytidine) in patients with adenocarcinoma of the pancreas. Invest New Drugs *12*, 29–34.

Ceyhan, G.O., Demir, I.E., Altintas, B., Rauch, U., Thiel, G., Müller, M.W., Giese, N.A., Friess, H., and Schäfer, K.H. (2008). Neural invasion in pancreatic cancer: A mutual tropism between neurons and cancer cells. Biochem. Biophys. Res. Commun.

Chambers, A.F., and Matrisian, L.M. (1997). Changing views of the role of matrix metalloproteinases in metastasis. J. Natl. Cancer Inst.

Chanmee, T., Ontong, P., and Itano, N. (2016). Hyaluronan: A modulator of the tumor microenvironment. Cancer Lett.

Charbonnier, F., Périn, J.P., Mattei, M.G., Camuzat, A., Bonnet, F., Gressin, L., and Alliel, P.M. (1998). Genomic organization of the human SPOCK gene and its chromosomal localization to 5q31. Genomics.

Chauhan, V.P., Martin, J.D., Liu, H., Lacorre, D.A., Jain, S.R., Kozin, S. V., Stylianopoulos, T., Mousa, A.S., Han, X., Adstamongkonkul, P., et al. (2013). Angiotensin inhibition enhances drug delivery and potentiates chemotherapy by decompressing tumour blood vessels. Nat. Commun. *4*.

Chen, G., Tian, X., Liu, Z., Zhou, S., Schmidt, B., Henne-Bruns, D., Bachem, M., and Kornmann, M. (2010). Inhibition of endogenous SPARC enhances pancreatic cancer cell growth: Modulation by FGFR1-III isoform expression. Br. J. Cancer *102*, 188–195.

Chen, J., Wang, M., Xi, B., Xue, J., He, D., Zhang, J., and Zhao, Y. (2012). SPARC is a key regulator of proliferation, apoptosis and invasion in human ovarian cancer. PLoS One.

Chlenski, A., Liu, S., Crawford, S.E., Volpert, O. V., DeVries, G.H., Evangelista, A., Yang, Q., Salwen, H.R., Farrer, R., Bray, J., et al. (2002). SPARC is a key Schwannian-derived inhibitor controlling neuroblastoma tumor angiogenesis. Cancer Res.

Chlenski, A., Guerrero, L.J., Peddinti, R., Spitz, J.A., Leonhardt, P.T., Yang, Q., Tian, Y., Salwen, H.R., and Cohn, S.L. (2010). Anti-angiogenic SPARC peptides inhibit progression of neuroblastoma tumors. Mol. Cancer *9*, 1–10.

Chu, G.C., Kimmelman, A.C., Hezel, A.F., and DePinho, R.A. (2007). Stromal biology of pancreatic cancer. J. Cell. Biochem. *101*, 887–907.

Clark, C.E., Hingorani, S.R., Mick, R., Combs, C., Tuveson, D.A., and Vonderheide, R.H. (2007). Dynamics of the immune reaction to pancreatic cancer from inception to invasion. Cancer Res. *67*, 9518–9527.

Clezardin, P., Malaval, L., Ehrensperger, A. -S, DELMAS, P.D., DECHAVANNE, M., and MCGREGOR, J.L. (1988). Complex formation of human thrombospondin with osteonectin. Eur. J. Biochem.

Collisson, E.A., Sadanandam, A., Olson, P., Gibb, W.J., Truitt, M., Gu, S., Cooc, J., Weinkle, J., Kim, G.E., Jakkula, L., et al. (2011). Subtypes of pancreatic ductal adenocarcinoma and their differing responses to therapy. Nat. Med. *17*, 500–503.

Condeelis, J., and Pollard, J.W. (2006). Macrophages: Obligate partners for tumor cell migration, invasion, and metastasis. Cell *124*, 263–266.

Conroy, T., Desseigne, F., Ychou, M., Bouche, O., Guimbaud, R., Becouarn, Y., Adenis, A., Raoul, J.L., Gourgou-Bourgade, S., de la Fouchardiere, C., et al. (2011). FOLFIRINOX versus gemcitabine for metastatic pancreatic cancer. N Engl J Med.

Cullinan, S.A., Moertel, C.G., Fleming, T.R., Rubin, J.R., Krook, J.E., Everson, L.K., Windschitl, H.E., Twito, D.I., Marschke, R.F., Foley, J.F., et al. (1985). A Comparison of Three Chemotherapeutic Regimens in the Treatment of Advanced Pancreatic and Gastric Carcinoma: Fluorouracil vs Fluorouracil and Doxorubicin vs Fluorouracil, Doxorubicin, and Mitomycin. JAMA J. Am. Med. Assoc.

Dangi-Garimella, S., Krantz, S.B., Barron, M.R., Shields, M.A., Heiferman, M.J., Grippo, P.J., Bentrem, D.J., and Munshi, H.G. (2011). Three-dimensional collagen I promotes gemcitabine resistance in pancreatic cancer through MT1-MMP-mediated expression of HMGA2. Cancer Res.

Dangi-Garimella, S., Sahai, V., Ebine, K., Kumar, K., and Munshi, H.G. (2013). Three-Dimensional Collagen I Promotes Gemcitabine Resistance In Vitro in Pancreatic Cancer Cells through HMGA2-Dependent Histone Acetyltransferase Expression. PLoS One *8*, 1–9.

Demir, I.E., Friess, H., and Ceyhan, G.O. (2015). Neural plasticity in pancreatitis and pancreatic cancer. Nat. Rev. Gastroenterol. Hepatol.

Dhanesuan, N., Sharp, J.A., Blick, T., Price, J.T., and Thompson, E.W. (2002). Doxycycline-inducible expression of SPARC/Osteonectin/BM40 in MDA-MB-231 human breast cancer cells results in growth inhibition. Breast Cancer Res. Treat.

Diop-Frimpong, B., Chauhan, V.P., Krane, S., Boucher, Y., and Jain, R.K. (2011). Losartan inhibits collagen I synthesis and improves the distribution and efficacy of nanotherapeutics in tumors. Proc. Natl. Acad. Sci. *108*, 2909–2914.

Direkze, N.C., Hodivala-Dilke, K., Jeffery, R., Hunt, T., Poulsom, R., Oukrif, D., Alison, M.R., and Wright, N.A. (2004). Bone marrow contribution to tumor-associated myofibroblasts and fibroblasts. Cancer Res. *64*, 8492–8495.

Downward, J. (2003). Role of receptor tyrosine kinases in G-protein-coupled receptor regulation of Ras: transactivation or parallel pathways? Biochem J *376*, e9-10.

Ellenrieder, V., Alber, B., Lacher, U., Hendler, S.F., Menke, A., Boeck, W., Wagner, M., Wilda, M., Friess, H., Büchler, M., et al. (2000). Role of MT-MMPs and MMP-2 in pancreatic cancer progression. Int. J. Cancer *85*, 14–20.

Engel, J., Paulsson, M., Taylor, W., Sage, H., and Hogan, B. (1987). Calcium Binding Domains and Calcium-Induced Conformational Transition of SPARC/BM-40/Osteonectin, an Extracellular Glycoprotein Expressed in Mineralized and Nonmineralized Tissues. Biochemistry.

Erkan, M., Reiser-Erkan, C., Michalski, C.W., Deucker, S., Sauliunaite, D., Streit, S., Esposito, I., Friess, H., and Kleeff, J. (2009). Cancer-Stellate Cell Interactions Perpetuate the Hypoxia-Fibrosis Cycle in Pancreatic Ductal Adenocarcinoma. Neoplasia *11*, 497–508.

Esch, F.S., Shimasaki, S., Mercado, M., Cooksey, K., Ling, N., Ying, S., Ueno, N., and Guillemin, R. (1987). Structural Characterization of Follistatin: A Novel Follicle-Stimulating Hormone Release-Inhibiting Polypeptide from the Gonad. Mol. Endocrinol.

Esposito, I., Penzel, R., Chaib-Harrireche, M., Barcena, U., Bergmann, F., Riedl, S., Kayed, H., Giese, N., Kleeff, J., Friess, H., et al. (2006). Tenascin C and annexin II expression in the process of pancreatic carcinogenesis. J. Pathol. *208*, 673–685.

Feig, C., Gopinathan, A., Neesse, A., Chan, D.S., Cook, N., and Tuveson, D.A. (2012). The pancreas cancer microenvironment. Clin. Cancer Res. *18*, 4266–4276.

Fendrich, V., Esni, F., Garay, M.V.R., Feldmann, G., Habbe, N., Jensen, J.N., Dor, Y., Stoffers, D., Jensen, J., Leach, S.D., et al. (2008). Hedgehog Signaling Is Required for Effective Regeneration of Exocrine Pancreas. Gastroenterology.

Fernanda Ledda, M., Adris, S., Bravo, A.I., Kairiyama, C., Bover, L., Chernajovsky, Y., Mordoh, J., and Podhajcer, O.L. (1997). Suppression of SPARC expression by antisense RNA abrogates the tumorigenicity of human melanoma cells. Nat. Med.

Fitzgerald, M.C., and Schwarzbauer, J.E. (1998). Importance of the basement membrane protein SPARC for viability and fertility in Caenorhabditis elegans. Curr. Biol.

Framson, P.E., and Sage, E.H. (2004). SPARC and tumor growth: Where the seed meets the soil? J. Cell. Biochem.

Francki, A., Bradshaw, A.D., Bassuk, J.A., Howe, C.C., Couser, W.G., and Sage, E.H. (1999a). SPARC regulates the expression of collagen type I and transforming growth factor-β1 in mesangial cells. J. Biol. Chem. *274*, 32145–32152.

Francki, a, Bradshaw, a D., Bassuk, J. a, Howe, C.C., Couser, W.G., and Sage, E.H. (1999b). SPARC regulates the expression of collagen type I and transforming growth factor-beta1 in mesangial cells. J. Biol. Chem.

Froeling, F.E.M., Feig, C., Chelala, C., Dobson, R., Mein, C.E., Tuveson, D.A., Clevers, H., Hart, I.R., and Kocher, H.M. (2011). Retinoic acid-induced pancreatic stellate cell quiescence reduces paracrine Wntβ-catenin signaling to slow tumor progression. Gastroenterology *141*, 1486–1497.e14.

Funk, S.E., and Sage, E.H. (1991). The Ca2(+)-binding glycoprotein SPARC modulates cell cycle progression in bovine aortic endothelial cells. Proc. Natl. Acad. Sci. U. S. A.

Funk, S.E., and Sage, E.H. (1993). Differential effects of SPARC and cationic SPARC peptides on DNA synthesis by endothelial cells and fibroblasts. J. Cell. Physiol. *154*, 53–63.

Gao, J., Song, J., Huang, H., Li, Z., Du, Y., Cao, J., Li, M., Lv, S., Lin, H., and Gong, Y. (2010). Methylation of the SPARC gene promoter and its clinical implication in pancreatic cancer. J. Exp. Clin. Cancer Res. *29*, 1–9.

Ghaneh, P., Costello, E., and Neoptolemos, J.P. (2008). Biology and management of pancreatic cancer. Postgrad. Med. J. *84*, 478–497.

Gilmour, D.T., Lyon, G.J., Carlton, M.B.L., Sanes, J.R., Cunningham, J.M., Anderson, J.R., Hogan, B.L.M., Evans, M.J., and Colledge, W.H. (1998). Mice deficient for the secreted glycoprotein SPARC/osteonectin/BM40 develop normally but show severe age-onset cataract formation and disruption of the lens. EMBO J. *17*, 1860–1870.

Greiling, T.M.S., Stone, B., and Clark, J.I. (2009). Absence of SPARC leads to impaired lens circulation. Exp. Eye Res. *89*, 416–425.

Gress, T.M., Menke, A., Bachem, M., Ellenrieder, V., Weidenbach, H., Wagner, M., and Adler, G. (1998). Role of Extracellular Matrix in pancreatic diseases. 625–637.

Guerra, C., Schuhmacher, A.J., Cañamero, M., Grippo, P.J., Verdaguer, L., Pérez-Gallego, L., Dubus, P., Sandgren, E.P., and Barbacid, M. (2007). Chronic Pancreatitis Is Essential for Induction of Pancreatic Ductal Adenocarcinoma by K-Ras Oncogenes in Adult Mice. Cancer Cell *11*, 291–302.

Guerra, C., Collado, M., Navas, C., Schuhmacher, A.J., Hernández-Porras, I., Cañamero, M., Rodriguez-Justo, M., Serrano, M., and Barbacid, M. (2011). Pancreatitis-induced inflammation contributes to pancreatic cancer by inhibiting oncogene-induced senescence. Cancer Cell *19*, 728–739.

Guweidhi, A., Kleeff, J., Adwan, H., Giese, N.A., Wente, M.N., Giese, T., Büchler, M.W., Berger, M.R., and Friess, H. (2005). Osteonectin influences growth and invasion of pancreatic cancer cells. Ann. Surg. *242*, 224–234.

Haber, C.L., Gottifredi, V., Llera, A.S., Salvatierra, E., Prada, F., Alonso, L., Helene, S.E., and Podhajcer, O.L. (2008). SPARC modulates the proliferation of stromal but not melanoma cells unless endogenous SPARC expression is downregulated. Int. J. Cancer.

Habisch, H., Zhou, S., Siech, M., and Bachem, M.G. (2010). Interaction of stellate cells with pancreatic carcinoma cells. Cancers (Basel). *2*, 1661–1682.

Hahn, S. a, Schutte, M., Hoque, a T., Moskaluk, C. a, da Costa, L.T., Rozenblum, E., Weinstein, C.L., Fischer, A., Yeo, C.J., Hruban, R.H., et al. (1996). DPC4, a candidate tumor suppressor gene at human chromosome 18q21.1. Science (80-.).

Hambrock, H.O., Nitsche, D.P., Hansen, U., Bruckner, P., Paulsson, M., Maurer, P., and Hartmann, U. (2003). SC1/hevin: An extracellular calcium-modulated protein that binds collagen I. J. Biol. Chem.

Hambrock, H.O., Kaufmann, B., Müller, S., Hanisch, F.G., Nose, K., Paulsson, M., Maurer, P., and Hartmann, U. (2004). Structural characterization of TSC-36/Flik: Analysis of two charge isoforms. J. Biol. Chem.

Hao, N.B., Lü, M.H., Fan, Y.H., Cao, Y.L., Zhang, Z.R., and Yang, S.M. (2012). Macrophages in tumor microenvironments and the progression of tumors. Clin. Dev. Immunol. *2012*.

Hasselaar, P., and Sage, E.H. (1992). SPARC antagonizes the effect of basic fibroblast growth factor on the migration of bovine aortic endothelial cells. J. Cell. Biochem.

Heinemann, V., Hertel, L., Grindey, G., and Plunkett, W. (1988). Comparison of the cellular pharmacokinetics and toxicity of 2′, 2′-difluorodeoxycytidine and 1-β-d-arabinofuranosylcytosine. Cancer Res. 4024–4031.

Hessmann, E., Patzak, M.S., Klein, L., Chen, N., Kari, V., Ramu, I., Bapiro, T.E., Frese, K.K., Gopinathan, A., Richards, F.M., et al. (2018). Fibroblast drug scavenging increases intratumoural gemcitabine accumulation in murine pancreas cancer. Gut *67*, 497–507.

Hidalgo, M., and Eckhardt, S.G. (2001). Development of matrix metalloproteinase inhibitors in cancer therapy. J. Natl. Cancer Inst. *93*, 178–193.

Hingorani, S.R., Petricoin, E.F., Maitra, A., Rajapakse, V., King, C., Jacobetz, M.A., Ross, S., Conrads, T.P., Veenstra, T.D., Hitt, B.A., et al. (2003). Preinvasive and invasive ductal pancreatic cancer and its early detection in the mouse. Cancer Cell *4*, 437–450.

Hingorani, S.R., Zheng, L., Bullock, A.J., Seery, T.E., Harris, W.P., Sigal, D.S., Braiteh, F., Ritch, P.S., Zalupski, M.M., Bahary, N., et al. (2018). HALO 202: Randomized phase II Study of PEGPH20 Plus Nab-Paclitaxel/Gemcitabine Versus Nab-Paclitaxel/Gemcitabine in Patients With Untreated, Metastatic Pancreatic Ductal Adenocarcinoma. J. Clin. Oncol. *36*, 359–366.

Von Hoff, D.D., Ervin, T., Arena, F.P., Chiorean, E.G., Infante, J., Moore, M., Seay, T., Tjulandin, S.A., Ma, W.W., Saleh, M.N., et al. (2013). Increased survival in pancreatic

cancer with nab-paclitaxel plus gemcitabine. N Engl J Med.

Hohenester, E., Maurer, P., Hohenadl, C., Timpl, R., Jansonius, J.N., and Engel, J. (1996). Structure of a novel extracellular Ca2+-binding module in BM-40. Nat. Struct. Biol.

Hohenester, E., Maurer, P., and Timpl, R. (1997). Crystal structure of a pair of follistatin-like and EF-hand calcium-binding domains in BM-40. EMBO J.

Howlader, N., Am, N., M, K., J, G., N, N., Sf, A., Cl, K., M, Y., J, R., Z, T., et al. (2012). SEER Cancer statistics review 1975-2010. J. Natl. Cancer Inst. 1–109.

Hruban, R.H., Takaori, K., Klimstra, D.S., Adsay, N.V., Albores-Saavedra, J., Biankin, A. V., Biankin, S.A., Compton, C., Fukushima, N., Furukawa, T., et al. (2004). An illustrated consensus on the classification of pancreatic intraepithelial neoplasia and intraductal papillary mucinous neoplasms. Am. J. Surg. Pathol. *28*, 977–987.

Hwang, R.F., Moore, T., Arumugam, T., Ramachandran, V., Amos, K.D., Rivera, A., Ji, B., Evans, D.B., and Logsdon, C.D. (2008). Cancer-associated stromal fibroblasts promote pancreatic tumor progression. Cancer Res. *68*, 918–926.

Iacobuzio-Donahue, C.A., Ashfaq, R., Maitra, A., Adsay, N.V., Shen-Ong, G.L., Berg, K., Hollingsworth, M.A., Cameron, J.L., Yeo, C.J., Kern, S.E., et al. (2003). Highly Expressed Genes in Pancreatic Ductal Adenocarcinomas: A Comprehensive Characterization and Comparison of the Transcription Profiles Obtained from Three Major Technologies. Cancer Res. *63*, 8614–8622.

Ijichi, H., Chytil, A., Gorska, A.E., Aakre, M.E., Fujitani, Y., Fujitani, S., Wright, C.V.E., and Moses, H.L. (2006). Aggressive pancreatic ductal adenocarcinoma in mice caused by pancreas-specific blockade of transforming growth factor-β signaling in cooperation with active Kras expression. Genes Dev. *20*, 3147–3160.

Incio, J., Liu, H., Suboj, P., Chin, S.M., Chen, I.X., Pinter, M., Ng, M.R., Nia, H.T., Grahovac, J., Kao, S., et al. (2016). Obesity-induced inflammation and desmoplasia promote pancreatic cancer progression and resistance to chemotherapy. Cancer Discov. *6*, 852–869.

Infante, J.R., Matsubayashi, H., Sato, N., Tonascia, J., Klein, A.P., Riall, T.A., Yeo, C.,

Iacobuzio-Donahue, C., and Goggins, M. (2007). Peritumoral fibroblast SPARC expression and patient outcome with resectable pancreatic adenocarcinoma. J. Clin. Oncol. *25*, 319–325.

Ingham, K.C., Brew, S.A., and Migliorini, M. (2002). Type I collagen contains at least 14 cryptic fibronectin binding sites of similar affinity. Arch. Biochem. Biophys.

Iodice, S., Gandini, S., Istituto, I.E.O., Istituto, I.E.O., Iodice, S., Gandini, S., and Maisonneuve, P. (2008). Tobacco and the Risk of Pancreatic Cancer : A Review and Meta-Analysis Tobacco and the risk of pancreatic cancer : a review and meta-analysis.

Ishii, G., Sangai, T., Oda, T., Aoyagi, Y., Hasebe, T., Kanomata, N., Endoh, Y., Okumura, C., Okuhara, Y., Magae, J., et al. (2003). Bone-marrow-derived myofibroblasts contribute to the cancer-induced stromal reaction. Biochem. Biophys. Res. Commun. *309*, 232–240.

Jabłońska-Trypuć, A., Matejczyk, M., and Rosochacki, S. (2016). Matrix metalloproteinases (MMPs), the main extracellular matrix (ECM) enzymes in collagen degradation, as a target for anticancer drugs. J. Enzyme Inhib. Med. Chem. *31*, 177–183.

Jackson, E.L., Willis, N., Mercer, K., Bronson, R.T., Crowley, D., Montoya, R., Jacks, T., and Tuveson, D.A. (2001). Analysis of lung tumor initiation and progression using conditional expression of oncogenic K-ras. 3243–3248.

Jacobetz, M.A., Chan, D.S., Neesse, A., Bapiro, T.E., Cook, N., Frese, K.K., Feig, C., Nakagawa, T., Caldwell, M.E., Zecchini, H.I., et al. (2013). Hyaluronan impairs vascular function and drug delivery in a mouse model of pancreatic cancer. Gut *62*, 112–120.

Januchowski, R., Świerczewska, M., Sterzyńska, K., Wojtowicz, K., Nowicki, M., and Zabel, M. (2016). Increased expression of several collagen genes is associated with drug resistance in ovarian cancer cell lines. J. Cancer.

Jones, S., Zhang, X., Parsons, D.W., Lin, J.C.-H., Leary, R.J., Angenendt, P., Mankoo, P., Carter, H., Kamiyama, H., Jimeno, A., et al. (2008). Core Signaling Pathways in Human Pancreatic Cancers Revealed by Global Genomic Analyses. Science (80-.). *321*, 1801–1806.

Kalluri, R., and Zeisberg, M. (2006). Fibroblasts in cancer. Nat. Rev. Cancer *6*, 392–401.

Kanda, M., Matthaei, H., Wu, J., Hong, S.M., Yu, J., Borges, M., Hruban, R.H., Maitra, A., Kinzler, K., Vogelstein, B., et al. (2012). Presence of somatic mutations in most early-stage pancreatic intraepithelial neoplasia. Gastroenterology *142*, 730–733.

Kanji, Z.S., Edwards, A.M., Mandelson, M.T., Sahar, N., Lin, B.S., Badiozamani, K., Song, G., Alseidi, A., Biehl, T.R., Kozarek, R.A., et al. (2018). Gemcitabine and Taxane Adjuvant Therapy with Chemoradiation in Resected Pancreatic Cancer: A Novel Strategy for Improved Survival? Ann. Surg. Oncol. *25*, 1052–1060.

Kanno, A., Satoh, K., Masamune, A., Hirota, M., Kimura, K., Umino, J., Hamada, S., Satoh, A., Egawa, S., Motoi, F., et al. (2008). Periostin, secreted from stromal cells, has biphasic effect on cell migration and correlates with the epithelial to mesenchymal transition of human pancreatic cancer cells. Int. J. Cancer *122*, 2707–2718.

Kano, M.R., Bae, Y., Iwata, C., Morishita, Y., Yashiro, M., Oka, M., Fujii, T., Komuro, A., Kiyono, K., Kaminishi, M., et al. (2007). Improvement of cancer-targeting therapy, using nanocarriers for intractable solid tumors by inhibition of TGF-beta signaling. Proc. Natl. Acad. Sci. *104*, 3460–3465.

Kelm, R.J., and Mann, K.G. (1991). The collagen binding specificity of bone and platelet osteonectin is related to differences in glycosylation. J. Biol. Chem.

Khan, S., Ebeling, M.C., Chauhan, N., Thompson, P.A., Gara, R.K., Ganju, A., Yallapu, M.M., Behrman, S.W., Zhao, H., Zafar, N., et al. (2016). Sensitivity of Gemcitabine in Pancreatic Cancer. *75*, 2292–2304.

Kikuta, K., Masamune, A., Watanabe, T., Ariga, H., Itoh, H., Hamada, S., Satoh, K., Egawa, S., Unno, M., and Shimosegawa, T. (2010). Pancreatic stellate cells promote epithelial-mesenchymal transition in pancreatic cancer cells. Biochem Biophys Res Commun.

Klimstra, D.S., and Longnecker, D.S. (1994). K-ras mutations in pancreatic ductal proliferative lesions. Am. J. Pathol. *145*, 1547–1550.

Knudsen, E.S., Vail, P., Balaji, U., Ngo, H., Botros, I.W., Makarov, V., Riaz, N., Balachandran, V., Leach, S., Thompson, D.M., et al. (2017). Stratification of pancreatic ductal adenocarcinoma: Combinatorial genetic, stromal, and immunologic markers. Clin. Cancer Res.

Koblinski, J.E., Kaplan-Singer, B.R., VanOsdol, S.J., Wu, M., Engbring, J.A., Wang, S., Goldsmith, C.M., Piper, J.T., Vostal, J.G., Harms, J.F., et al. (2005). Endogenous osteonectin/SPARC/BM-40 expression inhibits MDA-MB-231 breast cancer cell metastasis. Cancer Res.

Koukourakis, M.I., Giatromanolaki, A., Brekken, R.A., Sivridis, E., Gatter, K.C., Harris, A.L., and Sage, E.H. (2003). Enhanced expression of SPARC/osteonectin in the tumor-associated stroma of non-small cell lung cancer is correlated with markers of hypoxia/acidity and with poor prognosis of patients. Cancer Res.

Kupprion, C., Motamed, K., and Sage, E.H. (1998). SPARC (BM-40, osteonectin) inhibits the mitogenic effect of vascular endothelial growth factor on microvascular endothelial cells. J. Biol. Chem.

Lane, T.F., and Sage, E.H. (1994). The biology of SPARC, a protein that modulates cell-matrix interactions. FASEB J.

Lane, T.F., Iruela-Arispe, M.L., and Sage, E.H. (1992). Regulation of gene expression by SPARC during angiogenesis in vitro. Changes in fibronectin, thrombospondin-1, and plasminogen activator inhibitor-1. J. Biol. Chem.

Lane T. F and Sage Helene. (1994). The Biology of SPARC, a protein that modulates cell-matrix interactions. 121–144.

Lauth, M., Bergström, Å., Shimokawa, T., Tostar, U., Jin, Q., Fendrich, V., Guerra, C., Barbacid, M., and Toftgrd, R. (2010). DYRK1B-dependent autocrine-to-paracrine shift of Hedgehog signaling by mutant RAS. Nat. Struct. Mol. Biol.

Lee, J.J., Perera, R.M., Wang, H., Wu, D.-C., Liu, X.S., Han, S., Fitamant, J., Jones, P.D., Ghanta, K.S., Kawano, S., et al. (2014). Stromal response to Hedgehog signaling restrains pancreatic cancer progression. Proc. Natl. Acad. Sci.

Leslie, K., Gao, S.P., Berishaj, M., Podsypanina, K., Ho, H., Ivashkiv, L., and Bromberg, J. (2010). Differential interleukin-6/Stat3 signaling as a function of cellular context mediates Ras-induced transformation. Breast Cancer Res.

Lillie, R.D., Tracy, R.E., Pizzolato, P., Donaldson, P.T., and Reynolds, C. (1980). Differential staining of collagen types in paraffin sections: A color change in degraded forms. Virchows Arch. A Pathol. Anat. Histol. *386*, 153–159.

Liu, P., Lu, J., Cardoso, W. V, and Vaziri, C. (2008). The SPARC-related factor SMOC-2 promotes growth factor-induced cyclin D1 expression and DNA synthesis via integrin-linked kinase. Mol. Biol. Cell.

Lohr, M., Schmidt, C., Kluth, M., Mu, P., Nizze, H., and Jesnowski, R. (2001). Transforming Growth Factor- NL 1 Induces Desmoplasia in an Experimental Model of Human Pancreatic Carcinoma 1. Cancer Res. 550–555.

Lokeshwar, V.B., Obek, C., Soloway, M.S., and Block, N.L. (1997). Tumor-associated hyaluronic acid: a new sensitive and specific urine marker for bladder cancer. Cancer Res. *57*, 773–777.

Lowenfels, A.B., and Maisonneuve, P. (2004). Epidemiology and prevention of pancreatic cancer. Jpn.J.Clin.Oncol. *34*, 238–244.

Määttä, M., Soini, Y., Liakka, A., and Autio-Harmainen, H. (2000). Differential expression of matrix metalloproteinase (MMP)-2, MMP-9, and membrane type 1-MMP in hepatocellular and pancreatic adenocarcinoma: implications for tumor progression and clinical prognosis. Clin. Cancer Res. *6*, 2726–2734.

Mahlbacher, V., Sewing, A., Elsässer, H.P., and Kern, H.F. (1992). Hyaluronan is a secretory product of human pancreatic adenocarcinoma cells. Eur. J. Cell Biol.

Maisonneuve, P., and Lowenfels, A.B. (2010). Epidemiology of pancreatic cancer: An update. Dig. Dis. *28*, 645–656.

Mantoni, T.S., Schendel, R.R.E., Rödel, F., Al-Assar, O., Al-Assar, G.N.O., Masamune, A., and Brunner, T.B. (2008). Stromal SPARC expression and patient survival after chemoradiation for non-resectable pancreatic adenocarcinoma. Cancer Biol. Ther. *7*, 1806–1815.

Martinek, N., Zou, R., Berg, M., Sodek, J., and Ringuette, M. (2002). Evolutionary conservation and association of SPARC with the basal lamina in Drosophila. Dev. Genes Evol. *212*, 124–133.

Martinek, N., Shahab, J., Sodek, J., and Ringuette, M. (2006). Is SPARC an Evolutionarily Conserved Collagen Chaperone ? 296–305.

Martinek, N., Shahab, J., Saathoff, M., and Ringuette, M. (2011). Haemocyte-derived SPARC is required for collagen-IV-dependent stability of basal laminae in Drosophila embryos. J. Cell Sci.

Matthaei, H., Schulick, R.D., Hruban, R.H., and Maitra, A. (2011). Cystic precursors to invasive pancreatic cancer. Nat. Rev. Gastroenterol. Hepatol. *8*, 141–150.

Maurer, P., and Hohenester, E. (1997). Structural and functional aspects of calcium binding in extracellular matrix proteins. Matrix Biol.

Maurer, P., Mayer, U., Bruch, M., Jenö, P., Mann, K., Landwehr, R., Engel, J., and Timpl, R. (1992). High-affinity and low-affinity calcium binding and stability of the multidomain extracellular 40-kDa basement membrane glycoprotein (BM-40/SPARC/osteonectin). Eur. J. Biochem.

Mccleary-Wheeler, A.L., Mcwilliams, R., and Fernandez-Zapico, M.E. (2012). Aberrant signaling pathways in pancreatic cancer: A two compartment view. Mol. Carcinog. *51*, 25–39.

Miller, B.W., Morton, J.P., Pinese, M., Saturno, G., Jamieson, N.B., McGhee, E., Timpson, P., Leach, J., McGarry, L., Shanks, E., et al. (2015). Targeting the LOX/hypoxia axis reverses many of the features that make pancreatic cancer deadly: inhibition of LOX abrogates metastasis and enhances drug efficacy. EMBO Mol. Med. *7*, 1063–1076.

Minchinton, A.I., and Tannock, I.F. (2006). Drug penetration in solid tumours. Nat. Rev. Cancer *6*, 583–592.

Mini, E., Nobili, S., Caciagli, B., Landini, I., and Mazzei, T. (2006). Cellular pharmacology of gemcitabine. Ann. Oncol. *17*, 7–12.

Mizuguchi, Y., Yoshida, H., Yokomuro, S., Arima, Y., Mamada, Y., Taniai, N., Akimaru, K., and Tajiri, T. (2005). Collagen IV is a predictor for clinical course in patients with malignant obstructive jaundice. Hepatogastroenterology.

Moffitt, R.A., Marayati, R., Flate, E.L., Volmar, K.E., Loeza, S.G.H., Hoadley, K.A., Rashid, N.U., Williams, L.A., Eaton, S.C., Chung, A.H., et al. (2015). Virtual microdissection identifies distinct tumor- and stroma-specific subtypes of pancreatic ductal adenocarcinoma. Nat. Genet. *47*, 1168–1178.

Morris et al. (2010). KRAS, Hedgehog, Wnt and the twisted developmental biology of pancreatic ductal adenocarcinoma John. *292*, 342–351.

Motamed, K., and Sage, E.H. (1998). SPARC inhibits endothelial cell adhesion but not proliferation through a tyrosine phosphorylation-dependent pathway. J. Cell. Biochem.

Murphy, K.M., Brune, K.A., Griffin, C., Sollenberger, J.E., Petersen, G.M., Bansal, R., Hruban, R.H., and Kern, S.E. (2002). Evaluation of candidate genes MAP2K4, MADH4, ACVR1B, and BRCA2 in familial pancreatic cancer: deleterious BRCA2 mutations in 17%. Cancer Res. *62*, 3789–3793.

Nagaraju, G.P., Dontula, R., El-rayes, B.F., and Lakka, S.S. (2014). Molecular mechanisms underlying the divergent roles of SPARC in human carcinogenesis. Carcinogenesis *35*, 967–973.

Neesse, A., Michl, P., Frese, K.K., Feig, C., Cook, N., Jacobetz, M.A., Lolkema, M.P., Buchholz, M., Olive, K.P., Gress, T.M., et al. (2011). Stromal biology and therapy in pancreatic cancer. Gut *60*, 861–868.

Neesse, A., Frese, K.K., Bapiro, T.E., Nakagawa, T., Sternlicht, M.D., Seeley, T.W., Pilarsky, C., Jodrell, D.I., Spong, S.M., and Tuveson, D.A. (2013). CTGF antagonism with mAb FG-3019 enhances chemotherapy response without increasing drug delivery in murine ductal pancreas cancer. Proc. Natl. Acad. Sci. *110*, 12325–12330.

Neesse, A., Frese, K.K., Chan, D.S., Bapiro, T.E., Howat, W.J., Richards, F.M., Ellenrieder, V., Jodrell, D.I., and Tuveson, D.A. (2014). SPARC independent drug delivery and antitumour effects of nab -paclitaxel in genetically engineered mice. 974–983.

Neesse, A., Algül, H., Tuveson, D.A., and Gress, T.M. (2015). Stromal biology and therapy in pancreatic cancer: A changing paradigm. Gut *64*, 1476–1484.

Neoptolemos, J.P., Stocken, D.D., Bassi, C., Ghaneh, P., Cunningham, D., Goldstein, D., Padbury, R., Moore, M.J., Gallinger, S., Mariette, C., et al. (2010). Adjuvant Chemotherapy With Fluorouracil Plus Folinic Acid vs Gemcitabine Following Pancreatic Cancer Resection. September *304*, 1073–1081.

Neoptolemos, J.P., Palmer, D.H., Ghaneh, P., Psarelli, E.E., Valle, J.W., Halloran, C.M., Faluyi, O., O'Reilly, D.A., Cunningham, D., Wadsley, J., et al. (2017). Comparison of adjuvant gemcitabine and capecitabine with gemcitabine monotherapy in patients with resected pancreatic cancer (ESPAC-4): a multicentre, open-label, randomised, phase 3 trial. Lancet *389*, 1011–1024.

Noël, A., Jost, M., and Maquoi, E. (2008). Matrix metalloproteinases at cancer tumor-host interface. Semin. Cell Dev. Biol.

Norose, K., Clark, J.I., Syed, N.A., Basu, A., Heber-Katz, E., Sage, E.H., and Howe, C.C. (1998a). SPARC deficiency leads to early-onset cataractogenesis. Investig. Ophthalmol. Vis. Sci. *39*, 2674–2680.

Norose, K., Clark, J.I., Syed, N.A., Basu, A., Heber-Katz, E., Sage, E.H., and Howe, C.C. (1998b). SPARC deficiency leads to early-onset cataractogenesis. Investig. Ophthalmol. Vis. Sci.

Oettle, H., Neuhaus, P., Hochhaus, A., Hartmann, J.T., Gellert, K., Ridwelski, K., Niedergethmann, M., Zülke, C., Fahlke, J., Arning, M.B., et al. (2013). Adjuvant Chemotherapy With Gemcitabine and Long-term Outcomes Among Patients With Resected Pancreatic Cancer. Jama *310*, 1473.

Oettle et al. (2007). Adjuvant Chemotherapy With Gemcitabine vs Observation in Patients Undergoing Curative-Intent Resection of Pancreatic Cancer A Randomized Controlled Trial. Database *297*, 267–277.

Öhlund, D., Elyada, E., and Tuveson, D. (2014). Fibroblast heterogeneity in the cancer wound. J. Exp. Med.

Öhlund, D., Handly-Santana, A., Biffi, G., Elyada, E., Almeida, A.S., Ponz-Sarvise, M., Corbo, V., Oni, T.E., Hearn, S.A., Lee, E.J., et al. (2017). Distinct populations of inflammatory fibroblasts and myofibroblasts in pancreatic cancer. J. Exp. Med. jem.20162024.

Olive, K.P., Jacobetz, M.A., Davidson, C.J., Gopinathan, A., McIntyre, D., Honess, D., Madhu, B., Goldgraben, M.A., Caldwell, M.E., Allard, D., et al. (2009). Inhibition of Hedgehog Signaling Enhances Delivery of Chemotherapy in a Mouse Model of Pancreatic Cancer. Science (80-.). *324*, 1457–1461.

Ozawa, F., Friess, H., and Caliera, a T. (2001). Growth factors and their receptors in pancreatic cancer - Ozawa - 2000 - Teratogenesis, Carcinogenesis, and Mutagenesis - Wiley Online Library. Teratogenesis *44*, 27–44.

Özdemir, B.C., Pentcheva-Hoang, T., Carstens, J.L., Zheng, X., Wu, C.C., Simpson, T.R., Laklai, H., Sugimoto, H., Kahlert, C., Novitskiy, S. V., et al. (2014). Depletion of carcinoma-associated fibroblasts and fibrosis induces immunosuppression and accelerates pancreas cancer with reduced survival. Cancer Cell *25*, 719–734.

Parkin, D.., Bray, F.., and Devesa, S.. (2001). Cancer burden in the year 2000. The global picture. Eur. J. Cancer.

Patthy, L. (1991). Modular exchange principles in proteins. Curr. Opin. Struct. Biol.

Phillips, P.A., McCarroll, J.A., Park, S., Wu, M.-J., Pirola, R., Korsten, M., Wilson, J.S., and Apte, M. V (2003). Rat pancreatic stellate cells secrete matrix metalloproteinases: implications for extracellular matrix turnover. Gut.

Pickart, L., and Lovejoy, S. (1987). Biological Activity of Human Plasma Copper-Binding Growth Factor Glycyl-L-Histidyl-L-Lysine. Methods Enzymol.

Pickart, L., Freedman, J.H., Loker, W.J., Peisach, J., Perkins, C.M., Stenkamp, R.E., and Weinstein, B. (1980). Growth-modulating plasma tripeptide may function by facilitating copper uptake into cells. Nature *288*, 715–717.

Pollard, J.W. (2004). Opinion: Tumour-educated macrophages promote tumour progression and metastasis. Nat. Rev. Cancer *4*, 71–78.

Poschl, E. (2004). Collagen IV is essential for basement membrane stability but dispensable for initiation of its assembly during early development. Development.

Provenzano, P.P., Cuevas, C., Chang, A.E., Goel, V.K., Von Hoff, D.D., and Hingorani, S.R. (2012). Enzymatic Targeting of the Stroma Ablates Physical Barriers to Treatment of Pancreatic Ductal Adenocarcinoma. Cancer Cell *21*, 418–429.

Puolakkainen, P. a, Brekken, R. a, Muneer, S., and Sage, E.H. (2004). Enhanced growth of pancreatic tumors in SPARC-null mice is associated with decreased deposition of extracellular matrix and reduced tumor cell apoptosis. Mol. Cancer Res. *2*, 215–224.

Pylayeva-Gupta, Y., Lee, K.E., Hajdu, C.H., Miller, G., and Bar-Sagi, D. (2012). Oncogenic Kras-Induced GM-CSF Production Promotes the Development of Pancreatic Neoplasia. Cancer Cell.

Qian, X., Rothman, V.L., Nicosia, R.F., and Tuszynski, G.P. (2001). Expression of thrombospondin-1 in human pancreatic adenocarcinomas: Role in matrix metalloproteinase-9 production. Pathol. Oncol. Res. *7*, 251–259.

Rahib, L., Smith, B.D., Aizenberg, R., Rosenzweig, A.B., Fleshman, J.M., and Matrisian, L.M. (2014). Projecting cancer incidence and deaths to 2030: The unexpected burden of thyroid, liver, and pancreas cancers in the united states. Cancer Res. *74*, 2913–2921.

Raines, E.W., Lane, T.F., Iruela-Arispe, M.L., Ross, R., and Sage, E.H. (1992). The extracellular glycoprotein SPARC interacts with platelet-derived growth factor (PDGF)-AB and -BB and inhibits the binding of PDGF to its receptors. Proc. Natl. Acad. Sci. U. S. A.

Rhim, A.D., Oberstein, P.E., Thomas, D.H., Mirek, E.T., Palermo, C.F., Sastra, S.A., Dekleva, E.N., Saunders, T., Becerra, C.P., Tattersall, I.W., et al. (2014). Stromal elements act to restrain, rather than support, pancreatic ductal adenocarcinoma. Cancer Cell *25*, 735–747.

Rizzato, C., Campa, D., Pezzilli, R., Soucek, P., Greenhalf, W., Capurso, G., Talar-wojnarowska, R., Heller, A., Jamroziak, K., Khaw, K., et al. (2013). ABO blood groups

and pancreatic cancer risk and survival : Results from the PANcreatic Disease ReseArch (PANDoRA) consortium. 1637–1644.

Robinson, E., Foty, R., and Corbett, S. (2004). Fibronectin Matrix Assembly Regulates alpha5beta1-mediated Cell Cohesion. Mol. Biol. Cell.

Romberg, R.W., Werness, P.G., Lollar, P., Riggs, B.L., and Manns, K.G. (1985). Isolation and Characterization of Native Adult Osteonectin" J. Biol. Chem.

Rosenblatt, S., Bassuk, J. a, Alpers, C.E., Sage, E.H., Timpl, R., and Preissner, K.T. (1997). Differential modulation of cell adhesion by interaction between adhesive and counter-adhesive proteins: characterization of the binding of vitronectin to osteonectin (BM40, SPARC). Biochem. J.

Sage, H., Johnson, C., and Bornstein, P. (1984). Characterization of a novel serum albumin-binding glycoprotein secreted by endothelial cells in culture. J. Biol. Chem. *259*, 3993–4007.

Sage, H., Vernon, R.B., Funk, S.E., Everitt, E.A., and Angello, J. (1989). SPARC, a secreted protein associated with cellular proliferation, inhibits cell spreading in vitro and exhibits Ca+2-dependent binding to the extracellular matrix. J. Cell Biol.

Said, N., Socha, M.J., Olearczyk, J.J., Elmarakby, A.A., Imig, J.D., and Motamed, K. (2007). Normalization of the Ovarian Cancer Microenvironment by SPARC. Mol. Cancer Res. *5*, 1015–1030.

Said, N., Frierson, H.F., Sanchez-Carbayo, M., Brekken, R.A., and Theodorescu, D. (2013). Loss of SPARC in bladder cancer enhances carcinogenesis and progression. J. Clin. Invest. *123*, 751–766.

Sato, N., Fukushima, N., Maehara, N., Matsubayashi, H., Koopmann, J., Su, G.H., Hruban, R.H., and Goggins, M. (2003). SPARC/osteonectin is a frequent target for aberrant methylation in pancreatic adenocarcinoma and a mediator of tumor-stromal interactions. Oncogene *22*, 5021–5030.

Sato, N., Kohi, S., Hirata, K., and Goggins, M. (2016). Role of hyaluronan in pancreatic cancer biology and therapy: Once again in the spotlight. Cancer Sci.

Schäfer, H., Geismann, C., Heneweer, C., Egberts, J.H., Korniienko, O., Kiefel, H., Moldenhauer, G., Bachem, M.G., Kalthoff, H., Altevogt, P., et al. (2012). Myofibroblast-induced tumorigenicity of pancreatic ductal epithelial cells is L1CAM dependent. Carcinogenesis *33*, 84–93.

Schiemann, B.J., Neil, J.R., and Schiemann, W.P. (2003). SPARC inhibits epithelial cell proliferation in part through stimulation of the transforming growth factor-beta-signaling system. Mol. Biol. Cell.

Schneider, G., Siveke, J.T., Eckel, F., and Schmid, R.M. (2005). Pancreatic cancer: Basic and clinical aspects. Gastroenterology *128*, 1606–1625.

Schneiderhan, W., Diaz, F., Fundel, M., Zhou, S., Siech, M., Hasel, C., Moller, P., Gschwend, J.E., Seufferlein, T., Gress, T., et al. (2007). Pancreatic stellate cells are an important source of MMP-2 in human pancreatic cancer and accelerate tumor progression in a murine xenograft model and CAM assay. J. Cell Sci. *120*, 512–519.

Schnepp, A., Lindgren, P.K., Hülsmann, H., Kröger, S., Paulsson, M., and Hartmann, U. (2005). Mouse testican-2: Expression, glycosylation, and effects on neurite outgrowth. J. Biol. Chem.

Schubbert, S., Shannon, K., and Bollag, G. (2007). Hyperactive Ras in developmental disorders and cancer. Nat. Rev. Cancer *7*, 295–308.

Shek, F.W., Benyon, R.C., Walker, F.M., McCrudden, P.R., Pender, S.L., Williams, E.J., Johnson, P.A., Johnson, C.D., Bateman, A.C., Fine, D.R., et al. (2002). Expression of transforming growth factor-beta 1 by pancreatic stellate cells and its implications for matrix secretion and turnover in chronic pancreatitis. Am J Pathol *160*, 1787–1798.

Sherman, M.H., Yu, R.T., Engle, D.D., Ding, N., Atkins, A.R., Tiriac, H., Collisson, E.A., Connor, F., Van Dyke, T., Kozlov, S., et al. (2014). Vitamin D receptor-mediated stromal reprogramming suppresses pancreatitis and enhances pancreatic cancer therapy. Cell *159*, 80–93.

Sherman-Baust, C.A., Weeraratna, A.T., Rangel, L.B.A., Pizer, E.S., Cho, K.R., Schwartz, D.R., Shock, T., and Morin, P.J. (2003). Remodeling of the extracellular matrix through overexpression of collagen VI contributes to cisplatin resistance in ovarian cancer cells. Cancer Cell.

Shi, C., Hruban, R.H., and Klein, A.P. (2009). Familial pancreatic cancer. Arch. Pathol. Lab. Med. *133*, 365–374.

Shin, M., Mizokami, A., Kim, J., Ofude, M., Konaka, H., Kadono, Y., Kitagawa, Y., Miwa, S., Kumaki, M., Keller, E.T., et al. (2013). Exogenous SPARC suppresses proliferation and migration of prostate cancer by interacting with integrin β1. Prostate.

Siegel, R., Miller, K.D., and Ahmedin, J. (2017). Cancer Statistics 2017. CA CANCER J CLIN 2017 *67*, 7–30.

Singha, N.C., Nekoroski, T., Zhao, C., Symons, R., Jiang, P., Frost, G.I., Huang, Z., and Shepard, H.M. (2015). Tumor-Associated Hyaluronan Limits Efficacy of Monoclonal Antibody Therapy. Mol. Cancer Ther. *14*, 523–532.

Sinn, M., Sinn, B. V., Striefler, J.K., Lindner, J.L., Stieler, J.M., Lohneis, P., Bischoff, S., Bläker, H., Pelzer, U., Bahra, M., et al. (2014). SPARC expression in resected pancreatic cancer patients treated with gemcitabine: results from the CONKO-001 study. Ann. Oncol. *25*, 1025–1032.

Sinn, M., Bahra, M., Liersch, T., Gellert, K., Messmann, H., Bechstein, W., Waldschmidt, D., Jacobasch, L., Wilhelm, M., Rau, B.M., et al. (2017). CONKO-005: Adjuvant chemotherapy with gemcitabine plus erlotinib versus gemcitabine alone in patients after r0 resection of pancreatic cancer: A multicenter randomized phase III trial. J. Clin. Oncol. *35*, 3330–3337.

Sparmann, A., and Bar-Sagi, D. (2004). Ras-induced interleukin-8 expression plays a critical role in tumor growth and angiogenesis. Cancer Cell.

Stocken, D.D., Büchler, M.W., Dervenis, C., Bassi, C., Jeekel, H., Klinkenbijl, J.H.G., Bakkevold, K.E., Takada, T., Amano, H., and Neoptolemos, J.P. (2005). Meta-analysis of randomised adjuvant therapy trials for pancreatic cancer. Br. J. Cancer *92*, 1372–1381.

Sugimoto, H., Mundel, T.M., Kieran, M.W., and Kalluri, R. (2006). Identification of

fibroblast heterogeneity in the tumor microenvironment. Cancer Biol. Ther.

Sullivan, M.M., and Sage, E.H. (2004). Hevin/SC1, a matricellular glycoprotein and potential tumor-suppressor of the SPARC/BM-40/Osteonectin family. Int. J. Biochem. Cell Biol.

Suzuki, M., Hao, C., Takahashi, T., Shigematsu, H., Shivapurkar, N., Sathyanarayana, U.G., Iizasa, T., Fujisawa, T., Hiroshima, K., and Gazdar, A.F. (2005). Aberrant methylation of SPARC in human lung cancers. Br. J. Cancer.

Termine, J.D., Kleinman, H.K., Whitson, S.W., Conn, K.M., McGarvey, M.L., and Martin, G.R. (1981). Osteonectin, a bone-specific protein linking mineral to collagen. Cell *26*, 99–105.

Thayer, S.P., Di Magliano, M.P., Heiser, P.W., Nielsen, C.M., Roberts, D.J., Lauwers, G.Y., Qi, Y.P., Gysin, S., Fernández-del Castillo, C., Yajnik, V., et al. (2003). Hedgehog is an early and late mediator of pancreatic cancer tumorigenesis. Nature.

Theocharis, A.D., Skandalis, S.S., Gialeli, C., and Karamanos, N.K. (2016). Extracellular matrix structure. Adv. Drug Deliv. Rev. *97*, 4–27.

Thompson, D., and Easton, D.F. (2002). Cancer Incidence in BRCA1 mutation carriers. J. Natl. Cancer Inst. *94*, 1358–1365.

Thompson, C.B., Shepard, H.M., O'Connor, P.M., Kadhim, S., Jiang, P., Osgood, R.J., Bookbinder, L.H., Li, X., Sugarman, B.J., Connor, R.J., et al. (2010). Enzymatic Depletion of Tumor Hyaluronan Induces Antitumor Responses in Preclinical Animal Models. Mol. Cancer Ther. *9*, 3052–3064.

Tomotaki, S., Mizumoto, H., Hamabata, T., Kumakura, A., Shiota, M., Arai, H., Haginoya, K., and Hata, D. (2016). Severe Hemolytic Jaundice in a Neonate with a Novel COL4A1 Mutation. Pediatr. Neonatol.

Tramacere, I., Scotti, L., Jenab, M., Bagnardi, V., Bellocco, R., Rota, M., Corrao, G., Bravi, F., Boffetta, P., and Vecchia, C. La (2010). Alcohol drinking and pancreatic cancer risk: a meta-analysis of the dose-risk relation. *1486*, 1474–1486.

Tremble, P.M., Lane, T.F., Sage, E.H., and Werb, Z. (1993). SPARC, a secreted protein associated with morphogenesis and tissue remodeling, induces expression of metalloproteinases in fibroblasts through a novel extracellular matrix-dependent pathway. J. Cell Biol. *121*, 1433–1444.

Turati, F., Edefonti, V., Bosetti, C., Ferraroni, M., Malvezzi, M., Franceschi, S., Talamini, R., Montella, M., Levi, F., Maso, L.D., et al. (2013). Family history of cancer and the risk of cancer: a network of case–control studies. Ann. Oncol. 24.

Tuveson, D.A., Zhu, L., Gopinathan, A., Willis, N.A., Kachatrian, L., Grochow, R., Pin, C.L., Mitin, N.Y., Taparowsky, E.J., Gimotty, P.A., et al. (2006). Mist1-KrasG12Dknock-in mice develop mixed differentiation metastatic exocrine pancreatic carcinoma and hepatocellular carcinoma. Cancer Res. *66*, 242–247.

Vannahme, C., Schübel, S., Herud, M., Gösling, S., Hülsmann, H., Paulsson, M., Hartmann, U., and Maurer, P. (1999). Molecular cloning of testican-2: Defining a novel calcium-binding proteoglycan family expressed in brain. J. Neurochem.

Vannahme, C., Smyth, N., Miosge, N., Gösling, S., Frie, C., Paulsson, M., Maurer, P., and Hartmann, U. (2002). Characterization of SMOC-1, a novel modular calcium-binding protein in basement membranes. J. Biol. Chem.

Vannahme, C., Gösling, S., Paulsson, M., Maurer, P., and Hartmann, U. (2003). Characterization of SMOC-2, a modular extracellular calcium-binding protein. Biochem. J.

Vernon, R.B., and Sage, H. (1989). The calcium-binding protein SPARC is secreted by Leydig and Sertoli cells of the adult mouse testis. Biol Reprod.

Vonlaufen, A., Joshi, S., Qu, C., Phillips, P.A., Xu, Z., Parker, N.R., Toi, C.S., Pirola, R.C., Wilson, J.S., Goldstein, D., et al. (2008a). Pancreatic stellate cells: Partners in crime with pancreatic cancer cells. Cancer Res. *68*, 2085–2093.

Vonlaufen, A., Phillips, P.A., Xu, Z., Goldstein, D., Pirola, R.C., Wilson, J.S., and Apte, M. V. (2008b). Pancreatic stellate cells and pancreatic cancer cells: An unholy alliance. Cancer Res.

Waddell, N., Pajic, M., Patch, A.M., Chang, D.K., Kassahn, K.S., Bailey, P., Johns, A.L., Miller, D., Nones, K., Quek, K., et al. (2015). Whole genomes redefine the mutational landscape of pancreatic cancer. Nature *518*, 495–501.

Wahi, M.M., Shah, N., Schrock, C.E., Rosemurgy, A.S., and Goldin, S.B. (2009). Reproductive Factors and Risk of Pancreatic Cancer in Women: A Review of the Literature. Ann. Epidemiol. *19*, 103–111.

Wang, H., Fertala, A., Ratner, B.D., Sage, E.H., and Jiang, S. (2005). Identifying the SPARC binding sites on collagen I and procollagen I by atomic force microscopy. Anal. Chem. *77*, 6765–6771.

Whatcott, C.J., Diep, C.H., Jiang, P., Watanabe, A., Lobello, J., Sima, C., Hostetter, G., Shepard, H.M., Von Hoff, D.D., and Han, H. (2015). Desmoplasia in primary tumors and metastatic lesions of pancreatic cancer. Clin. Cancer Res. *21*, 3561–3568.

Witkiewicz, A.K., McMillan, E.A., Balaji, U., Baek, G.H., Lin, W.C., Mansour, J., Mollaee, M., Wagner, K.U., Koduru, P., Yopp, A., et al. (2015). Whole-exome sequencing of pancreatic cancer defines genetic diversity and therapeutic targets. Nat. Commun. *6*.

WRANA, J.L., OVERALL, C.M., and SODEK, J. (1991). Regulation of the expression of a secreted acidic protein rich in cysteine (SPARC) in human fibroblasts by transforming growth factor β: Comparison of transcriptional and post-transcriptional control with fibronectin and type I collagen. Eur. J. Biochem. *197*, 519–528.

Xu, Y., Gurusiddappa, S., Rich, R.L., Owens, R.T., Keene, D.R., Mayne, R., Höök, a, and Höök, M. (2000). Multiple binding sites in collagen type I for the integrins alpha1beta1 and alpha2beta1. J. Biol. Chem.

Yahya, R.S., El-Bindary, A.A., El-Mezayen, H.A., Abdelmasseh, H.M., and Eissa, M.A. (2014). Biochemical evaluation of hyaluronic acid in breast cancer. Clin.Lab.

Yan, Q., and Sage, E.H. (1999). SPARC, a matricellular glycoprotein with important biological functions. J. Histochem. Cytochem. *47*, 1495–1505.

Yauch, R.L., Gould, S.E., Scales, S.J., Tang, T., Tian, H., Ahn, C.P., Marshall, D., Fu, L., Januario, T., Kallop, D., et al. (2008). A paracrine requirement for hedgehog signalling in cancer. Nature.

Yiu, G.K., Chan, W.Y., Ng, S.W., Chan, P.S., Cheung, K.K., Berkowitz, R.S., and Mok, S.C. (2001). SPARC (secreted protein acidic and rich in cysteine) induces apoptosis in ovarian cancer cells. Am. J. Pathol.

Yoshida, S., Yokota, T., Ujiki, M., Ding, X.Z., Pelham, C., Adrian, T.E., Talamonti, M.S., Bell, R.H.J., and Denham, W. (2004). Pancreatic cancer stimulates pancreatic stellate cell proliferation and TIMP-1 production through the MAP kinase pathway. Biochem Biophys Res Commun.

Yoshida, S., Ujiki, M., Ding, X.Z., Pelham, C., Talamonti, M.S., Bell, R.H., Denham, W., and Adrian, T.E. (2005). Pancreatic Stellate Cells (PSCs) express cyclooxygenase-2 (COX-2) and pancreatic cancer stimulates COX-2 in PSCs. Mol. Cancer.

Zhang, J.L., Chen, G.W., Liu, Y.C., Wang, P.Y., Wang, X., Wan, Y.L., Zhu, J., Gao, H.Q., Yin, J., Wang, W., et al. (2012). Secreted Protein Acidic and Rich in Cysteine (SPARC) Suppresses Angiogenesis by Down-Regulating the Expression of VEGF and MMP-7 in Gastric Cancer. PLoS One *7*, 1–10.

Zhou, H.Y., Salih, E., and Glimcher, M.J. (1998). Isolation of a novel bone glycosylated phosphoprotein with disulphide cross-links to osteonectin. Biochem. J.